The roles of two TIFY proteins in the regulation of the shoot apical meristem in *Arabidopsis thaliana*

Presented by
M.Sc. Pengfei Fan
born in: Shandong, China
Oral examination: 2024.07.31

Inaugural dissertation
for
obtaining the doctoral degree
of the
Combined Faculty of Mathematics, Engineering and Natural Sciences
of the
Ruprecht - Karls - University
Heidelberg

Presented by
M.Sc. Pengfei Fan
born in: Shandong, China
Oral examination: 2024.07.31

The roles of two TIFY proteins in the regulation of the shoot apical meristem in *Arabidopsis thaliana*

Referees: Prof. Dr. Jan Lohmann
Prof. Dr. Thomas Greb

TABLE OF CONTENTS

Abbreviations 1

Zusammenfassung 3

Abstract 5

1. Introduction 6

1.1 Stem cell control in the shoot apical meristem 6
1.1.1 Plant stem cells 6
1.1.2 The shoot apical meristem 6
1.1.3 Stem cell maintenance in the SAM 8
1.1.4 The roles of WUS in SAM signaling regulation 9
1.1.4.1 The role of WUS in hormone signaling 10
1.1.4.2 The role of WUS in response to environmental signals 11
1.1.5 Functional domains within the WUS protein 12
1.2 The plant hormone: Jasmonate 14
1.2.1 JA biosynthesis 14
1.2.2 JA transportation 15
1.2.3 JA signaling 15
1.2.4 The biological roles of JA in plants 17
1.2.4.1 The role of JA in response to wounding 17
1.2.4.2 The role of JA in other stress responses 18
1.2.4.3 The roles of JA in plant growth and development 18
1.3 The TIFY protein family in plants 21
1.3.1 Members of the TIFY protein family 21
1.3.2 The biological functions of TIFY proteins 22
1.3.2.1 ZIM and ZIMLs 22
1.3.2.2 JAZs 23
1.3.2.3 PPDs 23
1.3.2.4 TIFY8 24
1.4 Aim of my study 24

2. Materials 25

2.1 Plant materials 25
2.2 Bacterial strains 25
2.3 Chemicals and commercial kits 25
2.3.1 Plant growth medium 25
2.3.2 Antibiotics 25
2.3.3 Seed sterilization 26
2.3.4 Chemical treatment 26
2.3.5 Cloning 26
2.3.6 Tissue staining 26
2.3.7 Fixation 26
2.3.8 Agarose embedding 27
2.3.9 Probe synthesis for *in situ* hybridization 27

2.3.10 *In situ* hybridization 27
2.3.11 Agrobacteria infiltration 27
2.3.12 RNA extraction 28
2.3.13 cDNA synthesis 28
2.3.14 qPCR 28
2.3.15 Yeast-two hybrid 28
2.3.16 eChIP 28
2.4 Mediums and buffers 28
2.4.1 Plant growth medium 28
2.4.2 Yeast growth medium 29
2.4.3 DNA extraction 29
2.4.4 Agrobacteria infiltration 29
2.4.5 *In situ* hybridization 29
2.4.6 eChIP-qPCR 30
2.5 Instruments 31
2.5.1 Microscopes 31
2.5.2 Sectioning and embedding 31
2.5.3 PCR and qPCR 31
2.5.4 Plant growth and microbial cultivation 32
2.5.5 Others 32
2.5.6 Software 32

3. Methods 33

3.1 Plant growth 33
3.2 Cloning 33
3.3 CRISPR/Cas9 knockout system 34
3.4 Wounding and chemical treatment 34
3.5 PFA fixation 35
3.6 Microscopy 35
3.7 Image analysis 36
3.8 *In situ* hybridization 36
3.9 RNA extraction and qRT-PCR 37
3.10 Vibratome sectioning 37
3.11 Agrobacteria infiltration in *Nicotiana benthamiana* 37
3.12 AP-FRET experiment 38
3.13 Yeast-two-hybrid 38
3.14 eChIP-qPCR 39
3.15 Statistical analysis 39

4. Results 40

4.1 Stem cell maintenance in response to systemic wounding 40
4.1.1 Wounding treatment modulates inflorescence stem growth and SAM morphology 40
4.1.2 Exogenous JA treatment inhibits inflorescence stem growth and SAM activity 43
4.1.3 The JA pathway is required for wounding-induced stem growth inhibition 45
4.1.4 Characterization of the JA signaling components in the SAM 47
4.1.5 WUS regulates JA-mediated wounding response in the SAM 49
4.1.6 WUS interacts with JAZ3 52

4.1.7 *JAZ3* is expressed in the SAM 55
4.1.8 WUS promotes *JAZ3* expression 55
4.1.9 The function of JAZ3 in stem cell maintenance 57
4.1.10 JAZ3 is a potential regulator of flowering 58
4.1.11 JAZ3 regulates the stem growth in response to systemic wounding 60
4.2 The function of TIFY8 in stem cell maintenance 63
4.2.1 *TIFY8* is expressed in the SAM 63
4.2.2 TIFY8 interacts with WUS 64
4.2.3 The function of WUS in the transcriptional and translational regulation of TIFY8 66
4.2.4 The function of TIFY8 in stem cell maintenance in the SAM 66
4.2.5 TIFY8 is a potential regulator of root stem cell maintenance 69

5. Discussion 72

5.1 The inflorescence stem growth is reshaped by systemic wounding and exogenous JA 73
5.2 The cellular basis of the stem growth inhibition 74
5.3 Stem cell maintenance in response to systemic wounding and exogenous JA 75
5.4 The systemic wounding response is mediated by the JA pathway 76
5.5 The role of WUS in the regulation of JA signaling 78
5.6 The role of JAZ3 in response to JA signaling in the SAM 79
5.7 The biological significance of the interaction between JAZ3 and WUS 81
5.8 TIFY8 is a regulator of stem cell maintenance 82
5.9 Potential connection between TIFY8 and JAZ3 upon interacting with WUS 83
5.10 Conclusion 84

6. References 85

Publications 93

Acknowledgments 94

Appendix 95

Abbreviations

aa	Amino acid
Ac	Acetic acid
AOS	Allene oxide synthase
AP-FRET	Acceptor Photobleaching-Förster Resonance Energy Transfer
bp	Base pair
CDS	Coding sequence
ChIP-seq	Chromatin Immunoprecipitation Sequencing
CK	Cytokinin
CLV3	CLAVATA3
COI1	CORONATINE INSENSITIVE1
CRISPR	Clustered regularly interspaced short palindromic repeats
CZ	Central zone
DAPI	4′,6-diamidino-2-phenylindole
DEX	Dexamethasone
DNA	Deoxyribonucleic acid
eChIP	Enhanced chromatin immunoprecipitation
EDTA	Ethylenediaminetetraacetic acid
F	Phenylalanine
G	Glycine
GG	GreenGate
GR	Glucocorticoid receptor
h	Hour
I	Isoleucine
JA	Jasmonates
JAR1	JASMONATE RESISTANT 1
JAZ	JASMONATE-ZIM DOMAIN
K	Lysine
L	Leucine
LOX	13-Lipoxygenase
M	Molar
min	Minute
MS	Murashige and Skoog salts

NINJA	NOVEL INTERACTOR OF JAZ
NLS	Nuclear localization sequence
OC	Organizing center
P	Proline
PZ	Peripheral zone
QC	Quiescent center
qPCR	Quantitative polymerase chain reaction
qRT-PCR	Quantitative reverse transcription polymerase chain reaction
R	Arginine
RAM	Root apical meristem
RNA	Ribonucleic acid
RNA-seq	Next generation RNA sequencing
rpm	Revolutions per minute
RZ	Rib zone
S	Serine
s	Second
SAM	Shoot apical meristem
sgRNA	small guide RNA
T	Threonine
T-DNA	Transfer DNA
TPL	TOPLESS
TR7	Triple reporter
VSP2	VEGETATIVE STORAGE PROTEIN 2
WOX5	WUSCHEL RELATED HOMEOBOX 5
WT	Wild type
WUS	WUSCHEL
Y	Tyrosine
Y2H	Yeast-two-hybrid
ZIM	ZINC-FINGER EXPRESSED IN INFLORESCENCE MERISTEM

Zusammenfassung

Mit dem Ziel, dort zu blühen, wo sie gepflanzt wurden, sind Pflanzen in der Lage, ihr Wachstum und ihre Entwicklung als Reaktion auf Umweltsignale zu koordinieren und umzuprogrammieren. Diese bemerkenswerte Plastizität verdanken sie Pools von pluripotenten Stammzellen an ihren Wachstumspunkten. Im Sprossapikalmeristem (SAM) der Acker-Schmalwand (*Arabidopsis thaliana*) wird die Erhaltung der Stammzellen durch ein regulatorisches Netzwerk gesteuert, in dem die WUSCHEL (WUS)-CLAVATA3 (CLV3) Rückkopplungsschleife eine zentrale Rolle spielt. Obwohl die Regulierung der Stammzellenerhaltung durch interne entwicklungsbedingte Signale im SAM bis ins Detail geklärt ist, bleibt weitgehend unklar, wie das SAM externe Stresssignale wahrnimmt und darauf reagiert. In der Natur leiden Pflanzen häufig unter Verletzungsstress, der hauptsächlich durch Pflanzenfresser und abiotische Faktoren verursacht wird. Jasmonat (JA) ist das wichtigste Phytohormon, das die frühe Reaktion der Pflanzen auf Verwundungen reguliert. Es ist jedoch unklar, wie JA die Aktivität des SAM beeinflusst.

In meiner Dissertation habe ich die Aktivität des SAM als Reaktion auf systemische Verwundung untersucht. Ich fand heraus, dass eine langfristige Verwundung von Blättern das Wachstum der Blütenstängel hemmt und die Zellzahl des SAM verringert, und dass dieser Prozess durch den JA-Signalweg vermittelt wird. Auf molekularer Ebene löst exogenes JA die Vergrößerung der WUS-Proteindomäne aus. Im Gegenzug unterdrückt WUS frühe JA-Reaktionen im SAM und schützt so das Stammzellsystem vor den hemmenden Auswirkungen von Verwundungen. Folgerichtig fördert WUS direkt die Expression des JA-Signalrepressors *JASMONATE-ZIM DOMAIN 3* (*JAZ3*) und interagiert direkt mit dem JAZ3-Protein. Ähnlich wie WUS hemmt JAZ3 auch die Wirkung von Verwundungen. Im zweiten Teil meiner Studie habe ich die Funktion von TIFY8, einem mit JAZ3 verwandten Protein, bei der Erhaltung von Stammzellen untersucht. TIFY8 interagiert auch mit WUS, aber die Expression von *TIFY8* wird durch WUS nicht beeinflusst. Genetische Beweise zeigen, dass TIFY8 als positiver Regulator der Zellproliferation im SAM wirkt. Andererseits interagiert TIFY8 mit der WUSCHEL-RELATED HOMEOBOX 5 (WOX5) und reguliert möglicherweise die Erhaltung der Stammzellen im Wurzelapikalmeristem in einer negativen Art und Weise. Insgesamt deckt meine Studie einen neuartigen Mechanismus der durch JA vermittelten

Wahrnehmung und Weiterleitung systemischer Verletzungssignale im SAM auf. Darüber hinaus charakterisiert sie die unterschiedlichen Rollen von zwei TIFY-Proteinen, nämlich JAZ3 und TIFY8, bei der Regulierung der Stammzellenerhaltung.

Abstract

Aiming to bloom where they are planted, plants are capable of coordinating and reprograming their growth and development in response to environmental signals. This remarkable plasticity owes to pools of pluripotent stem cells at their growth points. In the shoot apical meristem (SAM) of *Arabidopsis thaliana*, the maintenance of stem cells is orchestrated by a regulatory network, in which WUSCHEL (WUS)-CLAVATA3 (CLV3) feedback loop plays a pivotal role. Although the regulation of stem cell maintenance by internal developmental cues in the SAM has been elucidated in some detail, how the SAM senses and responds to external stress signals remains mostly elusive. In nature, plants frequently suffer from wounding stress, which is mainly caused by herbivores and abiotic factors. Jasmonate (JA) is the key phytohormone that regulates plant early response to wounding. However, how JA impinges on the activity of the SAM is unclear.

In my thesis work, I investigated the activity of the SAM in response to systemic wounding in *Arabidopsis thaliana*. I found that long-term wounding treatment in leaves inhibits inflorescence stem growth and reduces cell number of the SAM and that this process is mediated by the JA pathway. At a molecular level, exogenous JA triggers the expansion of the WUS protein domain. In turn, WUS represses early JA responses in the SAM and thus protects the stem cell system from the inhibitory effects of wounding. Consistently, WUS directly promotes the expression of the JA signaling repressor *JASMONATE-ZIM DOMAIN 3* (*JAZ3*) and directly interacts with the JAZ3 protein. Similar to WUS, JAZ3 also inhibits the effect of wounding. In the second part of my study, I characterized the function of TIFY8, a protein related to JAZ3 in stem cell maintenance. TIFY8 also interacts with WUS, but the expression of *TIFY8* is not affected by WUS. Genetic evidence reveals that TIFY8 acts as a positive regulator of cell proliferation in the SAM. On the other hand, TIFY8 interacts with WUSCHEL-RELATED HOMEOBOX 5 (WOX5) and potentially negatively regulates stem cell maintenance in the root apical meristem. Overall, my study uncovers a novel mechanism of JA-mediated systemic wounding signal perception and transduction in the SAM. Additionally, it characterizes the distinct roles of two TIFY proteins, namely JAZ3 and TIFY8, in the regulation of stem cell maintenance.

1. Introduction

1.1 Stem cell control in the shoot apical meristem

1.1.1 Plant stem cells

As plants are immobile throughout their life cycle, their growth and development largely depend on where they are planted. To thrive in the changing environment, it is extremely important for plants to sense environmental cues and integrate them into their internal developmental regulations. As a result, the tailored morphological traits of plants by their surroundings confer significant advantages for plant adaption to their living environment.

This remarkable phenotypic plasticity of plants mainly relies on their ability to continuously form new organs after embryogenesis. It is imperative under stress-related conditions, in which plant organs or tissues are damaged. To maintain this plasticity, plant stem cells are essential. They are pluripotent and act as central hubs of cell division and differentiation, hence providing all cells to form the entire plant body.

Plant stem cells reside in stem cell niches known as meristems. Meristems can be classified into two types in plants: primary meristems and secondary meristems (Weigel & Jürgens, 2002). Primary meristems, including the shoot apical meristem (SAM) and the root apical meristem (RAM), are initiated during embryogenesis and give rise to most parts of the plant. Secondary meristems originate from primary meristems (Schweingruber & Börner, 2018). They contribute to plant secondary growth including stem thickening growth and lateral organ formation (Agusti & Greb, 2013). Representative examples of secondary meristems include the cambium, responsible for the radial stem growth, and the axillary meristem, responsible for branching in the aerial part of the plant.

1.1.2 The shoot apical meristem

The shoot apical meristem is a dome-like structure embedded in the inner part of the shoot apex. Despite the small and densely packed area, different types of cells within the SAM are precisely arranged and organized at a cellular level. The architecture of the SAM can be characterized by clonally distinct cell layers and different functional zones. In *Arabidopsis*, the top three clonal layers contain stem cells in the central region,

where cells are slowly dividing and generate distinct cell lineages (Figure 1.1 A). Specifically, L1 cells form the epidermis of organs, while L2 and L3 cells give rise to the large parts of the above-ground tissues and the vasculature of the stem (Carles & Fletcher, 2003). The organization of cell division in the first three layers is dynamically modified in terms of environmental conditions. In addition, based on the cellular and molecular identity of the cells, the SAM can be divided into different zones (Greb & Lohmann, 2016) (Figure 1.1 B). The central zone (CZ), located in the center region of the first top three cell layers, is marked by the expression of the gene encoding a small signaling peptide CLAVATA3 (CLV3). The CZ provides a reservoir of stem cells. Surrounding the CZ is the peripheral zone (PZ), where cells are dividing faster and finally contribute to the foundation of lateral organs. The organizing center (OC), located beneath the CZ, is characterized by the expression of *WUSCHEL* (*WUS*), a gene encoding a homeodomain transcription factor. The OC acts as an inductive niche for stem cells and monitors the stem cell population. The basal part of the SAM is the rib zone (RZ). During primordia and stem initiation, cells in the RZ contribute to the founder cells of vasculature tissues and other tissues in newly developing organs (Serrano-Mislata & Sablowski, 2018).

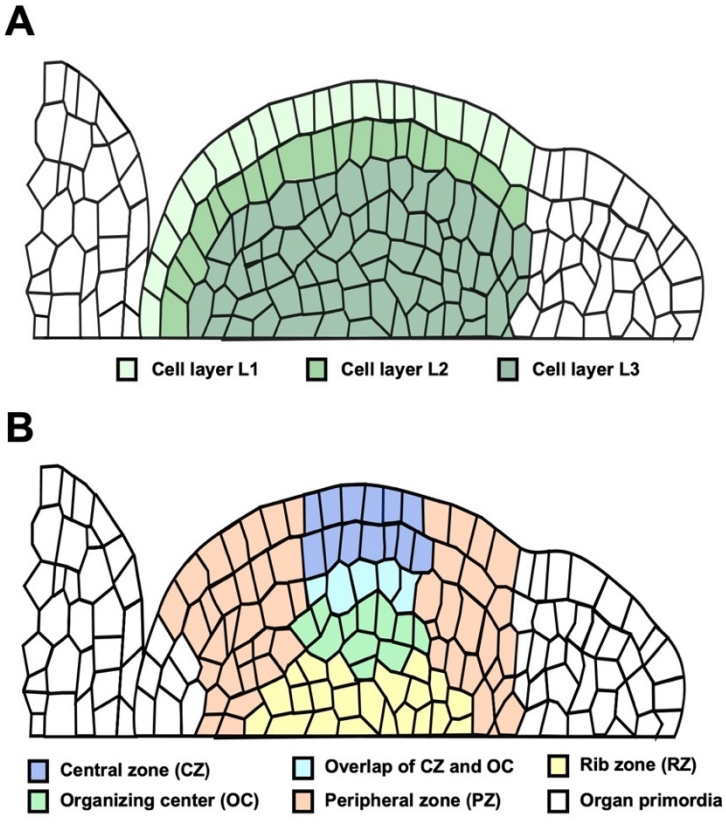


Figure 1.1: Schematic representation of the shoot apical meristem (SAM). **A**, schematic representation of the SAM characterized by layers. Labels of layers are adapted from Fuchs & Lohmann (2020). **B**, schematic representation of the SAM characterized by zones. Labels of functional domains are adapted from Thomas & Lohmann (2016).

1.1.3 Stem cell maintenance in the SAM

The dynamic balance between cell division and differentiation is properly maintained throughout the plant life cycle. In *Arabidopsis*, numerous regulatory circuits from different zones and layers contribute to the precise regulation of stem cell homeostasis in the SAM. The classic and fundamental regulatory cassette is the WUS-CLV3 negative feedback loop, which has been comprehensively studied (Figure 1.2). *WUS* is expressed in the cells of the OC (Mayer et al., 1998), while WUS protein can migrate to the CZ, where it activates *CLV3* expression through directly interacting with the regulatory elements in the genomic region of *CLV3* gene (Schoof et al., 2000; Yadav et al., 2011). In return, the secreted CLV3 peptide, along with the signaling cascades it activates, leads to the reduction of WUS activity (Brand et al., 2000) (Figure 1.2). Therefore, the stem cell population is dynamically maintained.

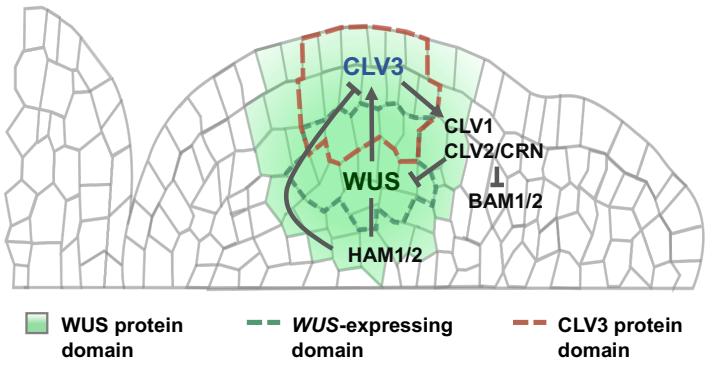


Figure 1.2: The core regulatory network of stem cell maintenance in the SAM.

The repression of WUS activity is under sophisticated regulation and is mainly achieved by the interaction between ligands and receptors (Figure 1.2). CLV3 is a signaling peptide belonging to the CLAVATA3/EMBRYO SURROUNDING REGION (CLE) peptide family (Wang & Fiers, 2010). The mutation of *CLV3* in *Arabidopsis* leads to enlarged inflorescence meristems due to the increased stem cell population (Clark et al., 1995). Additionally, multiple receptor-like kinases (RLKs),

receptor-like proteins (RLPs), and receptor-like cytoplasmic kinases (RLCKs) work coordinately in the CLV3-mediated pathway to regulate stem cell maintenance in the SAM (Somssich et al., 2016). The key RLK in the CZ is CLAVATA1 (CLV1). *CLV1* is specifically expressed in the CZ. The *clv1* mutant displays an enlarged SAM phenotype in *Arabidopsis* (Leyser & Furner, 1992). CLV1 itself, or together with the complex CLV2-CORYNE (CRN), interacts with CLV3 at the plasma membrane and transmits the signals into the cytosol via autophosphorylation, leading to the repression of WUS activity in the end (Figure 1.2) (Muller et al., 2008; Stone et al., 1998). Other identified RLKs involved in the WUS-CLV3 feedback loop include ERECTA (ER) (Chen et al., 2013; Mandel et al., 2014) as well as BARELY ANY MERISTEM 1 (BAM1) and BAM2, which function in the PZ (DeYoung et al., 2006; John et al., 2023). In addition, RECEPTOR-LIKE PROTEIN KINASE2 (RPK2) also regulates the CLV3 signal transduction. However, RPK2 acts as homo-oligomers without associating with the CLV1 and CLV2-CRN complex (Kinoshita et al., 2010). Although the peptides and receptors involved in the regulation of the SAM are well understood in some detail, the downstream signaling mechanism underlying how WUS activity is restricted remains ambiguous. Current studies reveal that phosphorylation, mitogen-activated protein kinase (MAPK) pathways, and the singling mediated by G-proteins are all involved in the downstream regulation of the CLV receptors (Betsuyaku et al., 2011; Ishida et al., 2014; Meng et al., 2012; Song et al., 2006).

1.1.4 The roles of WUS in SAM signaling regulation

As the master regulator of stem cell maintenance in the SAM, WUS acts as both a transcriptional activator and a repressor in a non-cell-autonomous manner (Daum et al., 2014; Haecker et al., 2004; Yadav et al., 2011).

Genetic evidence reveals that WUS is crucial for various developmental regulations in plants, as mutating WUS in *Arabidopsis* leads to detrimental effects on almost every developmental stage of the aerial parts of plants. During embryogenesis, *wus* mutants fail to form organized shoot meristems. In postembryonic development, abnormal vegetative and inflorescence shoot meristems in *wus* mutants are repetitively and ectopically initiated around the shoot apex and terminated prematurely (Laux et al., 1996). As a result, the overall shoot development is delayed and disrupted. In addition, *wus* mutants exhibit other developmental defects, including disordered phyllotaxis, abnormal stem growth, and improper branching. Furthermore, *wus* mutants display

premature termination in floral meristems and are defective in reproductive organ formation, hence they are infertile (Laux et al., 1996).

At the molecular level, WUS is involved in various regulatory modules. The distinct roles of WUS in different developmental regulations are largely dependent on the types of signaling pathways it associates with. Apart from the WUS-CLV3 regulatory loop in the SAM, WUS coordinates with other signaling pathways that are essential for the SAM in response to both internal developmental signals and external environmental signals.

1.1.4.1 The role of WUS in hormone signaling

WUS regulates cell proliferation and inhibits cell differentiation mainly through cytokinin and auxin signaling pathways in the SAM. These regulatory processes occur in a spatiotemporal manner.

cytokinin signaling is the central regulatory pathway of cell proliferation (Argueso et al., 2010). Components in the cytokinin signaling pathway are directly associated with WUS. Studies show that WUS activates cytokinin signaling while cytokinin induces *WUS* expression in return (Buechel et al., 2010; Gordon et al., 2009; Leibfried et al., 2005; Nimchuk et al., 2015). WUS directly represses the transcription of the type-A *ARABIDOPSIS RESPONSE REGULATOR (ARR)* genes, including *ARR7* and *ARR15*, which negatively regulate cytokinin signaling (Leibfried et al., 2005). In addition, cytokinin treatment in the SAM induces *WUS* expression in the OC with or without the CLV-mediated pathway (Gordon et al., 2009). Interestingly, a computational study suggests that cytokinin is crucial for positioning the OC domain in the SAM, as the WUS-expressing domain corresponds to the expression pattern of *ARABIDOPSIS HISTIDINE KINASEs* (*AHKs*), which encode cytokinin receptors (Chickarmane et al., 2012). In line with this result, recent studies further indicate that the positive cytokinin signaling regulators type-B ARRs directly activate *WUS* expression in both the SAM and axillary meristem (Meng et al., 2017; Xin et al., 2017).

Known as the key regulator for organogenesis, auxin signaling plays a pivotal role in primordia initiation in the SAM (Reinhardt et al., 2000). Of note, according to the distribution patterns of auxin biosensors, auxin response is lower in the CZ compared to that in the PZ, indicating that auxin signaling is repressed in stem cells (Ma et al., 2019). Further results suggest that the auxin minimum in the CZ is monitored by WUS. WUS represses the expression of auxin signaling activator *MONOPTEROS/AUXIN*

RESPONSE FACTOR 5(*MP/ARF5*) in the CZ. On the other hand, WUS targets the genomic regions of genes involved in auxin signaling and regulates the histone deacetylation of the targeted sites (Ma et al., 2019). Consistent with the lower auxin distribution observed in the CZ, Galvan-Ampudia et al. (2020) show that the auxin maxima only emerges in the PZ and is correlated with the position of new primordia formation. All these findings suggest that WUS potentially regulates the input and output of auxin signaling in the CZ to prevent cell differentiation, hence it maintains stem cell homeostasis in the SAM.

Auxin and cytokinin signaling pathways also functionally connect with each other, providing another regulatory layer in stem cell maintenance. MP/ARF5 inhibits cytokinin signaling in the SAM via directly repressing *ARR15* and *ARR7* expression (Zhao et al., 2010). In addition, MP/ARF5 also downregulates the expression of *DORNROSCHEN/ ENHANCER OF SHOOT REGENERATION 1* (*DRN/ ESR1*), which promotes *CLV3* expression probably in an indirect manner (Luo et al., 2018). This crosstalk ultimately finetunes *WUS* expression, which coordinates the rhythmic pace of cell proliferation and differentiation, together with the WUS-CLV3 regulatory system.

1.1.4.2 The role of WUS in response to environmental signals

The clear roles of WUS in sensing and responding to environmental stimuli are emerging. Light is one of the most important environmental cues for plant growth. It has been demonstrated that light regulates the process of organogenesis in the SAM through regulating auxin and cytokinin signaling pathways (Yoshida et al., 2011). Notably, Pfeiffer et al. (2016) found that light and sugar modulate *WUS* expression to terminate the stem cell dormancy during germination, which is mediated via the TARGET OF RAPAMYCIN (TOR) kinase signaling pathway. In the shoot apex, the regulation of light signal transduction is likely through the cytokinin pathway, in which cytokinin dehydrogenases CKX5 and CKX6 are involved (Pfeiffer et al., 2016). In addition, the SAM can also perceive the mineral nutrient signals through cytokinin signaling. The increasing nitrogen level in the soil induces cytokinin biosynthesis and precursor transportation, which subsequently triggers cytokinin signaling and *WUS* expression in the SAM (Landrein et al., 2018). Apart from the mineral signals, stem cell activity in the SAM is sensitive to the oxygen level. In general, the stem cell niche is under hypoxic conditions (Weits et al., 2019). Oxygen acts as a diffused signal regulating the stem cell activity. At the molecular level, increasing the oxygen level

promotes the degradation of LITTLE ZIPPER2 (ZPR2) via the N-degron pathway. Subsequently, the downstream targets of ZPR2, namely Class III HOMEODOMAIN LEUCINE ZIPPER (HD-ZIPIII) transcription factors and HECATE (HEC), modulate the *WUS* expression in response to the increasing oxygen level in the SAM (Weits et al., 2019).

Stress-related signals can also be perceived by the WUS-CLV3 regulatory system. Reactive oxygen species (ROS) serve as important environmental signals that orchestrate the regulation of plant development under diverse stress conditions. In the SAM, different ROS species have distinct roles in stem cell maintenance. $O_2^{\cdot -}$ in the CZ of the SAM is responsible for maintaining stable *WUS* and *CLV3* expression, while H_2O_2 represses *WUS* expression and promotes cell differentiation in the PZ of the SAM (Zeng et al., 2017). Moreover, it has been reported that WUS responds to and represses cucumber mosaic virus (CMV) infection in the SAM by inhibiting the expression of genes encoding plant S-adenosyl-L-methionine–dependent methyltransferases. As a consequence, the global protein synthesis in the SAM is inhibited, thereby hampering the virus replication and preventing virus infection in the SAM (Wu et al., 2020). Furthermore, Zeng et al. (2021) report that WUS is activated at both transcriptional and translational levels by salt and osmotic stress. This process is mediated by the ethylene signaling pathway. The transcription factor ETHYLENE INSENSITIVE 3 (EIN3), a positive regulator of ethylene responses, directly activates the expression of *AGAMOUS-LIKE 22* (*AGL22*) in the stem cell niche and further activates the WUS-CLV regulatory cascade. Therefore, the activated stem cell activity facilitates the stem cell maintenance against the native stress signals.

1.1.5 Functional domains within the WUS protein

The essential role of WUS in stem cell maintenance highly depends on its protein function. The function of the WUS protein is versatile: it binds DNA, forms homo- and heterodimer, and interacts with other transcriptional regulators (Busch et al., 2010; Daum et al., 2014; Perales et al., 2016; Rodriguez et al., 2016; Sloan et al., 2020; Yadav et al., 2011).

The multifunctionality of WUS can be revealed from its protein structure. There are six characterized protein domains within the WUS protein (Figure 1.3). Starting from the N-terminus of the WUS protein sequence, the first protein domain is the homeodomain, which is responsible for DNA binding and conserved across the WUS homeobox-

containing (WOX) protein family (Haecker et al., 2004). The second protein domain is the dimerization domain, functioning in protein interactions and WUS dimerization. Unlike the homeodomain, the dimerization domain is not a canonical protein domain of the WOX protein family. In the middle of the WUS protein sequence, a specific region (203aa-235aa) is required for WUS interaction with HAIRY MERISTEM (HAM) proteins, and hence this region is referred to as HAM binding domain (HBD) (Zhou et al., 2015). HAMs are crucial for stem cell maintenance, which can interact with WOX proteins in both the SAM and the RAM. Associating with WUS, HAMs restrict the expression domain of *CLV3* within the top three layers in the SAM (Figure 1.2) (Zhou et al., 2018).

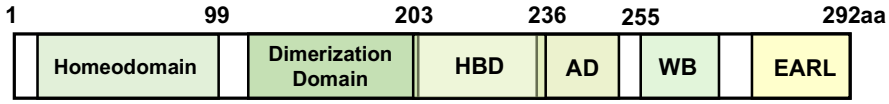


Figure 1.3: Schematic representation of functional domains within WUS. Numbers indicate the position of amino acids from the N-terminus of the protein. HBD: HAM binding domain; AD: acidic domain; WB: WUS-box; EARL: EAR-like domain.

At the C-terminus of the WUS protein resides the Ethylene-responsive element binding factor-associated Amphiphilic Repression (EAR)-like domain (EARL), which functions in transcriptional repression (Figure 1.3) (Ohta et al., 2001). Next to the EARL domain is the WUS-box domain, which is highly conserved in the WOX protein family (Haecker et al., 2004). The WUS-box is indispensable for the nuclear retention of WUS as well as the interaction between WUS and TOPLESS (TPL)/TOPLESS-RELATED (TPR) co-repressors for transcriptional repression (Rodriguez et al., 2016). The WUS function in stem cell maintenance is partially determined by the WUS-box (Dolzblasz et al., 2016). Another recognized domain near the C-terminus of WUS is the acidic domain (Figure 1.3), which is essential for its transcriptional activation activity and its regulatory role in female fertility (Dolzblasz et al., 2016).

1.2 The plant hormone: Jasmonate

Jasmonates (JA) and its derivatives are lipid-derived compounds (Wasternack, 2015). The initially identified bioactive form of JA is methyl jasmonate (MeJA), which is isolated from the flower of *Jasminum grandiflorum* (Demole et al., 1962). Since its discovery, the biosynthesis, distributions, signaling pathways, and biological functions of JA in plants have been substantially studied and elucidated. Nowadays, JA is considered as an important signaling phytohormone that not only plays an indispensable role in response to environmental stimuli but also modulates plant growth and development through the crosstalk with other pathways.

1.2.1 JA biosynthesis

The JA biosynthesis pathway is conserved across most land plants (Wasternack & Hause, 2013). It is initiated in plastids where α-linolenic acid (α-LeA) is released from galactolipids mediated by Phospholipase A1(PLA1) (Ishiguro et al., 2001) (Figure 1.4). In plastids, α-LeA is processed into *cis*-(+)-12-oxophytodienoic acid (OPDA), catalyzed by 13-Lipoxygenase (13-LOX), allene oxide synthase (AOS), and allene oxide cyclase (AOC) in sequence (Chauvin et al., 2013; Park et al., 2002). Subsequently, OPDA undergoes two main reaction steps catalyzed by OPDA reductase (OPR3) and fatty acid ß-oxidation machinery, and finally becomes (+)-*7-iso*-JA (Stintzi & Browse, 2000). However, to be converted into the bioactive form of JA, namely (+)-*7-iso*-JA-Ile (JA-lle), (+)-*7-iso*-JA needs to be catalyzed by JA-amino acid synthetase (JAR1) (Staswick & Tiryaki, 2004). JA-lle is the molecule directly involved in JA perception and signaling pathways. Apart from JA biosynthesis, JA metabolism also significantly influences the dynamic JA concentration in plants. Twelve metabolic pathways related to JA have been currently identified (Wasternack & Hause, 2013), which contributes to another regulatory layer in maintaining JA metabolic homeostasis.

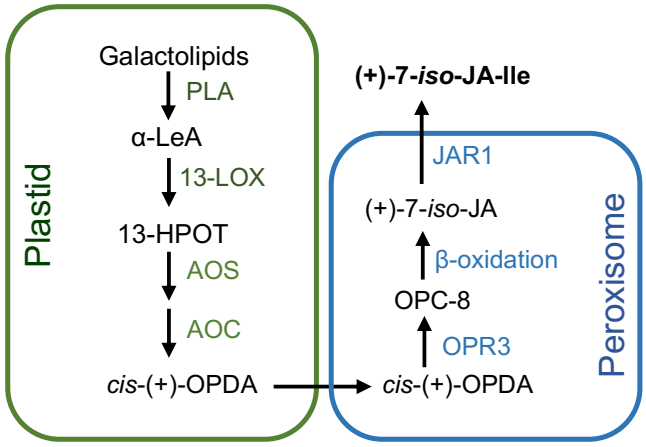


Figure 1.4: JA biosynthesis pathway from galactolipids. Key enzymes of each step are labeled beside the arrows. α-LeA: α-linolenic acid; 13-HPOT: (13S)-hydroperoxyoctadecatrienoic acid; *cis*-(+)-OPDA: *cis*-(+)-12-oxophytodienoic acid; OPC-8: 3-oxo-2-(2-pentenyl)-cyclopentane-1-octanoic acid. The figure is adapted from Wasternack & Song (2017).

1.2.2 JA transportation

It has been reported that JA and MeJA are mobile and can activate the expression of JA-responsive genes in the distal part of wounded tissues upon wounding treatment (Nguyen et al., 2017). It is tempting to ask whether JA mobility is directional and regulated by specific transporters like other plant hormones. Recent studies suggest that the ABC transporter Arabidopsis Jasmonate transporter 1 (JAT1/AtABCG16) is identified as a JA transporter within cells, which mediates JA export from cells and JA-Ile import into nuclei (Li et al., 2017). In the case of long-distance transport, JAT3 /ABCG6 and JAT4/ABCG20 function as the main transporters responsible for delivering JA through the phloem. JAT3 and JAT4 are crucial for facilitating the movement of JA from the wounded sites in leaves to the distal unwounded regions within the leaves (Li et al., 2020).

1.2.3 JA signaling

JA perception in plant cells is mainly through a co-receptor complex comprising the F-box protein CORONATINE INSENSITIVE1 (COI1) and JASMONATE-ZIM DOMAIN (JAZ). COI1 is part of the SKP1–CUL1–F-box protein (SCF) E3 ubiquitin ligase complex (SCF^{COI1}) and can interact with JAZs, which is mediated by JA-lles in a dose-dependent manner (Melotto et al., 2008; Xie et al., 1998; Yan et al., 2009). The

COI protein as the JA co-receptor is conserved among land plants but is not in algae, suggesting that JA signaling machinery may have occurred after plants resided in terrestrial environments (Han, 2017).

JAZ proteins are nuclear-localized repressors. When the level of JA is low in the cell, JAZs interact with MYC transcription factors (MYCs) and recruit the transcriptional repression complex, thereby repressing the expression of JA-responsive genes (Figure 1.5). However, upon the JA outburst in the cell, the COI1–JAZ co-receptor complex perceives the bioactive JA-lle, which leads to the degradation of JAZ proteins (Chini et al., 2007; Thines et al., 2007). Free from the repression by JAZs, MYCs activate JA-responsive gene expression (Wasternack & Song, 2017) (Figure 1.5).

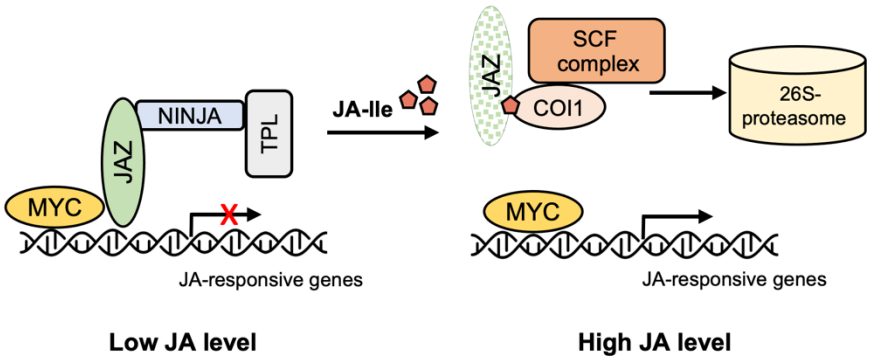


Figure 1.5: Simplified schematic representation of JA perception and signaling. The figure is adapted from Wasternack & Song (2017). The symbol of the DNA helix is from https://www.flaticon.com.

MYC proteins are responsible for the activation of JA-responsive gene expression. In *Arabidopsis*, there are four MYC proteins, namely MYC2, MYC3, MYC4, and MYC5. They all belong to the basic helix-loop-helix (bHLH) transcription factor family (Kazan & Manners, 2013). MYC proteins can form homo- or heterodimers and specifically bind to the G-box motif in the plant genome (Wang et al., 2017). Interestingly, MYC proteins orchestrate different layers of JA-induced transcriptional response. For example, MYC2 upregulates the expression of genes involved in the JA-mediated response to wounding while downregulating the expression of genes involved in the defense responses against necrotrophic pathogens (Lorenzo et al., 2004).

The conventional JA signaling machinery also contains other co-regulators essential for robust and efficient signaling transduction. NOVEL INTERACTOR OF JAZ (NINJA) interacts with both JAZs and TPL, serving as an adaptor that links JAZ and TPL

repressor complex (Pauwels et al., 2010) (Figure 1.5). MEDIATOR 25 (MED25), a subunit of the mediator complex, interacts with MYCs and initiates transcription processes (Cevik et al., 2012; Chen et al., 2012).

JA signaling is modulated by both positive and negative feedback loops. MYC2 and MYC3 can directly bind to the promoter regions of genes encoding enzymes involved in JA biosynthesis, such as *OPR3, AOS, LOC3, and AOC*, and promote their expression (Zander et al., 2020). This positive feedback circuit not only further amplifies the level of local JA response but also activates systemic JA signaling transduction. On the other hand, the expression of *JAZ*s is also directly activated by MYC proteins. Newly synthesized JAZ proteins interact with MYCs, thereby repressing JA-responsive gene expression (Howe et al., 2018). This negative feedback loop efficiently attenuates JA signaling and reduces the detrimental effects on plant fitness. Altogether, JA signaling is dynamically and precisely controlled in both temporal and spatial manners.

1.2.4 The biological roles of JA in plants

1.2.4.1 The role of JA in response to wounding

The perception of wounding is elicited by a range of molecules produced by insects or injured plants. These molecules are known as herbivore-associated molecular patterns (HAMPs) or damage-associated molecular patterns (DAMPs) (Campos et al., 2014; Wu & Baldwin, 2010). Following the recognition of HAMPs and DAMPs by plant cells, a series of downstream signals, including electrical signals, calcium waves, and reactive oxygen species, are stimulated and propagated as the first wave of wounding signals. After receiving the first wave of signals, JA signals are activated both locally and systemically as the main force of the second wave of wounding signals (Wang et al., 2019).

JA signaling plays a pivotal role in response to wounding stress. Evidence shows that *Arabidopsis* mutants that are deficient in JA biosynthesis and perception are significantly more susceptible to insect feeding than the wild type (Guo et al., 2018; Howe & Jander, 2008; Wang et al., 2019). The mechanical wounding in plant tissue caused by any factor is the typical trigger of the JA outburst in plants. Despite the very low basal concentration of JA in plant tissues under normal conditions, the level of JA is rapidly elevated both locally and systemically within one minute once the wounding is perceived by the plant (Glauser et al., 2009).

Upon insect feeding, the rapidly activated JA signaling renders substantial transcriptional reprogramming of genes related to anti-insect defense. This process is mainly achieved through the SCF^{COI1}-JAZ-MYC machinery. MYCs promote the expression of genes involved in the biosynthesis of proteinase inhibitors (PI), glucosinolates (GSs), and exopeptidases like leucine aminopeptidase (LAP), which are toxic to insect digestion systems (Boter et al., 2004; Schweizer et al., 2013). In addition, JAZs can interact with the WD-repeat/bHLH/MYB transcription factor complex, which regulates anthocyanin production and trichome formation upon wounding (Qi et al., 2011).

1.2.4.2 The role of JA in other stress responses

In response to biotic stress, JA regulates defense mechanisms through the crosstalk with other plant hormones. Together with ethylene signaling, the activation of JA signaling triggers the expression of defense genes including *PLANT DEFENSIN1.2* (PDF1.2), hence conferring plant resistance against necrotrophic pathogens (Zarei et al., 2011). In addition, JA and salicylic acid (SA) signaling share a specific group of downstream targets, and the two hormones antagonize each other in regulating gene expression against biotrophic pathogens (Wasternack & Hause, 2013).

JA signaling also contributes to the responses to abiotic stress including cold, heat, drought, salinity, heavy metals, and nutrient deficiency (Raza et al., 2021; Shikha et al., 2023). Exogenous JA application in plants, especially in roots, significantly alleviates the symptoms caused by abiotic stress on plant growth and development (Raza et al., 2021). The activation of JA signaling promotes plant resistance to abiotic stress mainly through three aspects: reshaping plant growth and development (Farhangi-Abriz & Ghassemi-Golezani, 2019; Ilyas et al., 2017), modulating the enzyme activities in a wide range of metabolism pathways (Huang et al., 2017), and regulating ion transports (Shikha et al., 2023). However, the molecular basis of how the JA signaling pathway contributes to stress responses remains elusive.

1.2.4.3 The roles of JA in plant growth and development

The JA pathway integrates the environmental cues into plant growth and developmental regulations. Here, the representative growth and developmental processes that JA regulates are illustrated.

Root development

Exogenous JA application inhibits primary root growth, which was used as a typical phenotypic criterion to screen JA signaling-related mutants in the early study of JA signaling pathway (Yan et al., 2009). At the cellular level, the inhibition of primary root growth by JA signaling is due to the repression of cell proliferation in the root meristem zone (MZ) and cell elongation in the elongation zone (EZ). Chen et al. (2011) found that exogenous JA repressed root stem cell activity, leading to abnormal cell division in the quiescent center (QC) and disordered columella stem cell differentiation. Further study indicates that MYC2 can directly target the promoter regions of *PLETHORA1* (*PLT1*) and *PLT2* and repress their expression. These two genes encode two AP2-domain transcription factors, which are the key regulators of root stem cell maintenance mediated by auxin signaling.

Apart from interacting with auxin signaling, JA signaling, together with ethylene signaling, inhibits primary root growth and regulates root hair formation. This process is achieved by the interaction between JAZ proteins and ETHYLENE INSENSITIVE 3(EIN3) and EIN3-LIKE1 (EIL1), which are essential transcription factors in ethylene signaling (Zhu et al., 2011). Despite its inhibitory role in primary root growth, JA promotes lateral root formation in *Arabidopsis*. One reported mechanism is through the activation of auxin biosynthesis, in which the JA signaling promotes the expression of *ETHYLENE RESPONSE FACTOR 109* (*ERF109*). As a consequence, ERF109 promotes the expression of *ANTHRANILATE SYNTHASE A1* (*ASA1*) and *YUCCA2* (*YUC2*), which encodes two crucial enzymes in auxin biosynthesis (Cai et al., 2014).

Stamen development

Mutants deficient in JA biosynthesis and signaling are male sterile in *Arabidopsis*, as these mutants display abnormal stamen development including shorter filaments and indehiscent anthers (Huang et al., 2017). Exogenous JA application can restore male fertility in the mutants of JA biosynthesis but not JA signaling. At the molecular level, two R2R3-MYB transcription factors, MYB21 and MYB24, are involved in the JA-mediated stamen development regulation. The double mutant *myb21 myb24* exhibits a completely male sterile phenotype. Moreover, JAZs interact with MYB21 and MYB24 and potentially repress their transcriptional activation function (Song et al., 2011). MYCs also interact with MYB21 and MYB24 and positively regulate stamen development (Qi et al., 2015).

Flowering

In plants, the transition from vegetative to reproductive growth is controlled by both endogenous developmental signals and environmental stimuli (Fornara et al., 2010). Activation of JA signaling represses the transition from vegetative to reproductive growth in *Arabidopsis*. Genetic and biochemical evidence shows that JAZ proteins interact with TARGET OF EAT1 (TOE1) and TOE2 to suppress their negative regulation of *FLOWERING LOCUS T* (*FT*) expression (Zhai et al., 2015). FT is a major component of florigen, which is required for the onset of flowering (Pin & Nilsson, 2012). When a high level of JA is accumulated in plants, degradation of JAZ1 releases the function of TOE1 and TOE2, thereby leading to the repression of *FT* to prevent flowering under stress conditions. In addition, MYC2/3/4 can inhibit *FT* expression by targeting the promoter region of *FT*, which provides another regulatory layer of JA-mediated inhibition of flowering in *Arabidopsis* (Wang et al., 2017).

Tissue regeneration

Increasing evidence indicates that JA plays an essential role in determining cell fate transition in various plant regeneration processes, such as tissue repair, callus formation, and *de novo* root or shoot regeneration (Zhang et al., 2023). One representative example is JA-mediated root tip repair upon wounding stress. Zhou et al. (2019) found that after laser ablation of the root tip, the wounding signals induced JA outbursts in the root. As a result, MYC2 activates the expression of *ERF115* and *ERF109.* ERF115 connects the SHORT ROOT (SHR)-SCARECROW (SCR)-RETINOBLASTOMA-RELATED (RBR) regulatory network and promotes cell division in the QC. On the other hand, ERF109 promotes *CYCLIN D6;1* (*CYCD6*) expression and regulates cell division. Taken together, the stem cell activity in the root is enhanced after tissue damage. Moreover, JA-induced *ERF109* expression regulates *de novo* root regeneration from detached leaves. In this process, ERF109 activates the auxin biosynthesis by promoting the expression of *ANTHRANILATE SYNTHASE α1* (*ASA1*), which is involved in the biosynthesis of auxin precursor (Zhang et al., 2019).

1.3 The TIFY protein family in plants

The TIFY protein family is a plant-specific protein family. It is named after the most conserved tify motif (TIF[F/Y]XG) in the ZIM domain possessed by all the members (Vanholme et al., 2007). The first identified TIFY protein is ZINC-FINGER PROTEIN EXPRESSED IN INFLORESCENCE MERISTEM (ZIM) in *Arabidopsis thaliana* (Shikata et al., 2004). Since the discovery of ZIM, an increasing number of proteins containing this conserved motif have been identified and classified into the TIFY protein family.

1.3.1 Members of the TIFY protein family

TIFY proteins can be further classified into two subgroups based on the presence of the C2C2-GATA zinc-finger domain (C2C2-GATA) (Figure 1.6). In *Arabidopsis*, the proteins of Class I are ZIM, ZML1 and ZML2. They contain the C2C2-GATA domain and the CCT domain (CONSTANS, CO-like, and TOC1), which is involved in protein interaction. Proteins in Class I possess DNA binding ability and are localized in the nucleus, thus they are considered as transcription factors (Vanholme et al., 2007).

Proteins in Class II lack the C2C2-GATA domain and are composed of JAZ proteins, TIFY8, and the PEAPOD (PPD) proteins, namely PPD1 and PPD2 . JAZ proteins are transcriptional repressors in JA signaling. TIFY8 is an atypical TIFY protein, and no other conserved domains have been characterized yet in its protein sequence. PPD1 and PPD2 have an additional PEAPOD domain and a divergent C-terminal Jas domain. Although some Class II proteins have been shown to localize in the nucleus, there is no clear evidence suggesting that they have DNA binding ability.

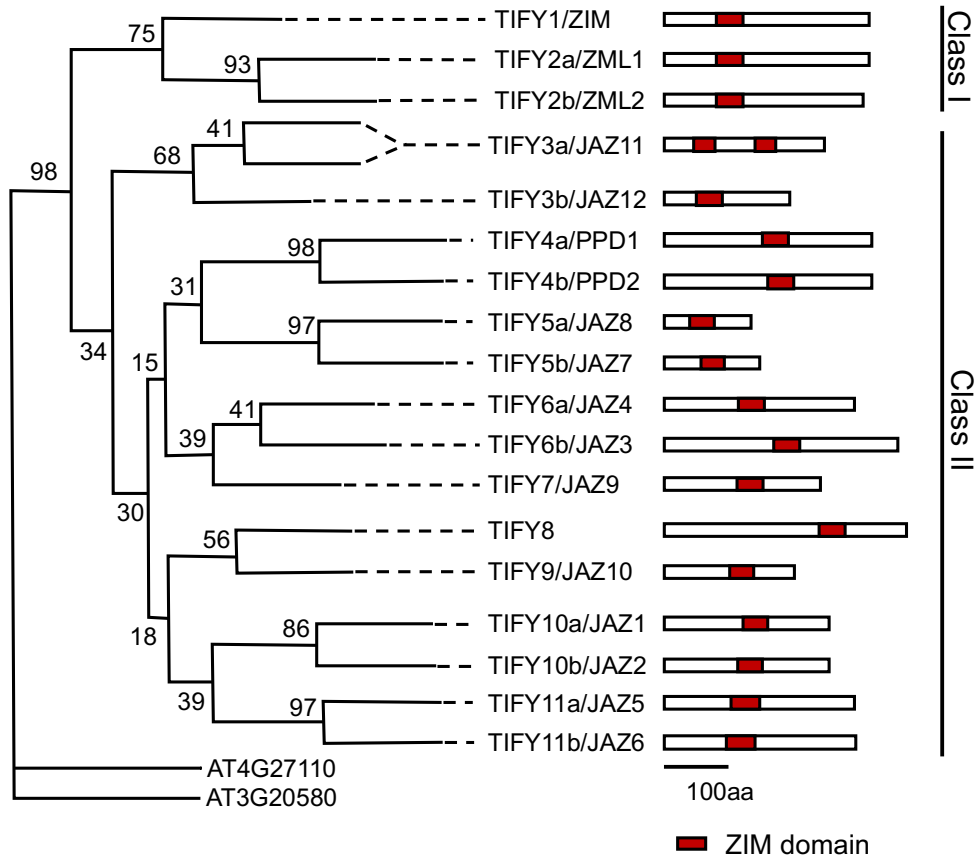


Figure 1.6: The TIFY protein family in *Arabidopsis thaliana*. The phylogenetic tree of 18 members in the *Arabidopsis* TIFY protein family was generated by Vanholme et al. (2007). The tree is constructed based on the ZIM domain protein sequence. AT4G27110 and AT3G20580 were selected as the outgroup. The figure is modified from Vanholme et al. (2007).

1.3.2 The biological functions of TIFY proteins

1.3.2.1 ZIM and ZIMLs

Class I proteins are putatively involved in inflorescence and flower development, as *ZIM* is specifically expressed in the shoot apex and flowers in *Arabidopsis*. However, the underlying regulation mechanism remains elusive. Nevertheless, plants overexpressing *ZIM* exhibit elongated hypocotyls and petioles, suggesting its role in regulating cell elongation (Shikata et al., 2004). Interestingly, ZIML1 and ZIML2 are required for the photoreceptor Cryptochrome 1 (CRY1)-mediated photoprotective response. Stimulated by high light, CRY1 activates the ZML1-ZML2 complex and

allows the ZML complex to bind to the cis-element of *CRY1*. As a result, high light-responsive genes are expressed (Shaikhali et al., 2012).

1.3.2.2 JAZs

JAZs are crucial repressors for all the JA-mediated regulation. they act as signaling hubs, linking JA signaling to other signaling pathways through protein interactions. There are 13 JAZ proteins in *Arabidopsis*, with only JAZ13 not classified as a member of the TIFY family, as it contains a divergent ZIM domain.(Thireault et al., 2015). The remaining 12 JAZ proteins are classified into five groups based on the phylogenetic analysis (Pauwels & Goossens, 2011). Despite the variance of functional domains among the five groups, there are three conserved domains in all JAZs proteins: an N-terminal domain (NT), a TIFY-containing ZIM domain, and a C-terminal Jas domain. The NT domain is responsible for the interaction with some transcription regulators, such as the Gibberellin repressor DELLA proteins (Hou et al., 2010; Zhu et al., 2011). The ZIM domain is necessary for the homo and hetero-dimerization between JAZs and the interaction with COI1 or NINJA (Pauwels et al., 2010; Wager & Browse, 2012). The Jas domain is required for the interaction with MYC proteins, COI, and a variety of other proteins mediated by the crosstalk between JA and other signaling pathways (Chini et al., 2007; Fernández-Calvo et al., 2011; Melotto et al., 2008; Tiancong Qi et al., 2011; Song et al., 2013). The Jas domain is characterized by a core amino acid sequence of S-L-X(2)-F-X(2)-K-R-X(2)-R and conserved P in the N-terminal and PY sequence in the C-terminal. Apart from the three domains mentioned above, some JAZs (JAZ5, JAZ6, JAZ7, JAZ8, JAZ13) have EAR motif, which is responsible for interaction with TOPLESS (TPL) proteins (Consortium et al., 2011).

1.3.2.3 PPDs

PPD1 and PPD2 are involved in the lamina size control and the regulation of dispersed meristematic cell (DMC) proliferation. Mutants with the deletion of PPD loci display dome-shaped leaves and abnormal shape of siliques (White, 2006). PPD2 can interact with NINJA and transcriptional repressor complexes in leaf cells. This complex plays an essential role in modulating cell cycle-related gene expression, such as *CYCD3* (Baekelandt et al., 2018).

1.3.2.4 TIFY8

TIFY8 is considered as an atypical TIFY protein due to the lack of additional domains presented in other members of the TIFY family. TIFY8 is characterized as a transcriptional repressor and can interact with several other proteins involved in different pathways. Potential interactors include RESPONSE REGULATOR 14 (ARR14) in cytokinin signaling, SPINDLY(SPY) in cytokinin and gibberellin signaling, OBERONs (OBEs) in the regulation of embryonic root meristem initiation, and NINJA in JA signaling (Cuéllar Pérez et al., 2014). However, the biological relevance of these interactions is still unclear. A recent study suggests that TIFY8 can interact with REVOLUTA (REV) and modulate leave senescence. The interaction represses the expression of *WRKY53*, which is a central activator of leaf senescence in *Arabidopsis* (Andrade Galan et al., 2023).

1.4 Aim of my study

While the fundamental mechanisms of stem cell regulation in the SAM have been elucidated, how the stem cell niche responds to wounding is still unclear. Since the JA pathway plays a crucial role in wounding signal perception and plant developmental regulation, I aimed to decipher the interplay between the stem cell regulatory network and the JA pathway in response to wounding. For my study, I followed three central goals:

1. Characterize the effects of systemic wounding on SAM activity.
2. Investigate the function of JA signaling in stem cell maintenance.
3. Investigate the role of WUS in the regulation of the JA pathway with a focus on TIFY proteins.

My results show that wounding acts on the SAM via the JA pathway and that conversely, WUS interacts with specific TIFY proteins, some of which have a role in inhibiting the JA response.

2. Materials

2.1 Plant materials

All the *Arabidopsis* plants used in this study are in Columbia ecotype (Col-0) background, except for *wus-7*, which is in Landsberg *erecta* (L*er*) background. All the information for plant materials is summarized in Table S2. All the transgenic lines used in this study are homozygous in the T3 generation or the T4 generation. To generate *tify8-cr1 clv3-10*, *tify8-cr2 clv3-10*, and *jaz3-cr tify8-cr1*, the heterozygous mutant allele of *tify8-cr1/tify8-cr2* was genotyped in the T2 generation and subsequently pollinated with the pollens of *clv3-10* mutants or the pollens of *jaz3-cr L30*. The double mutants *tify8-cr1 clv3-10, tify8-cr2 clv3-10, and jaz3-cr tify8-cr1* were identified by genotyping in the C2 generation. For CRISPR/Cas9 mutants used in this study, Cas9-editing cassettes were removed in *jaz3-cr L30*, *tify8-cr1 clv3-10*, and *jaz3-cr tify8-cr1* but not in the other mutant alleles.

2.2 Bacterial strains

The competent cells of *Escherichia coli* XL1 blue strain and the competent cells of *Agrobacterium tumefaciens* ASE and GV3101 strains were used in this study.

2.3 Chemicals and commercial kits

2.3.1 Plant growth medium

Murashige and Skoog salts (MS)	Duchefa Biochemie, Haarlem, Netherlands
2-(N-morpholino) ethanesulfonic acid (MES)	Carl Roth, Karlsruhe, Germany
Phyto agar	Duchefa Biochemie, Haarlem, Netherlands

2.3.2 Antibiotics

Hygromycin B	Roche, Basel, Switzerland
Ampicillin	Sigma-Aldrich, St. Louis, USA
Chloramphenicol	Carl Roth, Karlsruhe, Germany
Kanamycin	Carl Roth, Karlsruhe, Germany
Gentamycin	Sigma-Aldrich, St. Louis, USA

Spectinomycin	Sigma-Aldrich, St. Louis, USA
Tetracycline	Sigma-Aldrich, St. Louis, USA
Rifampicin	Carl Roth, Karlsruhe, Germany

2.3.3 Seed sterilization

Sodium hypochlorite solution, 12% Cl	Carl Roth, Karlsruhe, Germany
99% ethanol for seed sterilization	Heidelberg university, Germany
37 % HCl	Merck, Darmstadt, Germany

2.3.4 Chemical treatment

(+/-)-Jasmonic acid	Sigma-Aldrich, St. Louis, USA
Dexamethasone	Sigma-Aldrich, St. Louis, USA
Silwet® Gold	Spiess-Urania, Hamburg, Germany

2.3.5 Cloning

Phusion High-Fidelity DNA Polymerase	Thermo Scientific, Waltham, USA
dNTP mix	Thermo Scientific, Waltham, USA
Phusion HF buffer	Thermo Scientific, Waltham, USA
FastDigest Eco31I (IIs Class)	Thermo Scientific, Waltham, USA
FastDigest EcoR1	Thermo Scientific, Waltham, USA
FastDigest XhoI	Thermo Scientific, Waltham, USA
FastDigest BamHI	Thermo Scientific, Waltham, USA
T4 DNA ligase	Thermo Scientific, Waltham, USA
ATP solution	Thermo Scientific, Waltham, USA
JumpStartTM REDTaq®ReadyMixTM	Sigma-Aldrich, St. Louis, USA
FastDigest Buffer (10X)	Thermo Scientific, Waltham, USA
InnuPREP Plasmid Mini Kit	Analytik Jena, Jena, Germany
InnuPREP DOUBLEpure Kit	Analytik Jena, Jena, Germany
Phire™ Plant Direct PCR Master Mix	Thermo Scientific, Waltham, USA

2.3.6 Tissue staining

DAPI	Carl Roth, Karlsruhe, Germany
Propidium iodide (1mg/ml)	Sigma-Aldrich, St. Louis, USA

2.3.7 Fixation

Formaldehyde	AppliChem, Darmstadt, Germany
Glacial acetic acid	Sigma-Aldrich, St. Louis, USA
Ethanol	Fisher Scientific, Schwerte, Germany
Paraformaldehyde	Sigma-Aldrich, St. Louis, USA

2.3.8 Agarose embedding

Agarose, low gelling temperature	Sigma-Aldrich, St. Louis, USA

2.3.9 Probe synthesis for *in situ* hybridization

10x transcription buffer	Roche, Basel, Switzerland
RNase inhibitor	Roche, Basel, Switzerland
DIG RNA labeling mix	Roche, Basel, Switzerland
SP6 RNA Polymerase	Roche, Basel, Switzerland
T7 RNA polymerase	Roche, Basel, Switzerland
DNase I recombinant, RNase-free	Roche, Basel, Switzerland
Lithium chloride	Carl Roth, Karlsruhe, Germany
EDTA	Carl Roth, Karlsruhe, Germany
Deionized formamide	Carl Roth, Karlsruhe, Germany

2.3.10 *In situ* hybridization

Xylol	Carl Roth, Karlsruhe, Germany
Paraplast	Leica Biosystems, Nussloch, Germany
Glycin	Carl Roth, Karlsruhe, Germany
Dextrane sulfate	Carl Roth, Karlsruhe, Germany
Denhardt's solution	Sigma-Aldrich, St. Louis, USA
tRNA	Roche, Basel, Switzerland
$MgCl_2$	Carl Roth, Karlsruhe, Germany
NaCl	NeoFroxx, Einhausen, Germany
Tris	Carl Roth, Karlsruhe, Germany
Proteinase K, recombinant PCR grade	Roche, Basel, Switzerland
Formamide	Carl Roth, Karlsruhe, Germany
BSA	Carl Roth, Karlsruhe, Germany
Triton-X 100	Sigma-Aldrich, St. Louis, USA
Blocking reagent	Roche, Basel, Switzerland
Anti-Digoxigenin-AP Fab fragments	Roche, Basel, Switzerland
NBT-BCIP	Roche, Basel, Switzerland
Na_2CO_3	Sigma-Aldrich, St. Louis, USA
$NaHCO_3$	Sigma-Aldrich, St. Louis, USA
NaH_2PO_4	Sigma-Aldrich, St. Louis, USA
Na_2HPO_4	Sigma-Aldrich, St. Louis, USA
Sodium citrate	Sigma-Aldrich, St. Louis, USA

2.3.11 Agrobacteria infiltration

AcetoSyringone	Carl Roth, Karlsruhe, Germany

2.3.12 RNA extraction

RNeasy® Plant Mini kit	Qiagen, Hilden, Germany

2.3.13 cDNA synthesis

HiScript® III RT SuperMix for qPCR	Vazyme, Nanjing, China

2.3.14 qPCR

Luna® Universal qPCR master Mix	New England Biolabs, Ipswich, USA

2.3.15 Yeast-two hybrid

YPDA Broth	Takara, Kyoto, Japan
SD/-Leu/-Trp Broth	Takara, Kyoto, Japan
SD/-Ade/-His/-Leu/-Trp Broth	Takara, Kyoto, Japan
PEG3350	Carl Roth, Karlsruhe, Germany
Lithium acetate	Sigma-Aldrich, St. Louis, USA
Salmon sperm DNA	Invitrogen, Waltham, USA
Micro agar	Duchefa Biochemie, Haarlem, Netherlands
Adenine Hemisulfate	Duchefa Biochemie, Haarlem, Netherlands
X-α-Gal	Carl Roth, Karlsruhe, Germany

2.3.16 eChIP

HEPES	Carl Roth, Karlsruhe, Germany
Sodium deoxycholate	Sigma-Aldrich, St. Louis, USA
DTT	Sigma-Aldrich, St. Louis, USA
Protease inhibitor cocktail	Sigma-Aldrich, St. Louis, USA
Nonidet P-40	AppliChem, Darmstadt, Germany
iPure kit v2	diagenode, Milwaukee, USA
RFP-trap magetic agrose	chromotek, Planegg, Germany
Binding control magetic agrose	chromotek, Planegg, Germany
Isopropanol	Heidelberg university, Germany

2.4 Mediums and buffers

2.4.1 Plant growth medium

Plant 1/2 MS with agar (1 liter)	2.25g Murashige and Skoog salts (MS) 0.5g MES 8g phyto agar pH=5.7

2.4.2 Yeast growth medium

Master plate (500ml)	1 pouch of SD/-Leu/-Trp Broth 20mg Adenine Hemisulfate 10g micro agar
Selection plate (500ml)	1 pouch of SD/-Ade/-His/-Leu/-Trp Broth 10g micro agar

2.4.3 DNA extraction

DNA extraction buffer for genotyping	250mM Tris-HCl (pH=7.5) 250mM NaCl 25mM EDTA 0.5% SDS

2.4.4 Agrobacteria infiltration

Agrobacteria infiltration buffer	10 mM $MgCl_2$ 10 mM MES 0.15 mM AcetoSyringone

2.4.5 *In situ* hybridization

2x Hydrolysis Carbonate Buffer	120 mM Na_2CO_3 80 mM $NaHCO_3$
10xPBS	1.3 M NaCl 30 mM NaH_2PO_4 70 mM Na_2HPO_4
10xTBS	1M Tris pH 7.5 1.5 M NaCl
FAA fixation buffer	50% Ethanol 5% Glacial Acetic Acid 3.7% Formaldehyde
Proteinase-K buffer	100mM Tris pH 7.5 50mM EDTA pH 8.0
10x Salts	3M NaCl 100 mM Tris pH 8.0 50 mM EDTA 53.7 mM NaH_2PO_4 46.3 mM Na_2HPO_4

Hybridization mix	50% (deionized) formamide 10% Dextrane sulfate 1x in situ Salts 1x Denhardt' solution 0.5 mg/ml tRNA
Blocking solution	1% Blocking reagent 0.3% Triton-X 100 in 1% TBS
Antibody buffer	1% BSA 0.3% Triton-X 100 in 1% TBS
Detection buffer	100 mM Tris pH 9.5 50 mM $MgCl_2$ 100 mM NaCl
20xSSC	3M NaCl 0.3 M Na-citrate

2.4.6 eChIP-qPCR

Buffer S	50 mM HEPES-KOH (pH 7.5) 1 mM EDTA 1% Triton X-100 0.1% Sodium deoxycholate 1% SDS 1 mM DTT 1x Protease inhibitor cocktail 150 mM NaCl
Buffer F	50 mM HEPES-KOH (pH 7.5) 1 mM EDTA 1% Triton X-100 0.1% Sodium deoxycholate 1 mM DTT 1x Protease inhibitor cocktail 150 mM NaCl
Low-salt ChIP buffer	50 mM HEPES-KOH (pH 7.5) 150 mM NaCl 1 mM EDTA 1% Triton X-100 0.1% sodium deoxycholate

	0.1% SDS
High-salt ChIP buffer	50 mM HEPES-KOH (pH 7.5) 350 mM NaCl 1 mM EDTA 1% Triton X-100 0.1% sodium deoxycholate 0.1% SDS
ChIP wash buffer	10 mM Tris-HCl (pH 8.0) 250 mM LiCl 0.5% Nonidet P-40 1 mM EDTA 0.1% sodium deoxycholate
TE buffer	10 mM Tris-HCl (pH 8.0) 1 mM EDTA

2.5 Instruments

2.5.1 Microscopes

Confocal microscope Nikon A1	Nikon Instruments, Tokyo, Janpan
Leica confocal microscope STELLARIS 8	Leica Biosystems, Nussloch, Germany
SteREO Discovery.V20 microscope	Carl Zeiss, Jena, Germany
Zeiss Axio Imager M1 microscope	Carl Zeiss, Jena, Germany
Nikon SMZ 745	Nikon Instruments, Tokyo, Janpan
Digital Camera Nikon D5200	Nikon, Tokyo, Janpan

2.5.2 Sectioning and embedding

Leica ASP200 S Vacuum Tissue Processor	Leica Biosystems, Nussloch, Germany
Leica EG1160 Tissue Embedding Station	Leica Biosystems, Nussloch, Germany
Leica RM2255 Automated Microtome	Leica Biosystems, Nussloch, Germany
Leica VT1000 S vibratome	Leica Biosystems, Nussloch, Germany

2.5.3 PCR and qPCR

qTOWER^3 Real-time thermo cycler	Analytik Jena, Jena, Germany
Bio-Rad DNA Engine cycler	Bio-Rad, Hercules, USA
Nanodrop ND-1000	Nanodrop, Wilmington, USA

2.5.4 Plant growth and microbial cultivation

Conviron CMP6010	CONVIRON, Manitoba, Canada
Incubation Shaker Innova ® 44	New Brunswick Scientific, Edison, USA
Incubator Binder BD-Serie	Binder, Tuttlingen, Germany
Microbiological Safety Cabinet MSC1.2	Thermo Scientific, Waltham, USA

2.5.5 Others

Bioruptor® Pico sonication device	diagenode, Milwaukee, USA
Tissue Lyser II	Qiagen, Hilden, Germany
Milli-Q ® water system	Merck Millipore; Billerica, USA
Eppendorf Centrifuge 5424R	Eppendorf, Hamburg, Germany
Eppendorf Centrifuge 5810R	Eppendorf, Hamburg, Germany
Eppendorf Centrifuge 5424	Eppendorf, Hamburg, Germany
Eppendorf Thermomixer 5436	Eppendorf, Hamburg, Germany
NeoLabLine Rotator	neoLab Migge, Heidelberg, Germany
Analytical balance	Sartorius, Göttingen, Germany

2.5.6 Software

Microsoft Office 365 Pro Plus	Microsoft, Redmond, USA
R (4.2.1)	https://www.r-project.org
R Studio (2023.06.2+561)	https://posit.co/download/rstudio-desktop/
Endnote 21	Clarivate, Philadelphia, USA
Fiji (2.14.0)	https://imagej.net/software/fiji/
Knime (v4.5.0)	https://www.knime.com
Genious (9.1.8)	Dotmatics, Boston, USA
Inscape 1.3	https://inkscape.org
GraphPad prism 5	GraphPad Software, California, USA

3. Methods

3.1 Plant growth

Arabidopsis seeds for T1 selection were sterilized with 70% ethanol for 20 mins and then dried in sterile filter paper. Seeds for other purposes were sterilized by chlorine gas method for 4 hours. Seeds were sowed on the 1/2 MS medium plates with agar and stored at 4°C covered with Aluminum foil for two days. For transgenic line selection, Hygromycin B was added to the medium at a final concentration of 25μg/ml. Plates were then kept in the growth chamber for one week. Seedlings resistant to Hygromycin B were transferred into the soil. For seedlings used in the root phenotypic characterization, the plates were put vertically in the growth chamber. Plants transferred to the soil were grown in the growth room. The plants for flowering time measurement were grown in the controlled growth chamber (Conviron CMP6010). For the wounding treatment and JA treatment, plants were moved from the growth room to the controlled growth chamber when the treatments were started. *Arabidopsis* plants were grown at 22°C under long-day conditions (16h light/8h dark). *Nicotiana benthamiana* was grown in a growth chamber at 25°C under long-day conditions.

3.2 Cloning

The constructs generated using the GreenGate (GG) cloning system are listed in Table S3 and Table S4. To generate A, C, and E module vectors, targeting DNA fragments were first amplified by PCR. Templates for the PCR reaction are the complementary DNA (cDNA) for the C module and the genomic DNA for the A and E modules. Primers with corresponding overhang sequences are designed following the instruction (Lampropoulos et al., 2013). The reaction mixture contains the following ingredients: 16.5 μl purified PCR product, 1 μl empty module vector (100ng/μl), 0.5 μl Eco31I, 2 μl FD buffer, and MiliQ water to 20 μl. The digestion step was performed at 37°C for 1 hour, ending with deactivation at 80°C for 10 mins, followed by a two-hour ligation with T4 ligase at room temperature. The sequence of inserted DNA fragments in modules was confirmed by the Sanger sequencing (Eurofins Scientific, Luxemburg). To assemble GreenGate vectors, the reaction setting up is as follows: 0.75μl of the modules from A to F, 0.5μl of pGGZ, 2.0μl of the MiliQ water, 2.0μl of 10mM ATP,

1.0µl of 10xFD, 0.5µl of T4 ligase and 0.5µl of Eco31I. The GreenGate reaction is performed with 30 cycles of 37°C 1min and 16°C 1min, ending with 80°C deactivation for 10 mins.

To generate constructs for the yeast-two-hybrid (Y2H) experiment, CDS sequences of JAZ3 and TIFY8 were first amplified with the primers containing the restriction enzyme EcoRI cutting site in the 5'-prime and XhoI cutting site for JAZ3, BamHI cutting site for TIFY8 in 3'-prime. The purified PCR fragments and the destination vector pGADT7 (Takara, Kyoto, Japan) were digested by the corresponding restriction enzymes and assembled by T4 ligase for the prey vector. Construct for the bait, in which WUS assembled into vector pGBKT7 (Takara, Kyoto, Japan) was kindly provided by Thomas Greb's lab.

3.3 CRISPR/Cas9 knockout system

Constructs for CRISPR/Cas9 knockout mutants are generated based on Wang et al. (2015). Two suitable gRNAs for each targeted gene were selected on the CHOP CHOP program (http://chopchop.cbu.uib.no). To assemble the construct with gRNAs, a PCR reaction was performed, in which two gRNA sequences were incorporated into PCR forward and reverse primers. The plasmid pHEE2E-TRI was used as a template. PCR fragments were then purified and introduced into the destination vector pHEE401E, using the GreenGate reaction. To genotype transgenic plants in every generation, Thermo Scientific™ Phire™ Plant Direct PCR Master Mix was used for DNA extraction and PCR reaction. Primers used for PCR reactions are listed in Table S5. The edited plants were selected by PCR and then confirmed by Sanger sequencing.

3.4 Wounding and chemical treatment

The wounding treatment started when the main inflorescence stem was 0-0.5cm after plant bolting. The wounding treatment in one leaf was introduced by punching four small holes with forceps (Figure S1). For the seven-day wounding treatment, three leaves were wounded every day for 6 days and further experiments were conducted on the seventh day. As for the wounding treatment for imaging the SAM of *TR7* reporters, the wounding treatment was performed every day until the length of the inflorescence stem reached 10-12cm. For the short-term wounding treatment, 6 leaves were wounded twice. Samples were collected 4 hours after the first time of the wounding treatment.

For all the JA treatments, the (+/-)-Jasmonic acid was used. The final concentration of JA in all the JA treatments is 50 μM, which is diluted from 200mM JA stock with 100% ethanol as solvent. JA solution with 0.015% Silwet was sprayed directly on the apex of the inflorescence. Mock treatments were all the same as JA treatments except without JA. JA treatment started when the main stem was 0-0.5cm after bolting. For the SAM imaging, the long-term JA treatment was performed twice every day at the same time point for 4 days or 8 days. The SAMs were imaged on the fifth day or the ninth day accordingly. For the stem length measurement, the long-term JA treatment was performed twice every day at the same time point for 6 days. The stem length was measured on the seventh day. Short-term JA treatment was performed every 1 hour until samples were collected.

For the dexamethasone (DEX) treatment, 10 μM DEX solution with 0.015% Silwet was sprayed on the apex of the inflorescence twice in 2 hours. Mock treatments were all the same as DEX treatments except without DEX.

3.5 PFA fixation

To prepare the 4% PFA fixation solution, 20g of paraformaldehyde powder was added to 500 mL 1XPBS buffer. The powder was gradually dissolved by heating and adding NaOH tablets to PH=6.9. To fix the SAMs, shoot apexes of inflorescences were put into 4% PFA fixation solution under vacuum for 15 mins. Then the vacuum was released, and the samples were gently shaken. Another 15-minute fixation under vacuum was performed. After fixation, samples were washed with 1% PBS twice.

3.6 Microscopy

Images for *in situ* hybridization were obtained using Zeiss Imager M1. Images for the apex of inflorescences were taken by SteREO Discovery V20 microscope. For imaging the SAM, the apex of the inflorescence was first dissected with forceps under stereo microscopy and inserted in the 2% agarose medium. For DAPI staining, the dissected meristem was immersed in 20μl DAPI for 1 min. For Propidium iodide (PI) staining, roots of five-day-old seedlings were immersed in PI for 1.5 mins before imaging. Confocal images were taken by confocal microscope Nikon A1 with a CFI Apo LWD 25× water immersion objective. To image *TR7* lines, the imaging setting followed Wenzl and Lohmann (2023). Sections by vibratome were imaged by Leica confocal

microscope STELLARIS 8 with HC PL APO CS2 20x/0.75 DRY objective. The setting used is as follows: Ex:473nm, Em:478-550nm for GFP.

3.7 Image analysis

For image analysis of *TR7* reporter lines, the procedure followed the description in Wenzl and Lohmann (2023) (Figure S2). The quantification of the SAM area and the measurement of the primary root length were performed using Fiji software. The area of the SAM was manually selected, and the size of the selected area was calculated.

3.8 *In situ* hybridization

For the probe synthesis, CDS sequences of genes of interest were first amplified from corresponding C-module vectors, using primers containing the sequences of T7 and SP6 promoters. After PCR products were purified, the following ingredients were added into the in vitro transcription reaction mix: 2.0 µl 10x transcription buffer; 1.0 µl RNase inhibitor (20 units); 2.0 µl 10x Dig NTP mix; 2.0µl Enzyme (SP6 RNA Polymerase or T7 RNA polymerase); 13µl template cDNA (200ng). The reaction mix was then incubated for 2 hours at 37°C. DNA in the reaction product was removed by adding 2 µl RNase free DNase (20 units). Solution was then incubated for 15 mins at 37°C and the reaction was then terminated by adding 2 µl of 0.2 M EDTA (pH8.0). The synthesized probes were then precipitated by adding 2.5 µl of 4M LiCl and 75 µl of 100% EtOH to the mixture and incubated at -20°C overnight. The pellet was collected by centrifugation at 4°C for 30 mins with maximum speed and washed with cold 80% ethanol. The pellet was dried and dissolved with 50µl of deionized formamide.

For the paraffin embedding, samples were first fixed with the FAA solution and were processed following an *in situ* fixation program in Leica Asp200 for the automated vacuum and paraffin infiltration. Samples are embedded and sectioned at 8 µm and then transferred to water on the X-tra^{TM} Adhensive precleaned micro slides (Leica Biosystems, Germany). Slides were heated at 42°C overnight.

The hybridization was performed as described in Medzihradszky et al. (2014). 8 µl probe solution was added into the 100 µl hybridization mix for each slide. The hybridization was performed at 55°C overnight. After washing and blocking, slides were applied with 100 µl antibody solution (1:1250) for 90 mins. The signal detection was performed by NBT-BCIP after washing.

3.9 RNA extraction and qRT-PCR

Total RNA from the shoot apex of the inflorescence was isolated using the RNeasy® Plant Mini kit. 1000ng RNA for each sample was used for reverse transcription with a cDNA synthesis kit following the protocol. qPCR was performed with the following program: 95°C 1min, 40 cycles of 95°C for 10s, 60°C for 20s and 72°C for 20s, ended with melting curve from 72°C to 95°C, with ΔT =0.5 °C every 15s. The reaction mixture contained 10µl of qPCR master mix,l of the primer mix (10µM), 1µl reverse-transcribed cDNA, and 8µl of water. Three technical repeats were performed. *PROTEIN PHOSPHATASE 2A SUBUNIT A3* (*PP2A*) was used as the normalizer. Data were analyzed using the $2^{-\Delta\Delta CT}$ method.

3.10 Vibratome sectioning

The shoot apex was first fixed with 4% PFA. Samples were then embedded in 7% low melting agarose. After the agarose was solidified, the agarose blocks with samples were cut into smaller blocks with blades and then sectioned into 70µm-thick slices by vibratome. Slices were immediately checked and imaged under the confocal microscope.

3.11 Agrobacteria infiltration in *Nicotiana benthamiana*

The *Agrobacterium tumefaciens* strain ASE carrying the construct of interest from glycerol stock was first inoculated in Luria–Bertani (LB) medium with agar and antibiotics at 28°C in the incubator for one day. The refreshed clones were liquid-cultured at 28°C in the shaker overnight. Bacteria cells were collected by centrifugation (5000 xg, 10 mins) and then resuspended in the infiltration buffer. The concentration of bacteria culture for infiltration was adjusted to OD_{600} =0.5-0.75 and different infiltration combinations were mixed with equal concentration. The bacterial mixture was infiltrated into the abaxial leaf surface of 4 to 5-week-old *Nicotiana benthamiana* plants using 1ml syringes. Plants were then put back in the growth chamber for two days.

3.12 AP-FRET experiment

The FRET experiment was performed two days after Agrobacteria infiltration. A small piece of infiltrated leaves was shortly vacuumed in distilled water by the syringe before imaging. The FRET setting is as follows: phase I: pre-bleaching, acquisition, no delay, 3 pictures; phase II, bleaching, photobleaching, 1 step; phase III, post-bleaching, acquisition, no delay, 7 pictures. After photobleaching, the fluorescence intensity of the donor (GFP) and acceptor (mCherry) were recorded. The FRET efficiency is calculated according to the following formula:

$$E(\%)=\frac{I_{GFP(post-bleach)}-I_{GFP(pre-bleach)}}{I_{GFP(post-bleach)}}x\,100$$

3.13 Yeast-two-hybrid

The protocol is adapted from de Folter and Immink (2011) and the user manual of Yeastmaker™ Yeast Transformation System 2 (Takara, Kyoto, Japan). The stock of the Yeast strain AH109 was first refreshed in YPDA medium at 30°C for three days. 2-3 colonies were inoculated in 2ml liquid YPDA medium at 30°C with shaking at 180rpm overnight. The culture was transferred into 50ml liquid medium for another incubation for 6-8h. For co-transformation of both the bait and prey vector, the liquid culture was aliquoted into 2ml for each transformation and centrifuged for 10s at 13000 rpm. The pellet was resuspended and incubated in 1 ml of 100 mM LiAc for 1 min. The mixture was then centrifuged for 10s at 13000 rpm. The following were added into the pellet: 240 µl of 50% PEG; 36 µl of 1 M LiAc; 5 µl of salmon sperm DNA (10 mg/ml); 3 µl of plasmid DNA (~0.5–1.5 µg); 67 µl of MilliQ water. After vortexed for 1min, the mixture was incubated for 20–30 mins at 42°C in a water bath. The treated yeast cells were collected by centrifugation for 10s at 13000 rpm and resuspended in 100 µl of MilliQ water. The yeast solution was then plated on the master plate (SD medium –Leu/–Trp). Plates were then incubated for 3 days at 30°C. Three single colonies grown in the selection plate were picked and suspended in 50 µl MiliQ water individually. 5µl solution for each colony was dropped on master plates and selection plates (SD –Leu/–Trp/–His/–Ade) with X-α-Gal. Plates were incubated at 30°C for three days.

3.14 eChIP-qPCR

The enhanced chromatin immunoprecipitation (eChIP) protocol was adapted from (Zhao et al., 2020). 5-day-old seedlings of *UBQ10: mCherry-GR-WUS* and *UBQ10: mCherry-GR* were incubated in the 1/2 MS liquid medium with 10 μM DEX for 4 hours. After confirming the DEX induction worked by confocal microscope imaging, plant tissues were fixed with 1% formaldehyde under vacuum for a total of 10 mins. The fixation was stopped by 0.2 M glycine for 5 mins and samples were dried and collected with the liquid nitrogen. The chromatin was sheared by sonication (6 cycles of 30s on and 30s off, with high frequency) to average fragment sizes of 200-600bp. Sonicated samples were incubated with binding control magnetic agarose beads for 2 hours for preabsorption. 1% volume of sample is used as input. Immunoprecipitation was performed by incubating sonicated samples with RFP-Trap beads overnight. After immunoprecipitation, samples were washed with a series of buffers. iPure kit v2 was used for DNA purification. For qPCR analysis, three biological replicates were performed with 0.1g of seedlings for each biological replicate. Two technical repeats were performed. Analysis was performed according to the Percent Input Method, in which the raw Ct of the IP sample was first normalized to Ct of input subtracted with dilution factor and then normalized to the control sample.

3.15 Statistical analysis

Data from qRT-PCR and eChIP-qPCR were analyzed with the two-tailed Student's t-test. Data from the rest of the experiments were first applied to the Shapiro-Wilk normality test for normal distribution assessment in R (4.2.1). If the P-value >0.05, the data were assumed to be normally distributed. The following analysis was performed in the GraphPad Prism 5. The two-tailed Students' t-test or one-way ANOVA with the Tukey test was performed accordingly for the normally distributed data. The Wilcoxon rank-sum test or the Kruskal-Wallis test followed by Dunn's multiple comparison test was performed accordingly for the data that were not normally distributed.

4. Results

4.1 Stem cell maintenance in response to systemic wounding

4.1.1 Wounding treatment modulates inflorescence stem growth and SAM morphology

At the beginning of my study, I first asked how the wounding stress affected SAM development. It has been reported that repeatedly wounding leaves of *Arabidopsis* significantly reduced the leaf size as well as the fresh weight of the above-ground part of plants (Zhang & Turner, 2008). However, whether the wounding signals influence the function of the SAM remains elusive.

To seek the answer to my question and explore the physiological and cellular basis behind it, I first need to design a suitable wounding experimental system. There are three general concerns for the experimental design: first, the wounding response needs to be efficiently stimulated in the SAM, as the SAM is located in the inner part of the shoot; second, the wounding treatment should minimize any other side effects on plant growth and development as much as possible; third, the wounding treatment should mimic the natural wounding stress.

As wounding triggers systemic responses in plants, I decided to wound the rosette leaves of *Arabidopsis*. Therefore, the systemic wounding signal was expected to be transmitted to the SAM. To generate the wound in the leaves, I used the forceps to prick small holes in the leaf surface but not in the leaf veins (Figure S1). The reason for choosing this method is to minimize the area of tissue damage as much as possible, as the side effects of tissue damage on plants may interfere with the observation of the effects of wounding signaling transduction. Every day, four holes were made in one leaf, and three leaves were wounded. Given that the inflorescence meristem is more feasible to dissect than the vegetative SAM, I started the wounding treatment with plants after floral transition with the inflorescence stem length of 0-0.5cm.

After the seven-day wounding treatment, wounded plants displayed shorter inflorescence stems compared to mock plants (Figure 4.1 A and B). This result suggests that the wounding effects in leaves can systemically inhibit the growth of the inflorescence stem.

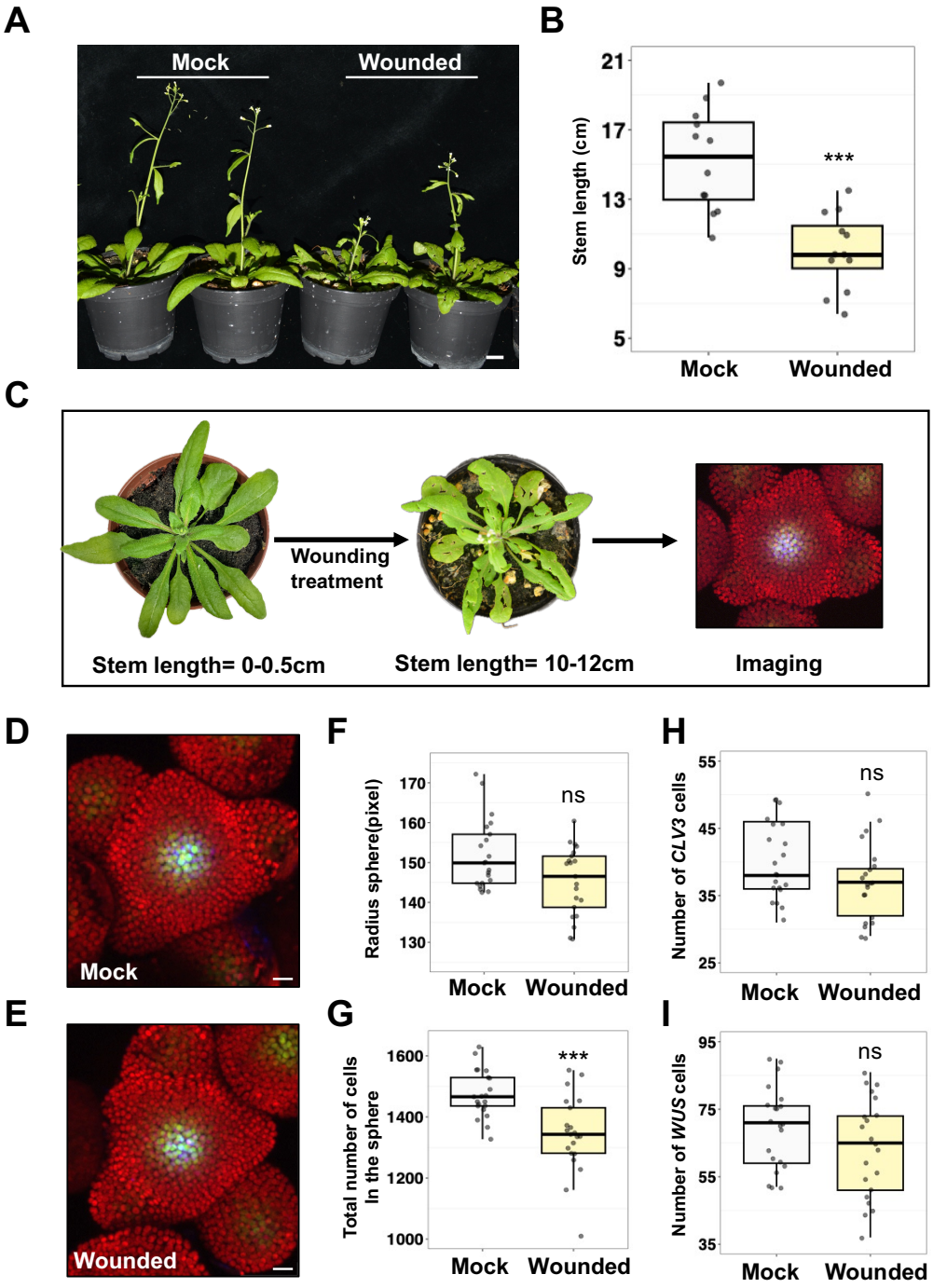


Figure 4.1: The seven-day wounding treatment modulates inflorescence stem growth and SAM morphology. A, mock and wounded triple reporter transgenic lines (*TR7*) after seven-day wounding treatment. Scale bar = 1cm. **B**, main stem length quantification of plants after seven-day wounding treatment (n =11). **C**, the modified method for wounding treatment. **D-E**, the volume view of the representative Z-stack images from the SAMs of mock (**D**) or wounded (**E**) *TR7* plants. Scale bar =10µm. **F-I**, SAM morphology analysis of mock and wounded plants using the computational analysis pipeline. Three biological replicates (n ≥ 10 in each replicate) were performed. Data of two replicates were presented here (n =21). Statistical analysis: two-tailed Student's t-tests for **B** and **G-I**, Wilcoxon rank-sum test for **F**. ***P < 0.001, ns = not significant.

Next, to explore the effects of wounding on SAM homeosis at a cellular level, I took advantage of the 3D imaging system developed by Dr. Christian Wenzl in our lab (Wenzl & Lohmann, 2023). In this system, three transcriptional reporters, including *CLV3:mTagBFP2-NLS*, *WUS:2xVENUS-NLS,* and *UBQ10:3xmCherry-NLS*, were combined into one transgenic line named triple reporter (*TR7*). The image analysis workflow enables us to simultaneously observe a series of SAM parameters (Figure S2). As wounding had a significant impact on the inflorescence stem growth and the SAM morphology changes during this growth process, the timepoint for SAM imaging was chosen based on inflorescence stem length (10-12 cm) independently of the age of respective plants (Figure 4.1 C). With the computational analysis pipeline, we can evaluate the size of the SAM with the parameter of "radius sphere" and the cell number of the SAM with the "total number of cells in the sphere".

After imaging the SAMs of mock and wounded plants (Figure 4.1 D and E), I performed the analysis pipeline. The results suggested that despite the rosette leaves being wounded, the cell number of the SAM in wounded plants was significantly reduced compared to mock plants (Figure 4.1 G, Figure S3). However, the size of the SAM was slightly decreased by wounding (Figure 4.1 F, Figure S3). As for the number of cells expressing *WUS* or *CLV3*, the number of *CLV3* cells remained relatively constant after wounding, while the number of *WUS* cells was slightly decreased (Figure 4.1H and I, Figure S3). These results suggest that the systemic wounding treatment affects the SAM activity but not the regulation of the stem cell maintenance in the SAM, as systemic wounding reduces the cell number of the SAM, but not the cell number of stem cell regions.

Altogether, the results from the long-term wounding treatment suggest that wounding in leaves results in growth inhibition in the inflorescence stem. The systemic wounding signals can modulate the SAM morphology, namely reducing the cell number of the SAM but not affecting the regulatory system of stem cell maintenance.

4.1.2 Exogenous JA treatment inhibits inflorescence stem growth and SAM activity

As wounding treatment activates the systemic JA synthesis as well as signaling pathway in plants, I wondered whether JA pathways are required for the SAM response to systemic wounding. To test this hypothesis, I first did a seven-day JA treatment, in which 50μM JA solution was sprayed at the shoot apex (Figure 4.2 A, Figure S1). In line with the observed stem growth inhibition phenotype after systemic wounding treatment, JA-treated plants displayed shorter inflorescence stems compared to mock plants (Figure 4.2 B).

To evaluate the SAM morphology upon JA treatment at the cellular level, I imaged the SAM of *TR7* plants with five-day JA treatment and analyzed SAM parameters (Figure 4.2 C and D). Compared to mock plants, JA-treated plants exhibited lower numbers of cells in the SAM, while the size of the SAM of the JA-treated plants was the same as that of mock plants (Figure 4.2 E and F). These results are consistent with those obtained from the systemic wounding assay. However, the number of *CLV3* or *WUS*-expressing cells was significantly reduced upon JA treatment (Figure 4.2 G and H), indicating that stem cell maintenance was affected. This result suggests that, unlike the systemic wounding treatment, the application of exogenous JA can perturb the stem cell regulatory system. Moreover, the negative effect of JA on the SAM is enhanced with a longer period of treatment, as the size of the SAM, as well as the signal intensity of the *WUS* and the *CLV3* reporter, were significantly decreased after nine-day JA treatment (Figure 4.2I and Figure S4).

All these results reveal that the long-time JA treatment inhibits stem growth and reduces the number of cells in the SAM, which is consistent with the long-term wounding treatment. JA treatment also reduces the size of the *WUS* and *CLV3*-expressing domain in a dose-dependent manner, indicating the activation of JA pathways represses the WUS-CLV3 regulatory system.

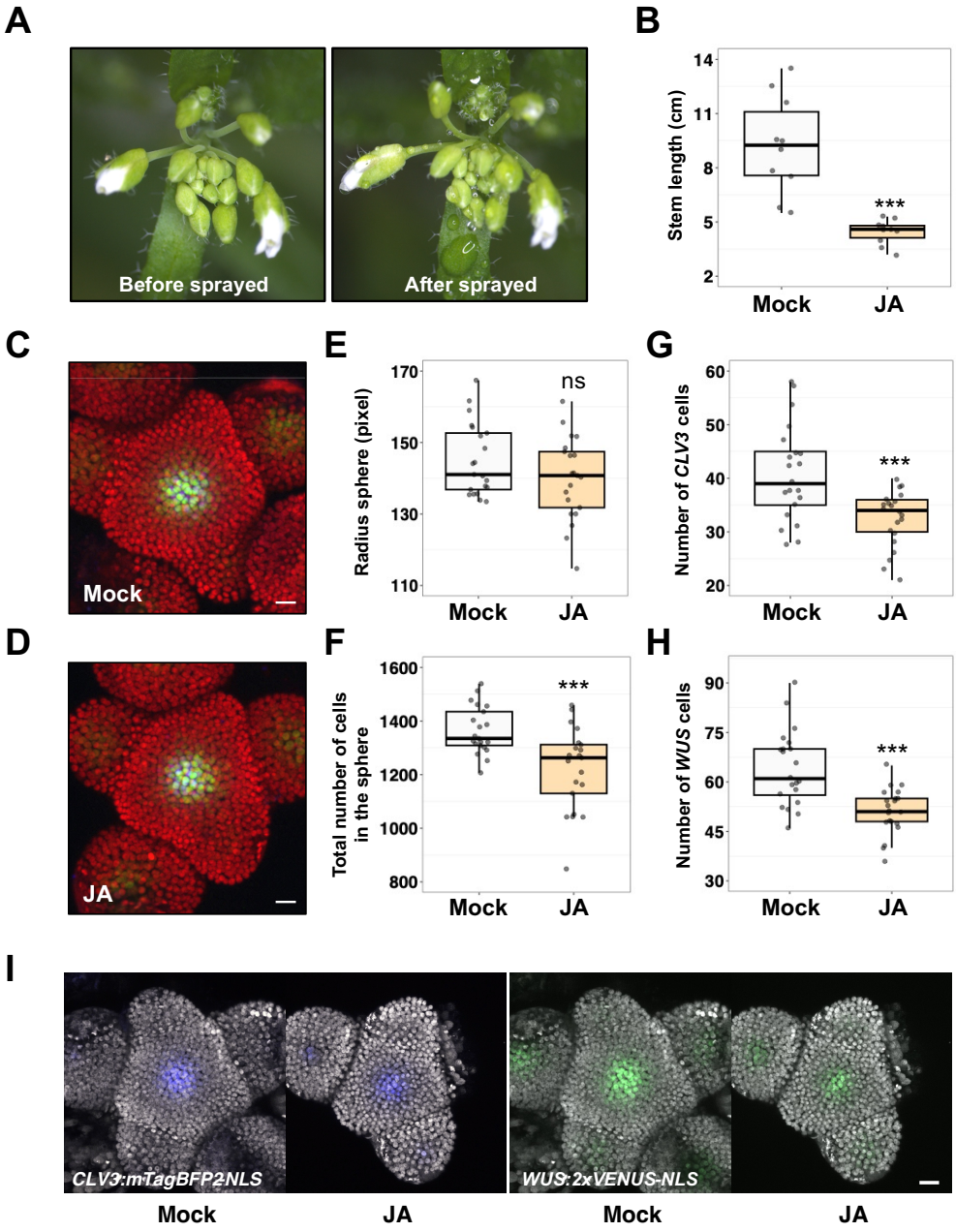


Figure 4.2: Long-term JA treatment represses inflorescence stem growth and SAM activity. A, the inflorescence tips before and after treatment with mock or JA solution. Long-term JA treatment started after floral transition (stem length = 0-0.5cm). **B**, main stem length quantification of plants with seven-day 50μM JA treatment (n =12). **C-D**, the volume view of the representative Z-stack images from the SAMs of mock (**C**) or JA-treated (**D**) *TR7* plants. Scale bar =10μm. **E-H**, SAM morphology analysis of five-day 50μM JA or mock-treated samples using computational image analysis pipeline. Data of two replicates are presented here (n =21). Statistical analysis: two-tailed Student's t-tests for **B** and **G-H**, Wilcoxon rank-sum test for **E.** ***P < 0.001, ns = not significant. **I**, Expression of *WUS* or *CLV3* domain of *TR7* with nine-day mock or 50μM JA treatment. The gray channel represents the expression of *UBQ10:3xmCherry-NLS* in *TR7*. Scale bar =10μm.

4.1.3 The JA pathway is required for wounding-induced stem growth inhibition

Regarding the similar effects of wounding and JA treatment on inflorescence stem growth and SAM morphology, it is reasonable to assume that JA mediates wounding-induced stem growth inhibition and SAM morphological modulation. However, systemic wounding triggers a series of signaling pathways in plants, which are potentially involved in the developmental regulation in response to wounding (Savatin et al., 2014). Therefore, more evidence is needed to determine whether JA pathways are required for wounding-induced stem growth inhibition.

To validate this hypothesis, I first checked whether the systemic wounding indeed stimulated the JA signaling in the SAM. To this end, I first selected four representative marker genes for JA early response as the readout for JA signaling activation in my wounding treatment assay (Acosta et al., 2013; Lorenzo et al., 2004; Zander et al., 2020). I checked the expression levels of these genes in the shoot apex upon wounding rosette leaves. According to the qPCR result, three out of four markers are significantly up-regulated four hours after wounding treatment (Figure 4.3 A), indicating that the wounding signal in leaves can trigger the JA signaling response in the shoot apex.

Next, I conducted the seven-day wounding treatment with mutants in JA signaling or JA biosynthesis. *coi1-21* is a missense allele induced by ethylmethane sulfonate (EMS) mutagenesis, in which the function of the JA co-receptor COI1 protein is impaired and JA signaling is blocked (He et al., 2012). However, unlike the strong allele of COI1, *coi1-21* is fertile and not completely insensitive to JA. Mutant *aos1-1* and *jar1-11* are two T-DNA insertion mutants affecting JA biosynthesis. The *aos1-1* mutant lacks the Allene Oxide Synthase, hence it fails to synthesize JA (Myers et al., 2023). The aos*1-1* mutant is sterile, but the sterility can be rescued by exogenous JA application. Mutant *jar1-11* is a weak allele of JAR1, in which JA is not efficiently catalyzed into bioactive JA-lle (Mahmud et al., 2022; Suza & Staswick, 2008).

According to the stem length measurement after the seven-day wounding treatment, *coi1-21* and *aos1-1,* but not *jar1-11*, displayed a weaker reduction in stem length upon wounding treatment compared to WT plants (Figure 4.3 B and C, Figure S5). Despite the low level of JA-lle in *jar1-11*, the plants still displayed WT-like stem growth inhibition level upon wounding, suggesting that even the low level of JA-lle is sufficient

for stem growth inhibition by systemic wounding, or other JA derivatives might also contribute to wounding signal transduction.

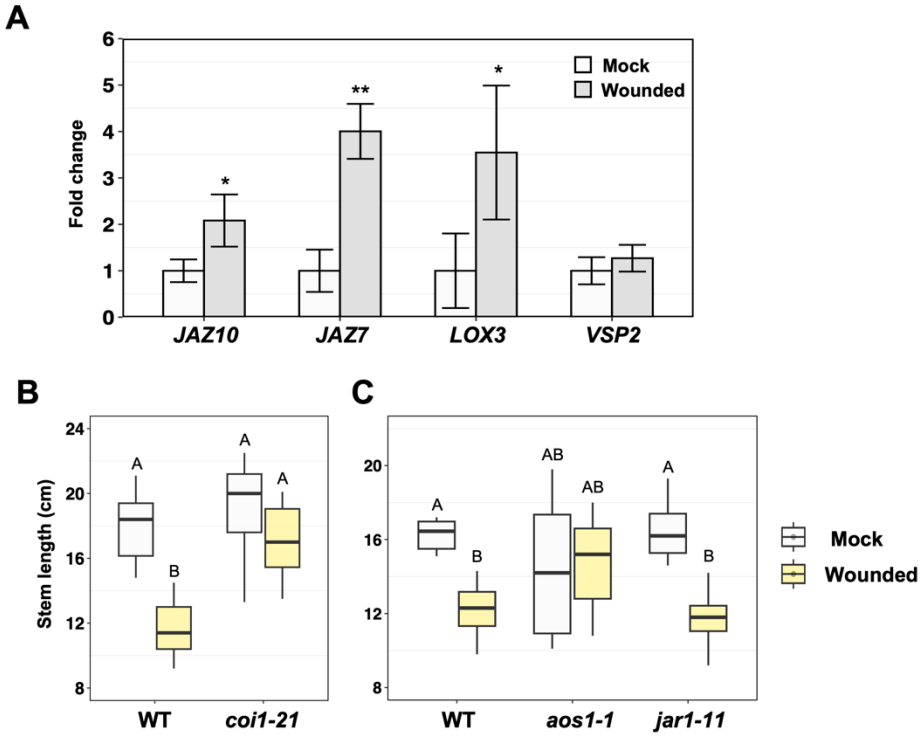


Figure 4.3: The JA pathway is involved in stem growth inhibition by wounding treatment. **A**, expression of marker genes of early JA response after wounding treatment. The error bar is the mean ± standard deviation (sd) of qPCR results from three biological replicates. Statistical analysis: two-tailed Student's t-tests. *P < 0.05, **P < 0.01. **B-C**, measurement of stem length of WT, *coi1-21* (**B**), *aos1-1,* and *jar1-11* (**C**) with seven-day wounding treatment. Statistical analysis: One-way ANOVA (Tukey's test). P < 0.01. three biological replicates were performed (n=15) for **B**. Two biological replicates were performed (n=10) for **C**. One biological replicate was presented here.

Together, all these data suggest that JA is responsible for both the systemic wounding signal transduction from leaves to shoot apex and the wounding-induced stem growth inhibition. Moreover, both JA biosynthesis and signaling are essential for this long-distance wounding signal transduction. Similar to the primary root growth inhibition assay to JA response in the root, the stem growth measurement can be considered as an approach to evaluate the shoot apex sensitivity to JA or wounding treatment in my experimental system.

4.1.4 Characterization of the JA signaling components in the SAM

Given that the JA signaling response can be activated in the SAM and the exogenous JA negatively affects stem cell maintenance (Figure 4.2 and Figure 4.3), I asked how the JA response is mechanistically regulated in the SAM at a molecular level. To answer this question, I first focused on investigating the key components of the JA signaling in the shoot apex. It has been reported that the regulation of JA biosynthesis and signaling varies between root and shoot (Acosta et al., 2013). Therefore, identifying the group of components particularly involved in JA signaling in the SAM is essential. To this end, I first focused on the key regulators in JA signaling and observed the expression pattern of these components in the SAM.

I first checked the expression pattern of *COI1*, which is the co-receptor of JA. As I failed to image the mRNA accumulation of *COI1* in the SAM by *in situ* hybridization, I acquired the translational reporter *COI1:COI1-GFP* (Larrieu et al., 2015). As shown in the 3D and cross-section image, COI1 was universally distributed in the SAM (Figure 4.4 A). The protein accumulation pattern of COI1 proves the presence of the canonical JA co-receptor in the SAM. Next, I checked the mRNA accumulation pattern of the four *MYC*s genes, which are the key activators of JA-responsive gene expression. According to the results from *in situ* hybridization, only the mRNA signal of *MYC3* can be detected in the SAM (Figure 4.4 B). Also, a higher signal of the *MYC3* probe is detected in the rib zone compared to other regions in the SAM. It is possible that technical issues, such as the probe efficiency, might have resulted in the poor signal detection. Nevertheless, these results suggest that the *MYC* gene, at least *MYC3*, is expressed in the SAM.

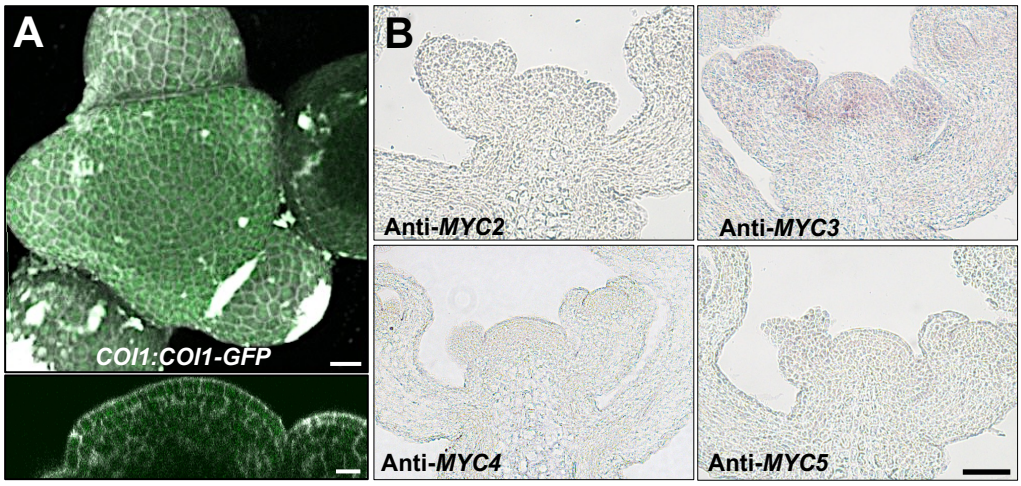


Figure 4.4: Expression pattern of representative components in JA signaling cassette. **A**, representative volume view and central cross-section of the SAM of *COI1:COI1-GFP*. Scale bar = 10 μm. The gray channel depicted the stained SAM with DAPI. **B**, the expression pattern of four *MYC* genes in the SAM. N = 4 -10. Scale bar = 50 μm. SAMs were imaged when the stem length of the plants was 5-8cm.

Next, I observed the expression pattern of *JAZ* genes, which encode JA co-receptors as well as JA signaling repressors. Given that there are 13 *JAZ* genes in *Arabidopsis*, I first selected four genes as primary candidates, which are *JAZ2*, *JAZ3*, *JAZ5*, and *JAZ6* (Table S1). These four genes are potential targets of the key stem cell regulator WUS based on the results of ChIP-seq and RNA-seq done by my colleagues (Ma et al., 2019). *In situ* hybridization results showed that *JAZ3* mRNA was mainly accumulated in the organizing center and the rib zone while *JAZ5* mRNA was weakly detected in the center of the SAM (Figure 4.5). No signal was detected in the SAM with *JAZ2* or *JAZ6* probes, indicating the expression of these genes is repressed in the SAM. The distinct expression pattern of the four *JAZ* genes indicates that the expression of *JAZs* is differentially regulated in the SAM.

As part of feedback regulation, *JAZ* expression is also activated by exogenous JA treatment (Zander et al., 2020). Therefore, I wondered if *JAZ* genes in the SAM could be derepressed with exogenous JA application. Indeed, the expression of *JAZ2*, *JAZ3,* and *JAZ5* is significantly enhanced upon JA treatment (Figure 4.5). However, the expression of *JAZ6* is relatively weak in the SAM despite its strong expression in the stem beneath the SAM upon JA treatment. These results also confirm that JA signaling response can be activated in the SAM by the exogenous JA application.

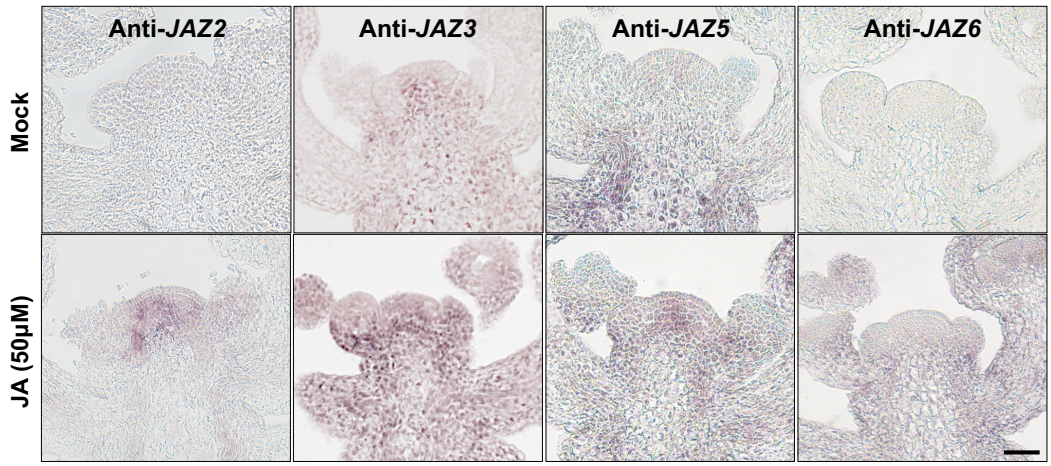


Figure 4.5: Expression pattern of WUS target genes in the SAM with or without JA treatment. Scale bar = 50 μm. N = 5-10. Sample were collected two hours after mock or 50 μM JA treatment. SAMs were collected when the stem length of the plants was 5-8cm.

Altogether, the observed expression pattern of JA signaling components reveals that the SAM possesses a distinct composition of JA activators and repressors from other tissues, confirming the tissue-specific regulation of JA signaling in plants. Furthermore, JA-responsive genes tend to be repressed in the SAM but can be derepressed when JA signaling is activated, which indicates that JA signaling in the SAM is under the control of some specific regulatory machinery.

4.1.5 WUS regulates JA-mediated wounding response in the SAM

To further explore how JA signaling is regulated in the SAM, I first wondered whether the WUS-CLV3 regulatory system contributes to this regulation. WUS is the main regulator of stem cell maintenance and has been reported as a key node in various hormone signaling pathways. Therefore, I focused on investigating the role of WUS in the regulation of JA pathways in the SAM.

As the long-term JA treatment reduced the *WUS* and *CLV3* expressing domain in the SAM (Figure 4.2), I first asked whether WUS activity was also affected in the same way upon shorter-term JA treatment. Therefore, I observed the response of WUS protein to exogenous JA treatment using reporter line *WUS:WUS-linker-GFP wus* (GD44) generated by my colleagues (Daum et al., 2014). To avoid additional JA signaling interference caused by meristem dissection, I fixed the samples using paraformaldehyde (PFA) before dissecting inflorescences. To capture the potential changes in the WUS protein accumulation pattern, I imaged the meristems after 4-hour and 8-hour exogenous JA treatment.

The results show a dynamic response pattern of WUS protein to exogenous JA (Figure 4.6 A): the domain of WUS protein accumulation weakly expanded into the peripheral zone and the rib zone four hours after JA treatment and was restored to its initial size eight hours after JA treatment. This relatively swift change in the WUS distribution pattern indicates a fast response of the SAM after sensing the application of the exogenous JA. However, a complete view of the WUS domain in the rib zone is difficult to capture by the imaging system I used. One possible reason is that the Z-stack imaging encounters challenges with depth penetration, especially in deeper cell layers. To obtain a clear view of the rib zones, I took advantage of vibratome sectioning, in which I can first embed the inflorescence with low melting agarose medium and then section samples into slices with 70μm thickness. Using this method, I also observed the weak expansion of the WUS-GFP domain upon JA treatment in 4 hours (Figure 4.6 B).

Altogether, all these results suggest that WUS protein can be activated by exogenous JA treatment. However, this JA-induced WUS expansion is consistent but mild, indicating that the robust WUS activity regulation in the SAM is hard to perturbate by the short-term JA treatment.

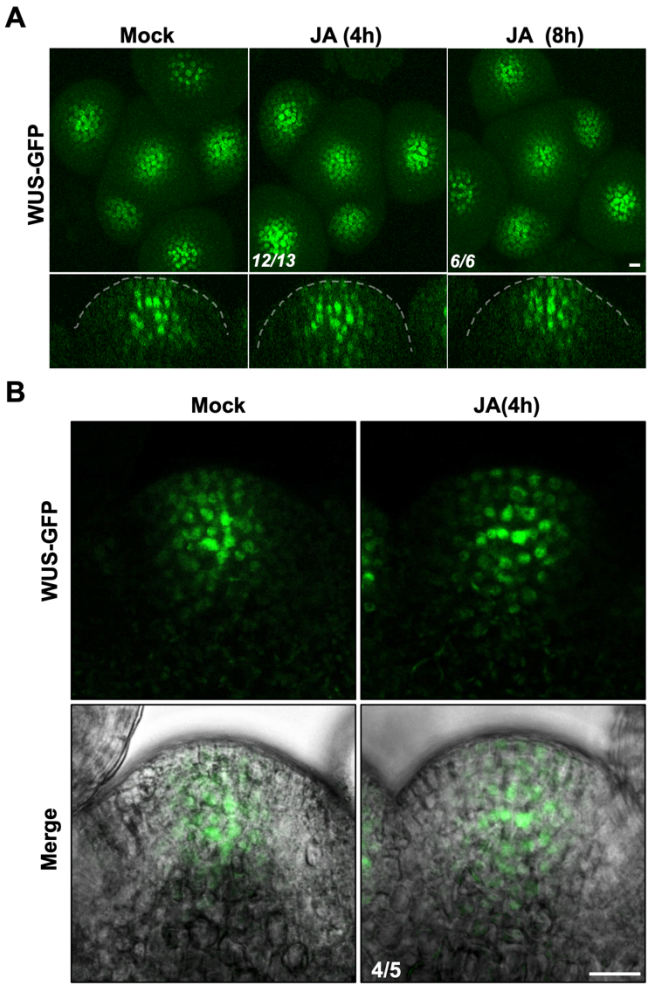


Figure 4.6: The accumulation of WUS protein is enhanced upon short-term JA treatment. A, representative maximum projection images from Z-stack images and central cross-section of SAM domain of *WUS:WUS-linker-GFP wus* plants with mock or 50μM JA treatment. SAMs were imaged directly after inflorescences were dissected. **B**, the GFP channel and the merge channel of the representative images of sectioned SAM of *WUS:WUS-linker-GFP wus* plants by vibratome after mock or 50μM JA treatment. Scale bar = 10 μm. The SAMs were imaged when the stem length of plants was 10-13cm.

Next, to investigate the role of WUS in the regulation of JA response in the SAM, I first evaluated the expression of early JA-responsive genes in the shoot apex of *clv3-10* mutant (Forner et al., 2015), in which WUS activity is enhanced in the absence of functional CLV3. Compared to WT, expression of the four genes is repressed in *clv3-*

10 without exogenous JA treatment (Figure 4.7 A). However, upon exogenous JA treatment, the expressions of these genes were differentially regulated compared to WT (Figure 4.7 B). *JAZ7* expression is upregulated in *clv3-10*, while *LOX3* expression is reduced. Expression of *VSP2* and *JAZ10* did not show significant change. As I only checked the gene expression level after the 2-hour 50μM JA treatment, it is also possible that the early JA response is regulated in a timer and dose-dependent manner in the SAM. Therefore, the result I observed only reflected the situation for a signal time point. Altogether, my current results suggest overexpressing WUS possibly represses the early JA signaling response in the SAM. When the JA level is elevated upon exogenous JA treatment, WUS regulates the expression of the JA-responsive genes distinctly.

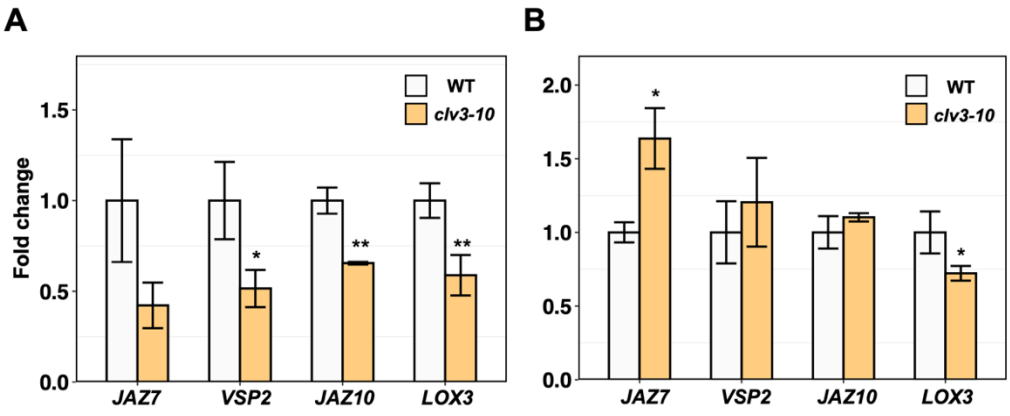


Figure 4.7: Expression of genes in early JA response is repressed in the *clv3-10* mutant. **A-B**, expression of marker genes of early JA response in the apex of the inflorescence of WT and *clv3-10* plants with mock (**A**) or 50μM JA treatment (**B**). The error bar is the mean ± sd of qPCR results from three biological replicates. Statistical analysis: two-tailed Student's t-tests. *P < 0.05, **P < 0.01. The apex of the inflorescence was collected when the stem length of plants was 10-13cm.

As the seven-day wounding and exogenous JA treatment inhibit the inflorescence stem growth (Figure 4.1 and Figure 4.2), I wondered if WUS also regulated the stem growth inhibition mediated by JA and wounding treatment. To this end, I conducted a seven-day JA treatment in *clv3-10* as well as *wus-7*, a weak mutant allele of *WUS* (Graf et al., 2010). Compared to WT, the stem growth of the *clv3-10* mutant was less sensitive to the exogenous JA whereas it was more sensitive in the *wus-7* mutant (Figure 4.8 A and B, Figure S6). Moreover, the stem growth of *clv3-10* is also less sensitive to the systemic wounding treatment (Figure 4.8 C, Figure S6). Altogether, these results

suggest WUS plays a positive role in alleviating stem growth inhibition in response to JA and wounding treatment.

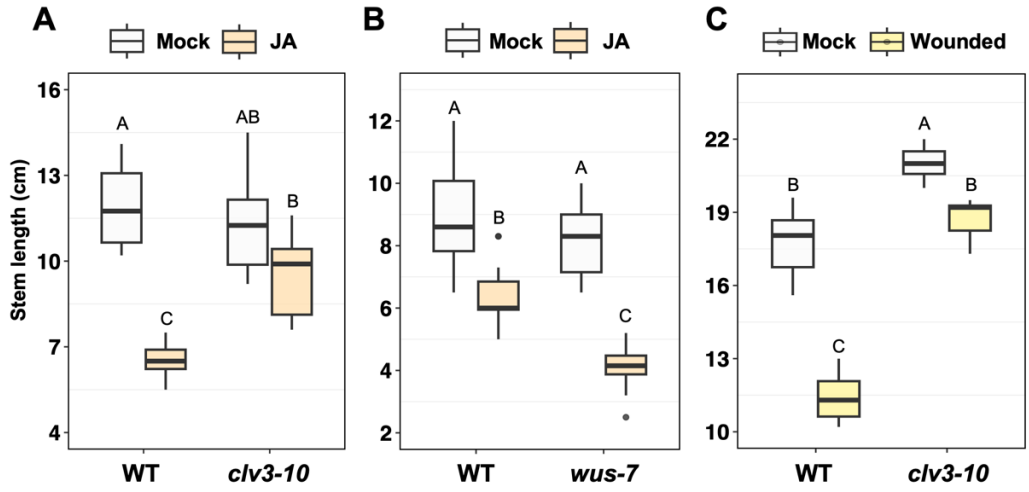


Figure 4.8: CLV3 and WUS are involved in the JA signaling mediated stem growth inhibition. A-B, measurement of stem length of WT, *clv3-10* (**A**) and *wus-7* (**B**) with seven-day 50μM JA treatment. **C**, measurement of stem length of WT and *clv3-10* with seven-day wounding treatment. Statistical analysis: One-way ANOVA (Tukey's test). $P < 0.01$. Three biological replicates were performed for treatment in *clv3-10* (n =10) and one replicate is presented here. One replicate is performed for treatment in *wus-7* (n =12).

4.1.6 WUS interacts with JAZ3

Although WUS potentially represses JA-responsive gene expression and alleviates the developmental effects caused by JA signaling, the molecular mechanism of these processes is still unclear. To further explore the molecular basis of the interaction between the WUS-directed regulatory system and JA signaling, I planned to first select a list of target genes that are not only involved in JA pathways but also potentially connected with WUS function. As for the second criterion, I focused on the genes regulated by WUS at a transcriptional level or the protein interactors of WUS, which are identified from the results of the ChIP-seq and RNA-seq in Ma et al. (2019), and the yeast-two-hybrid screening results from my colleague Dr. Athanasios Lampropoulos. The candidate genes are listed in the Table S1.

Among all these genes, I was particularly interested in the two WUS protein interactors, namely JAZ3 and TIFY8. JAZ3 is the repressor in the JA signaling pathway. TIFY8 belongs to the same protein family as JAZ3, but its function in JA signaling regulation is still unclear. During my study, accumulating evidence suggested that JAZ3 and

TIFY8 are involved in distinct regulatory processes in the SAM. Here, the investigation of the function of JAZ3 is presented.

To validate the potential interaction between WUS and JAZ3, I first did a yeast-two-hybrid assay using the co-transformation system, and the result showed a positive interaction between WUS and JAZ3 (Figure 4.9).

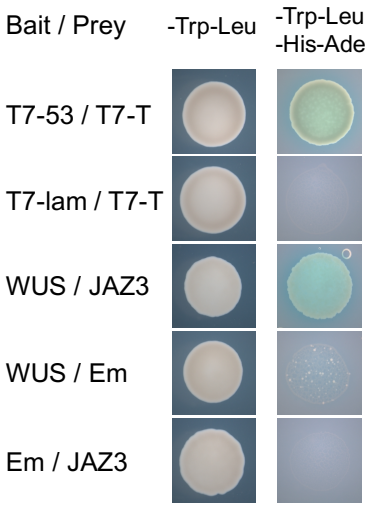


Figure 4.9: WUS interacts with JAZ3 in the Y2H assay. Successful co-transformations with different combinations of vectors were selected with minimal synthetic defined (SD) medium without leucine and tryptophan (-Trp -Leu). Positive interactions were selected on the SD medium without leucine, tryptophan, histidine, and adenine (-Trp -Leu -His -Ade). Colonies with positive protein interaction show a blue color by X-α-Gal treatment. The combination T7-T and T7-53 was used as positive control and T7-T and T7-lam were used as negative control. Em: Empty vector.

Next, I confirmed the interaction by using the AP-FRET system after transient co-expression of potential interaction partners in *Nicotiana benthamiana*. With this approach, I also screened the responsible domains or regions in WUS or JAZ3 required for their interaction. To this end, several truncated versions of proteins were designed (Figure 4.10 A and C). According to the results of FRET efficiency of different combinations, the C-terminal Jas domain in JAZ3 is required but not sufficient for WUS interaction (Figure 4.10 B, Figure S7). The Jas domain in JAZ3 is responsible for its interaction with MYC2 to repress JA signaling activation (Chini et al., 2007). Apart from the Jas domain, the region that contains the conserved ZIM domain is required for JAZ3 interaction with WUS (Figure 4.10 B, Figure S7). The ZIM domain of JAZ3 is

required for the turnover of JAZ3 protein, probably associated with the COI1-dependent 26S proteasome degradation (Chini et al., 2007).

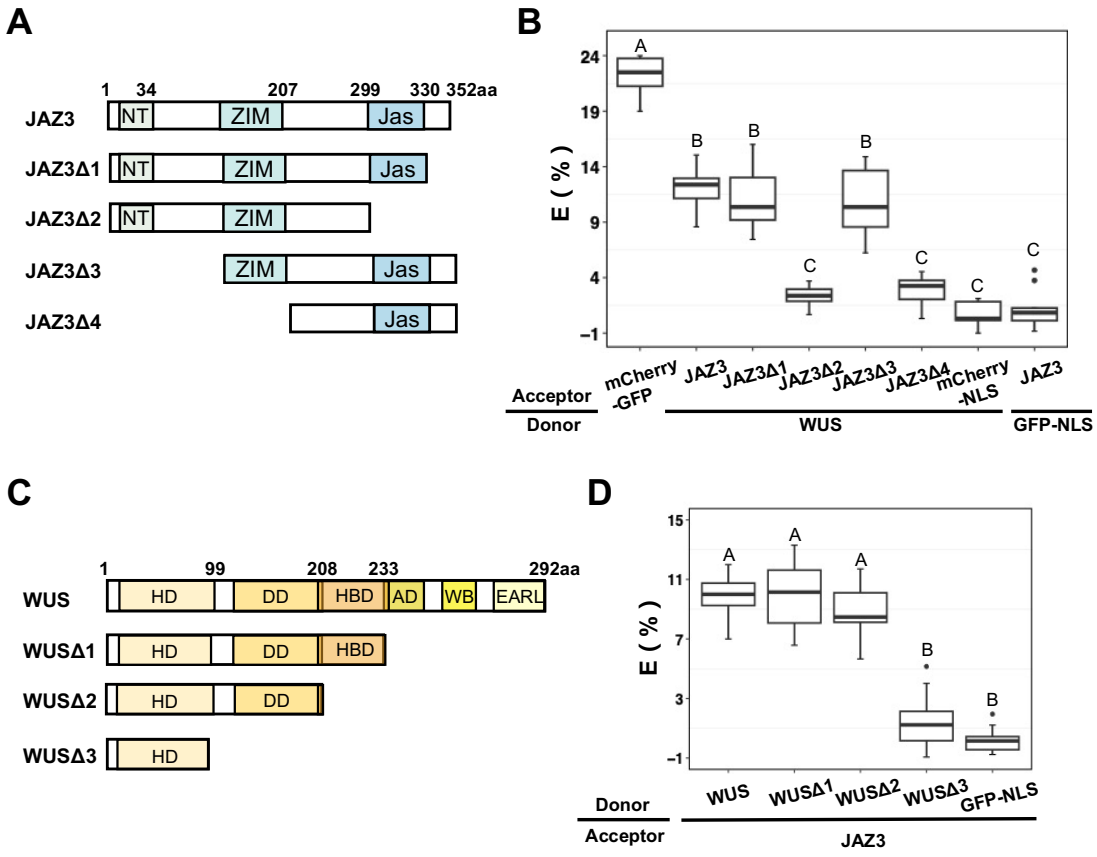


Figure 4.10: WUS interacts with JAZ3 in the AP- FRET assay. A, C: schematic representation of the truncated versions of JAZ3 (**A**) and WUS (**C**). Numbers indicate the start or end of different truncations in amino acids from the N-terminus of the protein. HD: homeodomain; DD: dimerization domain; HBD: HAM binding domain; AD: acidic domain; WB: WUS-box; EARL: EAR-like domain. **B**, **D**: AP-FRET experiments for protein interaction between WUS and truncated versions of JAZ3 (**B**), or protein interaction between truncated versions of WUS and JAZ3 (D). "Acceptor" refers to protein fused with mCherry. "Donor" refers to a protein fused with GFP. "E" refers to FRET efficiency. mCherry-GFP is used as the positive control, in which GFP is directly fused with mCherry. For each combination, the efficiencies of 10 nuclei were calculated in one biological replicate. Statistics were analyzed using one-way ANOVA with the Tukey test ($P<0.01$). Three biological replicates were performed and the result of one replicate is presented here.

On the other hand, the dimerization domain of WUS is required for WUS to interact with JAZ3, as deleting the dimerization domain in the WUSΔ3 version failed to interact with JAZ3 (Figure 4.10 D, Figure S7). Altogether, these results suggest that WUS interacts with JAZ3. This interaction may affect the regulation of JAZ3 repressor

function as well as JAZ3 protein degradation. Moreover, the unstructured region of WUS in the dimerization domain is required for interacting with JAZ3.

4.1.7 *JAZ3* is expressed in the SAM

To confirm whether the *JAZ3* expression pattern overlaps with the WUS domain, I did *in situ* hybridization and generated transcriptional and translational reporters of JAZ3. According to *in situ* hybridization results, the mRNA signal of *JAZ3* is specifically detected in the organizing center as well as the rib zone and the stem tissue beneath the rib zone (Figure 4.11 A). The *JAZ3* expression pattern presented in the transcriptional reporter *JAZ3: GFP-NLS* agreed with the result of *in situ* hybridization in the SAM (Figure 4.11 B). Also, *JAZ3* was expressed in initiating primordia according to *JAZ3: GFP-NLS*. As for the translational reporter *JAZ3: GFP-JAZ3*$_{CDS}$, no signal could be detected even in the homozygous lines. Considering that JAZ3 is easily degraded by JA signaling activation (Chini et al., 2007), the JAZ3 protein might not be stable in the SAM after the inflorescence dissection., which may consistently introduce wounding and trigger JA signaling in the SAM.

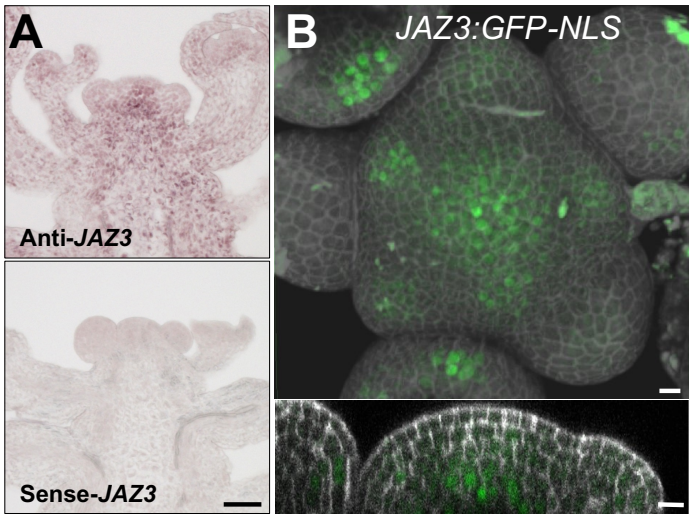


Figure 4.11: Expression pattern of *JAZ3* in the SAM. **A**, *In situ* hybridization in the SAM with anti-sense and sense probes of *JAZ3*. Scale bar=50 μm. **B**, representative volume view and central cross-section of the SAM of *JAZ3:GFP-NLS*. The gray channel depicted the stained SAM with DAPI. Scale bar = 10 μm. SAMs were imaged when the stem length of the plants was 5-8cm.

4.1.8 WUS promotes *JAZ3* expression

Given that WUS is a transcription factor and the expression pattern of *JAZ3* overlaps with the WUS domain, I wondered if WUS could regulate the expression of *JAZ3*. To

this end, I checked the expression pattern of *JAZ3* in *UBQ10: mCherry-GR-linker-WUS*. In this inducible expression system, ubiquitously expressed WUS in the cell is fused with glucocorticoid receptor (GR) and the translocation of the respective cytosolic fusion protein to the nucleus can be induced by DEX treatment (Ma et al., 2019). Results from *in situ* hybridization revealed the expression of *JAZ3* is enhanced by inducible overexpression of WUS-GR with DEX treatment (Figure 4.12 A). Next, I checked the expression of other JA signaling-related genes in the SAM (Figure 4.12 A). *JAZ2*, *JAZ5,* and *MYC3* displayed different expression patterns but their expression was not significantly enhanced by overexpressing WUS-GR.

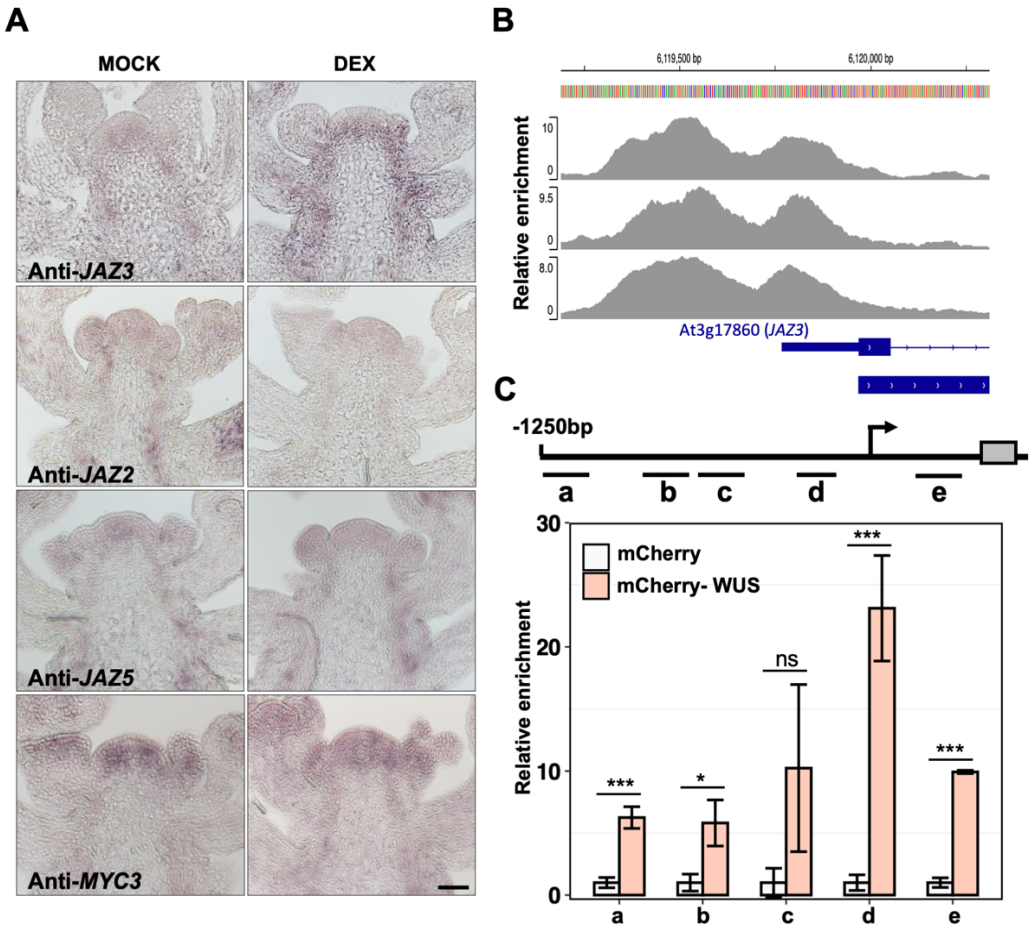


Figure 4.12: WUS promotes *JAZ3* expression in the SAM. **A**, expression pattern of selected candidates in the SAM of *UBQ10:mcherry-GR-linker-WUS* with or without dexamethasone (DEX) treatment. Scale bar = 50 µm. N ≥3. mCherry-WUS-GR in the SAM was induced by spraying 10 µM DEX on the shoot apex for two hours. SAMs were imaged when the stem length of the plants was 5-8cm. **B**, the relative enrichment of WUS-GR in the genomic regions of *JAZ3* identified by eChIP-seq. Three replicates are presented. The image was downloaded from Integrative Genomics Viewer. **C**, qPCR results of the enrichments of *JAZ3* fragments by eChIP. Regions a-d are located in the *JAZ3* promoter, while the region e is located in the 5'untranslated region of *JAZ3*. Five-day-old seedlings of *UBQ10:mCherry-GR-linker-WUS* and *UBQ10:mCherry-GR* were treated with DEX for 4 hours before they were collected for the eChIP experiment. The error bar is the mean ± sd of results from three biological replicates. Statistical analysis: two-tailed Student's t-tests, *P < 0.05, ***P < 0.001, ns =not significant.

Moreover, according to the profile of eChIP-seq with *UBQ10: mCherry-GR-linker-WUS* from my colleague Ines Hidalgo Prados, WUS can bind to *JAZ3* promoter regions, indicating that WUS was directly involved in the *JAZ3* transcriptional regulation (Figure 4.12 B). To confirm this result, I performed eChIP-qPCR with seedlings of the same transgenic lines used for eChIP-seq. The relative enrichment of WUS on the five regions of the *JAZ3* promoter and 5'untranslated region was checked (Figure 4.12 C). Compared to the control, in which mCherry-GR is ubiquitously expressed, mCherry-WUS-GR is significantly enriched in four out of five sites. The enrichment of regions near the transcription start site as well as the 5'-UTR of *JAZ3* is higher (Figure 4.12 C), suggesting that WUS indeed directly regulates the expression of *JAZ3*.

Overall, according to the results from the inducible WUS overexpression system, WUS not only interacts with JAZ3, but it can also directly bind to the *JAZ3* genomic region and activate the expression of *JAZ3* in the SAM. Therefore, JAZ3 is possibly an important node in the interplay between JA signaling and the regulatory system of stem cell maintenance.

4.1.9 The function of JAZ3 in stem cell maintenance

As JAZ3 interacts with WUS and WUS can regulate *JAZ3* expression (Figure 4.10 and Figure 4.12), I wondered whether JAZ3 was also involved in the regulation of stem cell maintenance mediated by WUS. To test this hypothesis, I generated *WUS:JAZ3* transgenic lines, in which the expression of *JAZ3* is enhanced in the *WUS*-expressing domain. To quantify the SAM phenotypes, I generated *WUS:JAZ3* transgenic lines in the *TR7* background and conducted the *TR7* analysis pipeline with homozygous *WUS:JAZ3/TR7* transgenic lines. Despite the variation between the two individual lines, the SAM of *WUS:JAZ3* displayed an overall slightly increased cell number, but a similar SAM size and number of *WUS* or *CLV3* cells as *TR7 (*Figure 4.13 A-D). Moreover, expressing JAZ3 under the *WUS* promoter did not alter the fasciated inflorescence phenotype of the *clv3-10* mutant (Figure 4.13 E).

Altogether, these results suggest overexpressing *JAZ3* does not affect stem cell maintenance in the SAM, at least it doesn't seem to affect WUS function. However, more evidence is needed to comprehensively characterize the function of JAZ3 in stem cell maintenance.

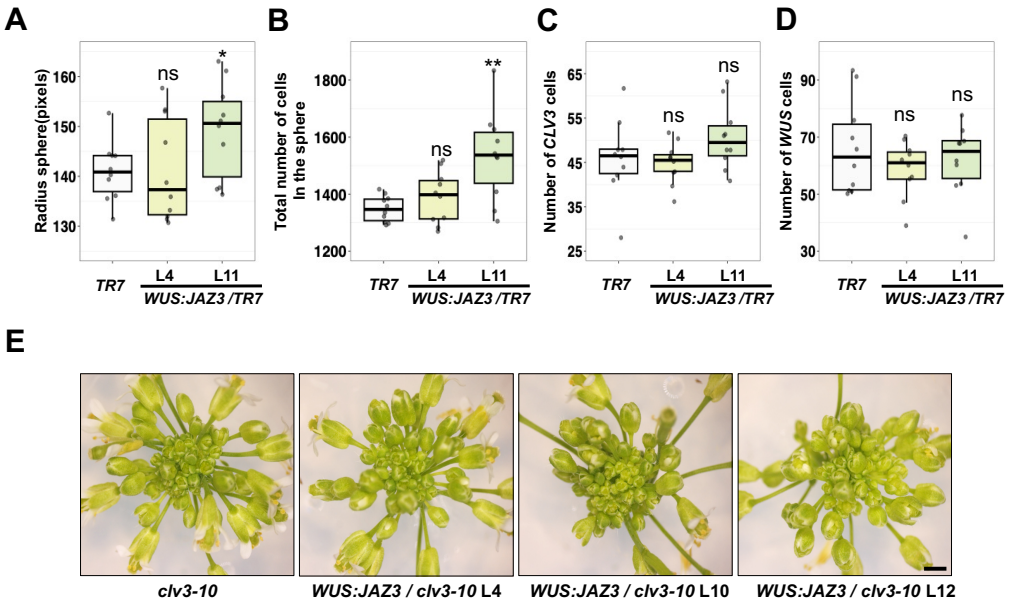


Figure 4.13: Overexpressing *JAZ3* in the *WUS* domain does not alter the SAM morphology. **A**, SAM morphology analysis of *TR7* and *WUS:JAZ3/TR7* by computational image analysis pipeline. The SAM was imaged when the stem length of the plant is 10-12cm. Statistical analysis: two-tailed Student's t-tests for **B-D**, Wilcoxon rank-sum test for **A**. *P < 0.05, **P < 0.01, ns =not significant. N=10. **E**, the inflorescence tip of *clv3-10* and *WUS:JAZ3 / clv3-10* in T3 generation. Scale bar =100 µm. The inflorescence tip was imaged when the stem length of the plant was 8-10cm.

4.1.10 JAZ3 is a potential regulator of flowering

To further decipher the function of JAZ3 in the SAM, I generated the *jaz3-cr* mutant using the CRISPR/Cas9 knockout system (Figure 4.14 A, Figure S8). Meanwhile, I also acquired the T-DNA insertion triple mutant *jaz3 jaz5-1 jaz10-1(jaz3/5/10)* (de Torres Zabala et al., 2016). Four weeks after germination, the mutants *jaz3-cr* and *jaz3/5/10* presented WT-like growth and developmental phenotypes, except for the shorter inflorescence stems compared to *TR7* (Figure 4.14 B). On the other hand, the inflorescence stems of *WUS:JAZ3/TR7* transgenic lines seem to be longer compared to *TR7* (Figure 4.14 C).

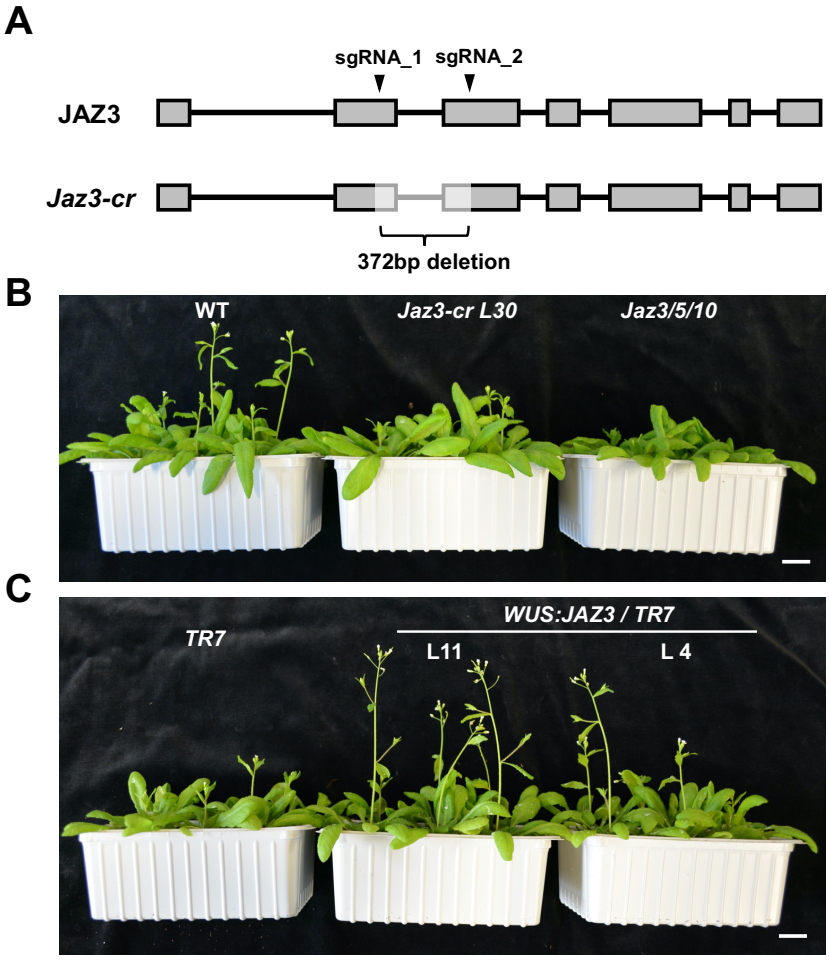


Figure 4.14: The inflorescence stem growth of *jaz3* mutants and *WUS:JAZ3* transgenic lines. A, Schematic graph of CRISPR/Cas9 knock-out *jaz3-cr* mutants. The grey box indicates exon, and the black line indicates intron. The arrowhead indicates the target site of sgRNA. **B**, four-week-old WT, *jaz3,* and *jaz3/5/10* mutant in Col-0 background. **C**, four-week-old *WUS:JAZ3* transgenic lines in *TR7* background. Scale bar = 2cm.

As the stem growth-related phenotype may be due to the regulation of flowering time, I measured the time to bolt and the number of rosette leaves after bolting of the listed genotypes. Compared to WT, the time to bolt is slightly delayed in *jaz3*-related mutants but is earlier in the transgenic lines in which overexpressing *JAZ3* or truncated *JAZ3* without Jas domain under *WUS* promoter (Figure 4.15 A and C, Figure S9 and S10). Also, *jaz3* mutants possessed more leaves after bolting while *WUS:JAZ3* and *WUS:JAZ3Δ2* possessed fewer leaves compared to WT(Figure 4.15 B and D, Figure S9 and S10). These results demonstrated that JAZ3 is a potential regulator of flowering, and the stem growth phenotypes of *jaz3* mutant and *WUS:JAZ3* transgenic lines are likely linked to flowering control.

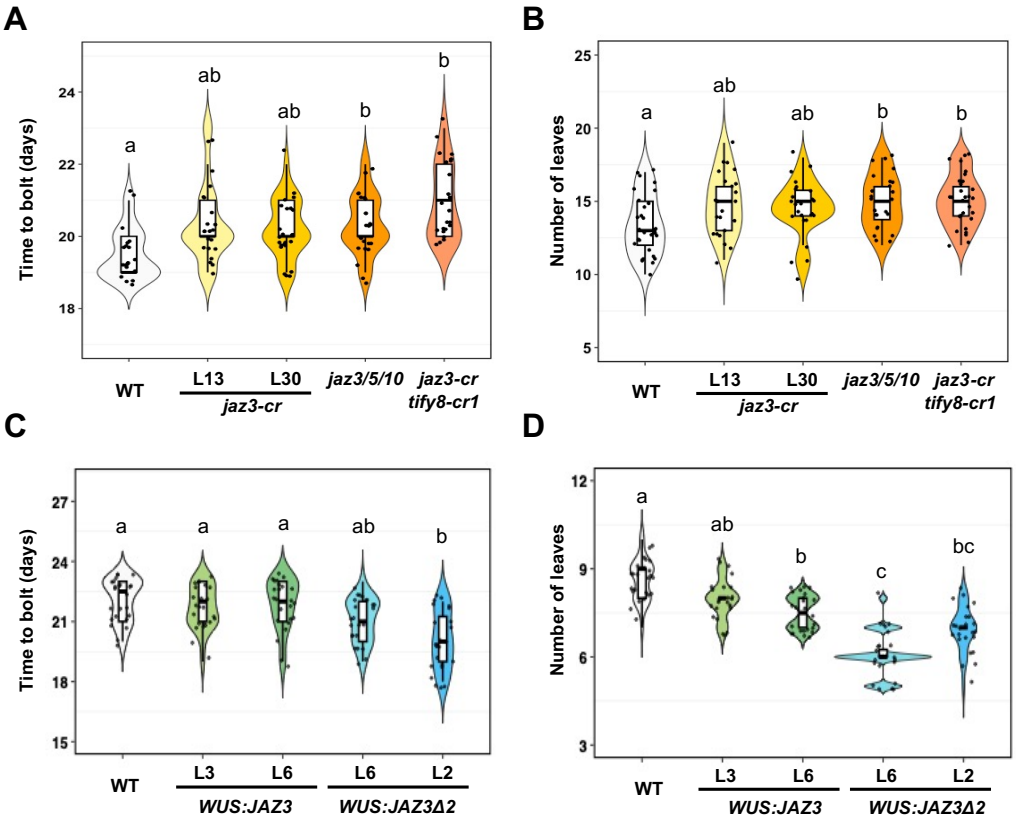


Figure 4.15: Flowering time of JAZ3-related mutants and transgenic lines. A-B, Time to bolt (**A**), and the number of leaves after bolting (**B**) of JAZ3-related mutants. **C-D**, Time to bolt (**C**), and the number of leaves after bolting (**D**) of *WUS:JAZ3* and *WUS: JAZ3Δ2.* Time to bolt was recorded when the bolted stem length was 0.5 cm, and the number of leaves was counted at the same time. N= 22-30. Three biological replicates were performed, and one replicate is presented here. Statistics were analyzed using the Kruskal-Wallis test followed by Dunn's multiple comparison test (P<0.05).

4.1.11 JAZ3 regulates the stem growth in response to systemic wounding

Given that WUS can alleviate the stem growth inhibition caused by exogenous JA and systemic wounding (Figure 4.8), I wondered whether JAZ3 could also be involved in this regulatory process. Therefore, I first explored the function of JAZ3 in wounding-mediated stem growth inhibition. To this end, I conducted the systemic wounding treatment in mutants *jaz3-cr*, *jaz3/5/10,* and *WUS:JAZ3* transgenic lines. As the difference in flowering time might affect the observation of the stem length, the wounding treatments all started when the stem length was 0-0.5cm after bolting.

Compared to WT, stem growth of *jaz3-cr* tended to be more sensitive to systemic wounding. However, the significance of the tendency varies among different biological replicates (Figure 4.16 A, Figure S11). This result suggests that JAZ3 and other

unknown regulators may act together to the stem growth regulation in response to systemic wounding. In *Arabidopsis*, the 13 JAZ proteins redundantly regulate the JA response in a tissue-specific manner (Chini et al., 2016). Therefore, other JAZ proteins apart from JAZ3 may contribute to the wounding-mediated stem growth regulation. Therefore, I performed the wounding treatment in *jaz3/5/10* together with the *jaz3-cr* single mutant. The stem length of the triple mutant *jaz3/5/10* was between WT and *jaz3-cr* after the long-term wounding treatment (Figure 4.16 A, Figure S11). It seems that the mutation in *JAZ5* and *JAZ10* did not enhance the sensitivity of the stem growth displayed in the *jaz3-cr* to the systemic wounding. However, considering that the significance of the phenotypes also depends on the types of mutagenesis, it is hard to conclude whether JAZ5 and JAZ10 share the same role as JAZ3 in the stem growth regulation upon wounding treatment so far.

In addition, compared to WT, the *WUS:JAZ3* transgenic lines displayed less inhibited stem growth upon systemic wounding (Figure 4.16 B, Figure S11), indicating that overexpressing *JAZ3* under *WUS* promoter can alleviate the stem growth inhibition upon systemic wounding treatment. Furthermore, to check whether the resistance to systemic wounding in *WUS:JAZ3* plants was correlated to the JA signaling in the apex of the inflorescence. I conducted the seven-day JA treatment in *WUS:JAZ3* transgenic lines and measured the stem length of treated plants. Compared to WT, *WUS:JAZ3* plants were more resistant to exogenous JA treatment (Figure 4.16 C, Figure S12). This result indicates that expressing JAZ3 in the *WUS* domain can repress the effect of JA response on stem growth. Altogether, JAZ3, the same as WUS, is a positive regulator in alleviating the stem growth inhibition induced by JA-mediated systemic wounding.

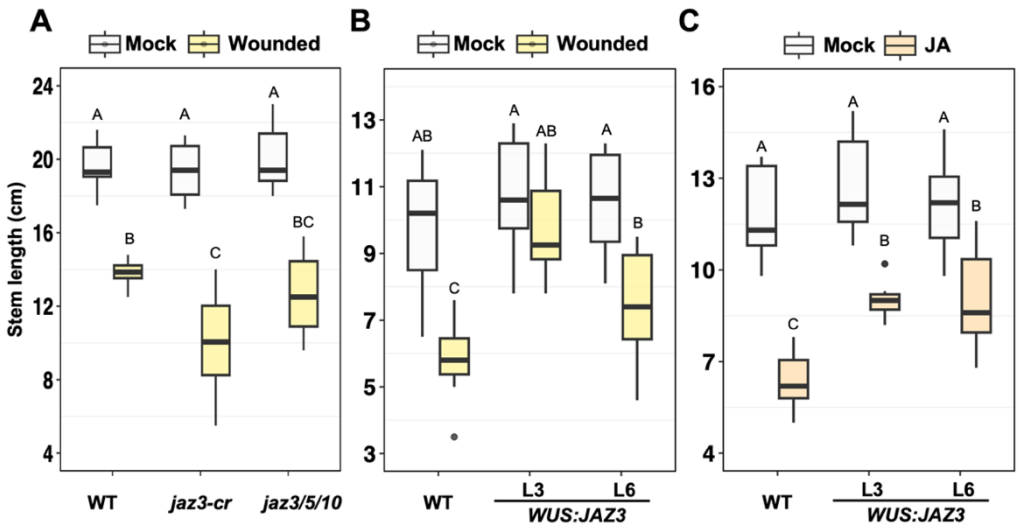


Figure 4.16: JAZ3 is involved in stem growth regulation in response to the JA mediated-systemic wounding. A, Stem length measurement of WT, *jaz3-cr L30*, and *jaz3/5/10* with mock or wounding treatment. N=10. Three biological replicates were performed for WT and *jaz3-cr L3*0, and two replicates for *jaz3/5/10*. **B**, Stem length measurement of WT and *WUS:JAZ3* with mock or wounding treatment. N=10. **C**, Stem length measurement of WT and *WUS:JAZ3* with mock or 50μM JA treatment. N=11. Three biological replicates were performed, and one replicate is presented here. Statistics analysis: one-way ANOVA with Tukey test (P<0.01)**.**

4.2 The function of TIFY8 in stem cell maintenance

The same as JAZ3, TIFY8 is identified as a potential WUS interactor from our yeast-two-hybrid screening profile. Although it belongs to the TIFY protein family and can interact with the adaptor protein NINJA similarly to JAZ3, the transgenic plants with altered *TIFY8* expression display WT-like JA sensitivity (Cuéllar Pérez et al., 2014). It is still disputable whether TIFY8 is directly involved in the JA-dependent regulatory processes. At the beginning of my study, I initially selected TIFY8 as a candidate of interest to investigate the molecular basis of JA signaling regulation in the SAM. However, accumulating evidence suggests that TIFY8 plays a distinct role from JAZ3 in regulating stem cell maintenance, which is associated with the WUS-CLV3 regulatory system instead of the JA signaling pathway.

4.2.1 *TIFY8* is expressed in the SAM

In Cuéllar Pérez et al. (2014), the GUS accumulation pattern in the *TIFY8:GUS-GFP* reporter suggests that *TIFY8* is expressed in the shoot apex of *Arabidopsis* seedlings. To confirm the expression pattern of *TIFY8* in the SAM, I first performed the *in situ* hybridization with the *TIFY8* probe. The result reveals that *TIFY8* is specifically expressed in the organizing center and the rib zone in the SAM (Figure 4.17 A). In addition, I generated two fluorescent reporter lines, namely *TIFY8:GFP-NLS* and *TIFY8:TIFY8*$_{CDS}$*-GFP*, to further evaluate the expression pattern of *TIFY8.* GFP driven by *TIFY8* promoter exhibited a broader expression pattern, while TIFY8-GFP is mainly restricted to the center of the SAM and the young primordia (Figure 4.17 B and Figure 4.19). The difference between the *in situ* hybridization result and the reporter lines suggests that the expression of *TIFY8* might undergo regulations at post-transcriptional and translational levels. Nevertheless, taking all these results together, *TIFY8* is expressed in the SAM and its expression domain partially overlaps with the WUS domain.

Next, to check whether the exogenous JA can alter the expression of *TIFY8* in the SAM, I performed the *in situ* hybridization with the *TIFY8* probe upon JA treatment. Compared to the mock, the expressing domain of *TIFY8* was mildly expanded in the JA-treated SAM (Figure 4.17 C). However, the change was not as significant as that of *JAZs* (Figure 4.5), indicating *TIFY8* may not be a JA early response gene in the SAM.

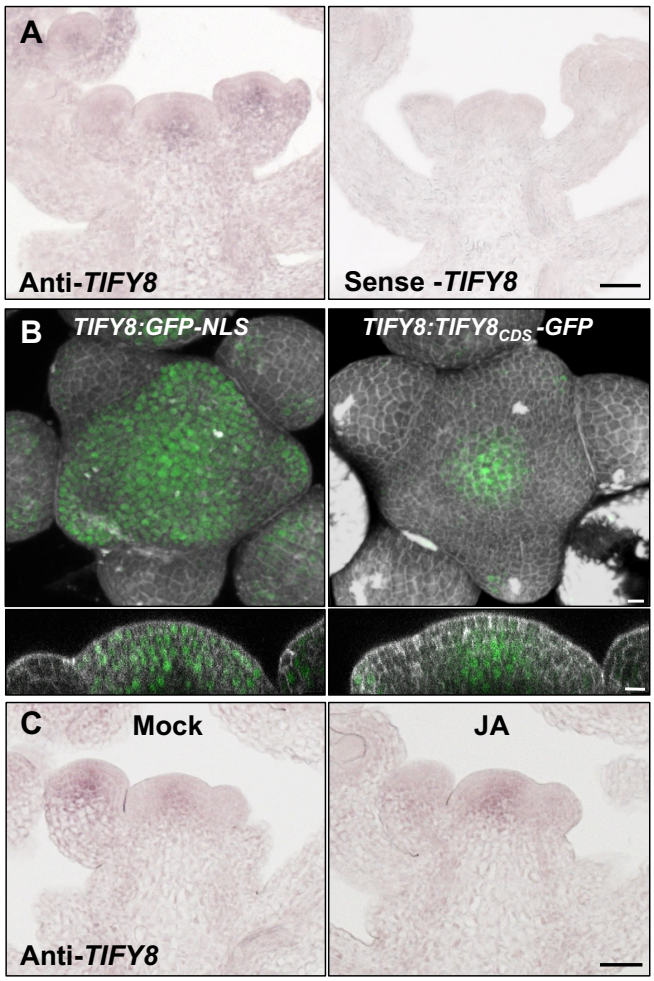


Figure 4.17: Expression pattern of *TIFY8* in the SAM. **A**, *In situ* hybridization in SAM with anti-sense and sense probes of *TIFY8*. Scale bar = 50μm. **B**, the expression pattern of GFP-NLS and TIFY8$_{CDS}$-GFP under *TIFY8* promoter. The gray channel depicted the DAPI-stained SAM. Scale bar = 10 μm. **C**, the expression pattern of *TIFY8* in the SAM with or without JA treatment. Sample were collected two hours after mock or 50μM JA treatment. Scale bar = 50 μm.

4.2.2 TIFY8 interacts with WUS

To validate the interaction between WUS and TIFY8, I did a yeast-two-hybrid as well as the AP-FRET in the transient co-expression system in *Nicotiana benthamiana.* The yeast-two-hybrid result confirmed the positive interaction between TIFY8 and WUS (Figure 4.18 A).

Next, I designed the truncated versions of the TIFY8 protein and used AP-FRET to map potential protein domains responsible for the interaction between WUS and TIFY8 (Figure 4.18 B). The deletion of the C-terminal ZIM domain (TIFY8Δ3) eliminates the WUS-TIFY8 interaction. Moreover, an uncharacterized region near the N-terminus of

TIFY8 is also responsible for interacting with WUS (Figure 4.18 C, Figure S13). Same as in the case of JAZ3, the dimerization domain of WUS is required for the interaction between TIFY8 and WUS (Figure 4.18 D, Figure S13). Altogether, both the ZIM domain of TIFY8 and the dimerization domain of WUS are required for the interaction between WUS and TIFY8, which is similar to the interaction between JAZ3 and WUS. The region near the N-terminus of TIFY8 is also essential for interacting with WUS.

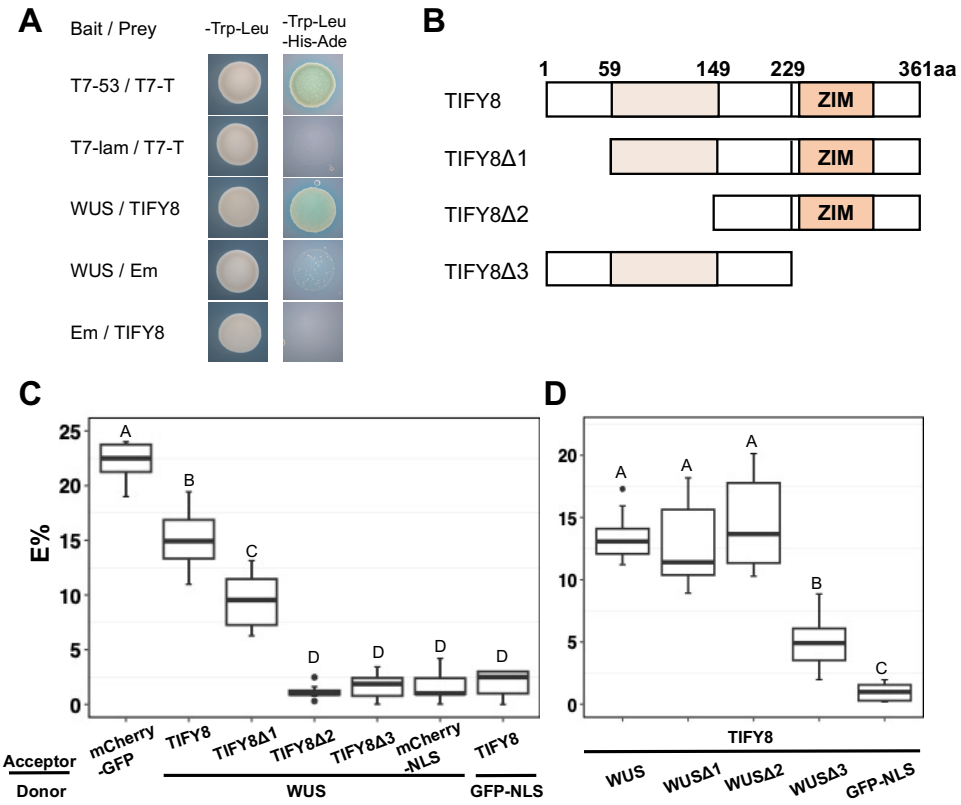


Figure 4.18: WUS interacts with TIFY8. A, WUS interacts with TIFY8 in the yeast-two-hybrid assay. The same experimental system was used as in Figure 4.9. Two biological replicates were performed. **B**, schematic representation of the sequence deletion assay of TIFY8. Numbers indicate the start or end of different truncations in amino acids from the N-terminus of the protein. **C-D**, AP-FRET experiments for protein interaction between WUS and truncated versions of TIFY8 (**C**), or protein interaction between truncated versions of TIFY8 and WUS(**D**). "Acceptor" refers to protein fused with mCherry. "Donor" refers to the protein fused with GFP. "E" refers to FRET efficiency. mCherry-GFP is used as the positive control. For each combination, the FRET efficiencies of ten nuclei were calculated in one biological replicate. Statistics were analyzed using one-way ANOVA with the Tukey test ($P<0.01$). Three biological replicates were performed, and one is presented here.

4.2.3 The function of WUS in the transcriptional and translational regulation of TIFY8

To investigate whether TIFY8 is regulated by WUS at either transcriptional or translational level, I generated transgenic lines combining *TIFY8* reporters and *UBQ10: mCherry-GR-linker-WUS*. These transgenic lines allow me to capture the dynamic changes of GFP-NLS or TIFY8$_{CDS}$-GFP upon inducible WUS overexpression. As shown in Figure 4.19, I did not observe any significant changes of the GFP signal in both transcriptional and translation reporters upon DEX treatment. Moreover, unlike the case for *JAZ3*, the *TIFY8* mRNA accumulation pattern is not changed two hours after DEX induction according to the *in situ* hybridization result (Figure S14). Therefore, overexpressing WUS does not alter the *TIFY8* expression and TIFY8 protein accumulation, suggesting that WUS may not regulate *TIFY8* expression or TIFY8 protein abundance. However, given that only the inducible system is used in my study, more evidence is needed to draw a complete picture of TIFY8 regulation associated with WUS.

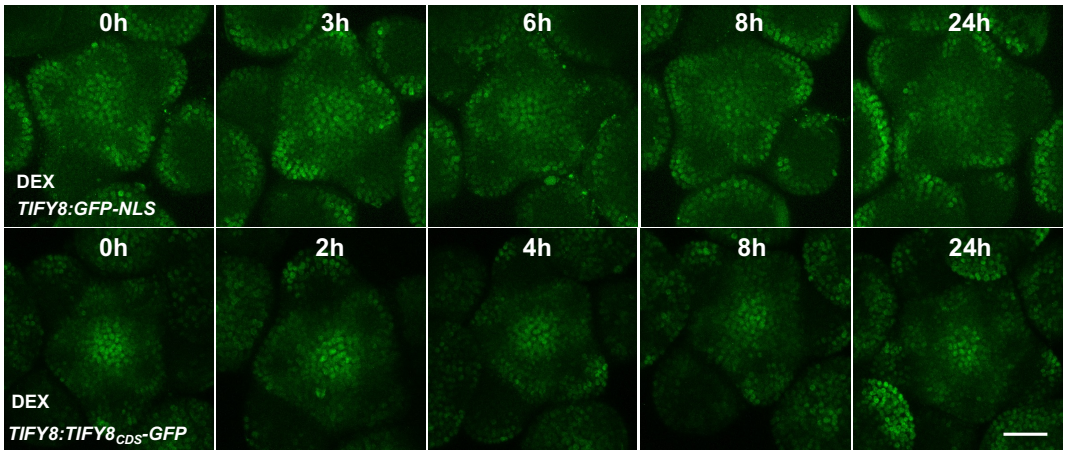


Figure 4.19: Inducible overexpression of WUS does not alter the expression of *TIFY8* and TIFY8 protein accumulation. Time-course imaging of expression pattern of GFP-NLS and TIFY8$_{CDS}$-GFP driven by *TIFY8* promoter under *UBQ10: mCherry-GR-linker-WUS* background with DEX treatment. N=3-4 at each time point. Scale bar = 50 μm.

4.2.4 The function of TIFY8 in stem cell maintenance in the SAM

As TIFY8 can interact with WUS, I reasoned that the biological role of TIFY8 could be linked to the function of WUS in regulating stem cell maintenance. To test this hypothesis, I generated CRISPR/Cas9 knockout mutants of *TIFY8* as well as the transgenic lines, in which TIFY8 is expressed under *WUS* or *CLV3* promoter. Two

mutant alleles were isolated (Figure 4.20 A, Figure S8). Mutant *tiyf8-cr1* contains a 953bp deletion while the allele *tiyf8-cr2* possesses single-nucleotide insertion before the first exon and another one in the second exon. Single mutant *tify8-cr1* exhibited a WT-like inflorescence phenotype. However, the mutation of *TIFY8* in the *clv3-10* background partially rescued the fasciated inflorescence phenotype of the *clv3-10* mutant (Figure 4.20 B). The result from the number of reproductive organs suggests that the rate of organ production in *clv3-10* is reduced when *TIFY8* is mutated (Figure 4.20 C).

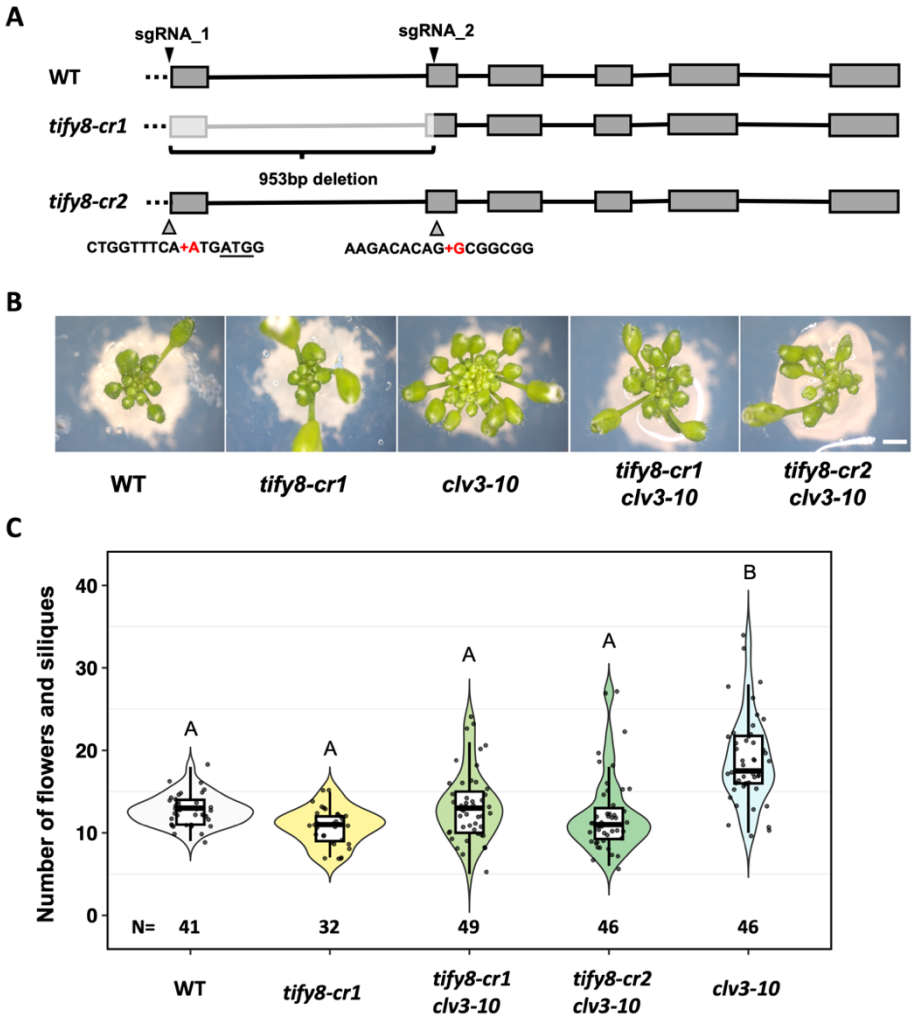


Figure 4.20: Mutation of TIFY8 partially rescues the inflorescence phenotype of *clv3-10* mutant. **A**, the schematic graph of CRISPR/Cas9 knock-out *tify8* mutants. Grey boxes indicate exons. Black lines indicate introns. dotted lines indicate the five prime untranslated regions. Black arrowheads indicate the targeted sites of sgRNA. Gray arrowheads indicate the single nucleotide insertion site. Letters with red color indicate the single inserted base pair. The translational initiation site is marked with the underline. **B**, inflorescence tip of WT, *tify8-cr1*, *clv3-10,* and *tify8-cr clv3-10* mutants. Scale bar = 100 µm. **C**, measurement of floral organs and siliques of represented genotypes. When stem length is 17-22cm, flowers in stage P13-20 were counted (Smyth et al., 1990). Statistical analysis: one-way ANOVA with the Tukey test ($P<0.01$). The results are from two biological replicates.

Next, to observe the SAM phenotypes, I dissected the inflorescence and quantified the area of the SAM of the listed genotypes. Compared to WT, *tify8-cr1* displayed a smaller SAM area (Figure 4.21 A and B). The same pattern was also shown in the *clv3-10* background (Figure 4.21 C). This phenotype was fully complemented when the reporter *TIFY8:TIFY8$_{CDS}$-GFP* was introduced into *clv3-10 tify8-cr1* double mutant background (Figure 4.21 D). Altogether, it appears that TIFY8 is involved in stem cell maintenance regulation. The mutation of *TIFY8* may prevent the excessive cell proliferation in the SAM of *clv3-10*, which is caused by the loss of WUS repression.

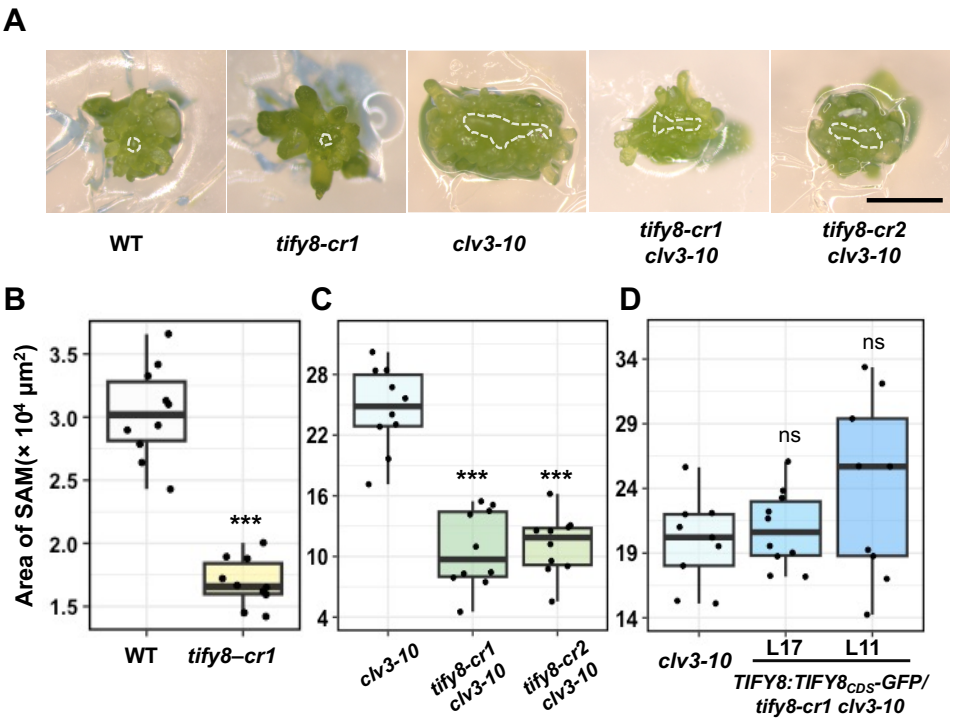


Figure 4.21: Mutation of TIFY8 reduces SAM size. **A**, SAM of WT, *tify8-cr1*, *clv3-10,* and *tify8-cr clv3-10* mutants. Scale bar = 100 μm. **B**, quantification of the area of the SAM of WT and *tify8–cr1*. **C**, quantification of the area of the SAM of *clv3-10* and *tify8-cr clv3-10* mutants. **D**, quantification of the area of the SAM of *clv3-10* and *TIFY8:TIFY8$_{CDS}$-GFP/tify8-cr1 clv3-10.* Statistical analysis: two-tailed Student's t-tests compared to control. ***P < 0.01. ns =not significant. N=9-10. SAMs were imaged when the stem length of the plant was 8-10cm.

In addition, I observed the inflorescence phenotypes of TIFY8-related transgenic lines, namely *WUS:TIFY8* and *CLV3:TIFY8*. *WUS:TIFY8* showed WT-like inflorescence (Figure 4.22 A), whereas the inflorescence tip of *CLV3:TIFY8* is enlarged compared to WT (Figure 4.22 B). Images of respective SAMs revealed cell over-proliferation occurred in the meristem of *CLV3:TIFY8* (Figure 4.22 C). Altogether, the genetic

evidence suggests that TIFY8 is involved in the regulation of cell proliferation in the SAM, which is potentially associated with the WUS-CLV3 regulatory loop.

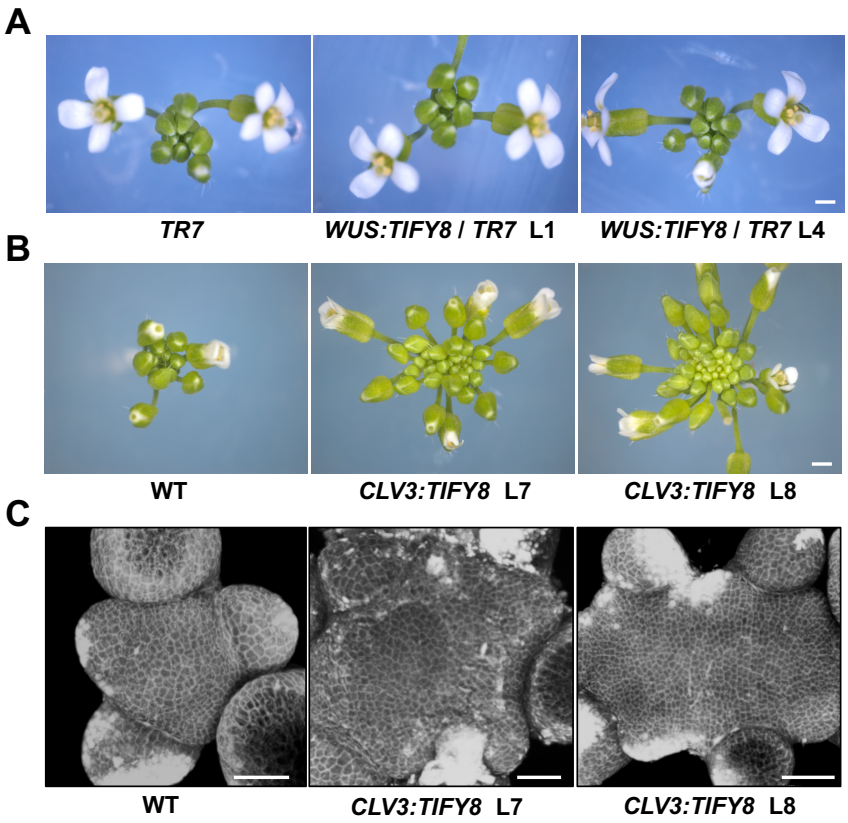


Figure 4.22: Ectopically expressing *TIFY8* in the *CLV3* domain results in enlarged meristems. A, inflorescence tip of *TR7* and *WUS:TIFY8* plants under *TR7* background. Scale bar = 100 µm. **B**, inflorescence tip of *WT* and *CLV3:TIFY8* plants. Scale bar = 100 µm. **C**, the volume views of Z-stack images of SAMs of WT and *CLV3:TIFY8* plants. The gray channel depicted the stained SAM with DAPI. Scale bar = 50µm. The inflorescence tips and SAMs were imaged when the stem length of the plant was 8-10cm.

4.2.5 TIFY8 is a potential regulator of root stem cell maintenance

It has been reported that *TIFY8* is also expressed in the root tip (Cuéllar Pérez et al., 2014). To assess the TIFY8 expression pattern in detail, I imaged the root tip of *TIFY8:TIFY8*$_{CDS}$*-GFP* reporter. TIFY8-GFP is accumulated in the quiescent center, columella cells, and the stele initials (Figure 4.23 A). This pattern overlapped with that of WOX5, a transcription factor of the WUSCHEL-related homeobox gene family and the key regulator in root stem cell maintenance. Moreover, AP-FRET results suggested that TIFY8 interacted with WOX5, indicating that TIFY8 might be directly associated with the WOX5 function (Figure 4.23 B). All these results suggest that TIFY8 might be a conserved interactor with the WOX proteins.

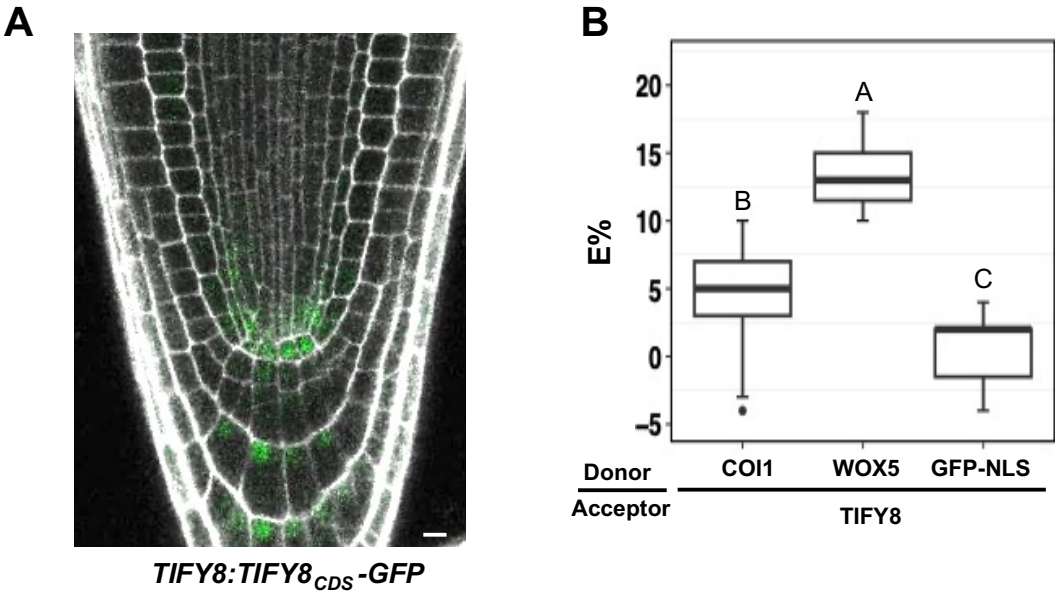


Figure 4.23: TIFY8 interacts with WOX5. A, accumulation pattern of TIFY8 protein in root tips. The gray channel depicts a stained root tip with Propidium iodide. scale bar = 10 μm. Roots were imaged five days after germination. **B**, AP-FRET experiments for protein interaction between TIFY8 and COI1 or WOX5. For each combination, the efficiencies from 8-10 nuclei were calculated in one replicate. "Acceptor" refers to the protein fused with mCherry. "Donor" refers to the protein fused with GFP. "E" refers to FRET efficiency. Results from two biological replicates were presented. Statistics were analyzed using one-way ANOVA with Tukey test ($P<0.01$).

Considering that WOX5 functions in inhibiting the columella stem cell differentiation in the root stem cell niche (Sarkar et al., 2007), TIFY8 may be also involved in the regulation of columella stem cell maintenance through interacting with WOX5. To test this hypothesis, I observed the root stem cell niche organization of *tify8-cr1* at a cellular level. In comparison to WT, about half of the *tify8-cr1* mutants observed exhibited an additional cell layer in the distal area beneath the quiescent center (Figure 4.24 A and B). The cells in this cell layer were similar in size to columella stem cells, indicating that they were likely undifferentiated. However, the results presented here are not sufficient to determine the identity of this additional cell layer. Reporter lines of the marker genes expressed in columella stem cells are necessary to confirm the cell identity. In addition, the primary root length of *tify8-cr1* exhibited no difference compared to that of WT (Figure 4.24 C), suggesting that loss of *TIFY8* function may not affect the primary root growth. Altogether, TIFY8 is possibly involved in the distal stem cell maintenance in the root stem cell niche through interacting with WOX5.

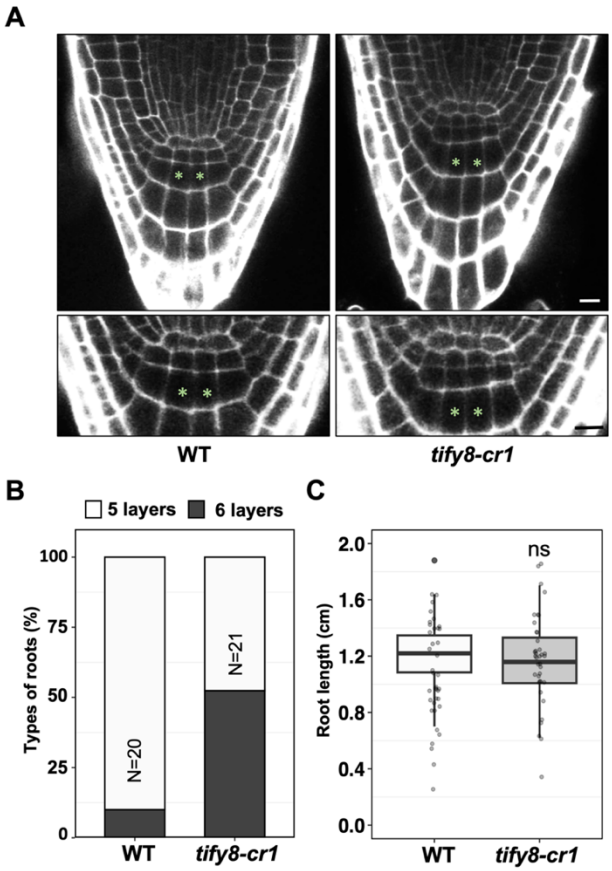


Figure 4.24: The function of TIFY8 in the root development. A, representative images of the root stem cell niche patterning in 5-day-old seedlings of WT and *tify8-cr1*. *The g*rey channel depicts a stained root tip with Propidium iodide. scale bar = 10 μm. The lower panels are the higher magnification of the upper panels. The asterisks indicate the fourth cell layer from the tip of the root. **B**, the frequency of roots with different cell layer numbers beneath the QC in WT and *tify8-cr1*. The terms "5 layers" and "6 layers" refer to roots containing either five or six cell layers beneath the QC. respectively. **C**, quantification of the primary root length of listed genotypes. The primary root length was measured five days after germination. Statistical analysis: two-tailed Student's t-tests. ns =not significant. N= 38.

5. Discussion

The stem cells in the SAM contribute to the great developmental plasticity of the plant aerial part, which is crucial for plant growth and development in their entire life cycles. With an increasing number of advanced studies, now we have a comprehensive and profound view of the molecular mechanisms of the interplay between the regulation of stem cell maintenance and plant internal signaling pathways. However, how stem cell maintenance is regulated in response to environmental signals, especially stress-related signals, remains mostly elusive.

In the main part of my Ph.D study, I explored how the systemic wounding signal modulates the SAM morphology and the inflorescence stem development, and how the SAM responds to the wounding signal (Figure 5.1). Systemic wounding inhibits stem growth by reducing the cell number of the SAM, but the population of stem cells is not affected. Furthermore, JA signaling plays a pivotal role in the systemic wounding response in the SAM, which is associated with the function of WUS. At a molecular level, when the leaves are not systemically wounded, WUS represses the early JA-responsive gene expression together with the JA signaling repressor JAZ3, hence the JA signaling is maintained at a resting level in the SAM (Figure 5.1 B). When the wounding response from the leaves reaches the SAM (Figure 5.1 A), WUS protein activity can be activated upon the JA outburst. In addition, WUS enhances *JAZ3* expression, thereby repressing the JA response in the SAM (Figure 5.1 C) As a result, stem cell maintenance is achieved and the stem growth inhibition by the systemic wounding is alleviated.

In addition, the function of TIFY8 in stem cell maintenance is characterized in this study. Unlike JAZ3, TIFY8 seems not to be directly involved in the response to JA in the SAM. However, TIFY8 can interact with WUS and WOX5. The accumulation pattern of TIFY8 overlaps with the *WUS*-expressing domain as well as the *WOX5*-expressing domain. Moreover, genetic evidence suggests that TIFY8 is involved in the regulation of stem cell maintenance in both the SAM and the RAM. In the SAM, TIFY8 acts as a positive regulator of cell proliferation, potentially associating with WUS function. In the RAM, TIFY8 seems to regulate the columella stem cell maintenance through interacting with WOX5. However, the clear molecular mechanism of TIFY8 function in stem cell maintenance awaits to be unveiled.

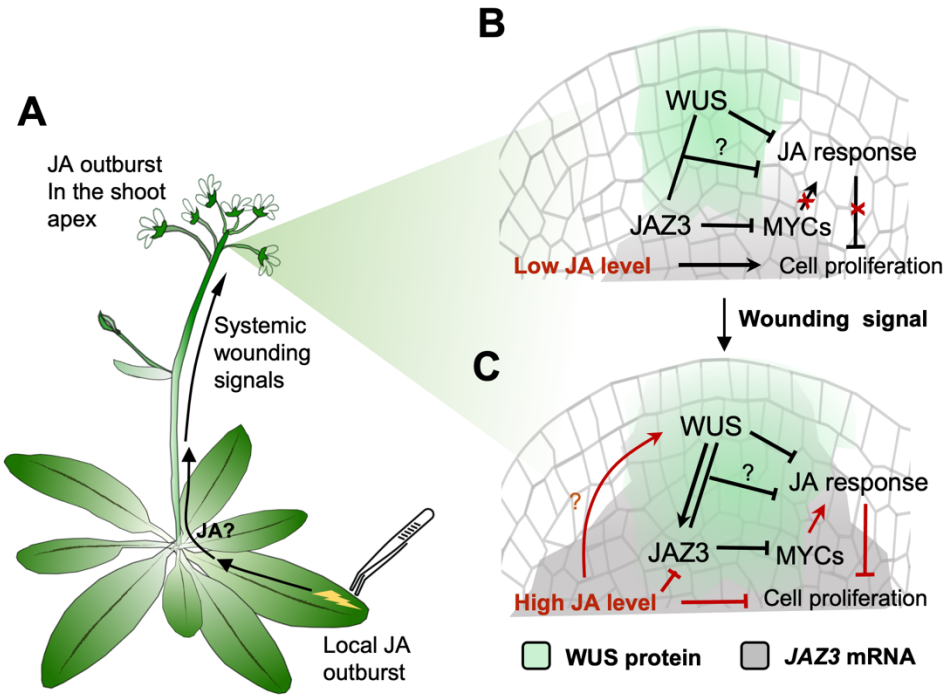


Figure 5.1: Theoretical model for the regulation of the SAM in response to systemic wounding. When the level of JA in the SAM is low, JA response is repressed by WUS and JAZ3 (**B**). Wounding treatment in leaves triggers local and systemic JA response. The systemic wounding signals travel from leaves to the shoot apex and stimulate the JA outburst in the SAM (**A**). The JA outburst in the SAM leads to JAZ3 degradation, hence the JA signaling is activated by MYCs. On the other hand, the WUS protein domain is expanded upon the JA outburst. WUS promotes *JAZ3* expression and represses JA-responsive gene expression together with the newly synthesized JAZ3 proteins. Therefore, the inhibition of cell proliferation as well as the inflorescence stem growth by JA response is alleviated (**C**). The icon of the forceps is from https://www.flaticon.com.

5.1 The inflorescence stem growth is reshaped by systemic wounding and exogenous JA

It has been reported that wounding in the leaves of *Arabidopsis s*eedlings inhibits the growth of the unwounded root (Schulze et al., 2019). However, whether wounding stunts plant growth systemically in other unwounded tissues remains elusive. Results in my study reveal that growth inhibition can also occur systemically in the inflorescence stem when the leaves are wounded, which further confirms the profound effect of systemic wounding on plant growth and development.

Wounding triggers the JA outburst in plants. The long-term wounding treatment can systemically induce the endogenous JA signal transduction (Acosta et al., 2013). On the other hand, the JA signaling is locally induced by the exogenous JA application.

Two treatments differ from the JA signals input, but they both can trigger the JA response in the shoot apex. Interestingly, spraying JA on the shoot apex is sufficient to inhibit the inflorescence stem growth. This result indicates that the shoot apex could be the main region responsible for the wounding-induced stem growth inhibition. However, it is hard to compare the effects of growth inhibition by the endogenous JA or the exogenous JA in my study, as the level of bioactive JA forms has not been measured yet. This can be achieved using liquid chromatography-mass spectrometry (LCMS) in the future (Mahmud et al., 2022).

The observed phenotype of inhibited stem growth upon systemic wounding and exogenous JA treatment provides a representative example of how plant growth is re-modulated under stress conditions. In response to stresses, the trade-off between plant growth and defense favors actions for stress resistance (Züst & Agrawal, 2017). At the molecular level, stress-responsive pathways are promptly activated on a large scale. Conversely, plant growth and development are temporally retarded. Therefore, more energy and resources can be allocated to defense activities. From this point of view, stem growth inhibition can be considered as a strategy of plants to reprogram developmental processes against systemic wounding stress.

5.2 The cellular basis of the stem growth inhibition

A key question regarding stem growth inhibition is whether it mainly results from the inhibition of cell division, cell elongation, or both processes. It has been reported that the JA signaling induced by wounding hampers leaf growth by inhibiting cell division rather than reducing cell expansion (Zhang & Turner, 2008). While JA inhibits primary root growth by repressing both cell proliferation and cell elongation (Chen et al., 2011). However, in Chen et al. (2011), seeds were directly germinated in the growth medium with JA. The entire primary root, including the meristematic zone and the elongation zone, is directly exposed to the exogenous JA in the medium. This differs from the treatment in my study, in which only the shoot apex was directly treated with JA. Therefore, the altered cell division or cell elongation in the shoot apex may directly lead to the inhibition of inflorescence stem growth upon JA treatment.

Unlike the well-characterized root development, the regulatory mechanisms of stem development remain to be deciphered. At a cellular level, the stem elongation is driven by cell proliferation in the rib zone and relatively slower cell division followed by rapid

cell expansion in the internode (Serrano-Mislata & Sablowski, 2018). At the molecular level, the cell division in the rib zone is regulated by the gibberellin (GA) signaling pathway and BEL1-like (BLH) transcription factors (Bencivenga et al., 2016; Serrano-Mislata et al., 2017).

From the result of my study, systemic wounding treatment reduces the number of cells in regions excluding the central zone and organizing center. Therefore, the cell number of the rib zone and the peripheral zone is likely reduced by wounding. In addition, the reduced number of *WUS* cells by JA treatment indicates that cell division in the organizing center and the rib zone may be affected by JA treatment. Moreover, overexpressing JA signaling repressor *JAZ3* under the *WUS* promoter can alleviate stem growth inhibition by wounding (Figure 4.16 B, Figure S11). All this information suggests that the inhibited cell division within the *WUS* expressing domain is likely responsible for the inhibition of stem growth upon wounding treatment. However, the contribution of cell elongation, if any, in the rib zone cannot be ruled out, as our imaging system cannot capture the entire sub-apical region of the SAM, and the change of the cell size is not evaluated in my study. Moreover, it is also unclear whether the internode elongation in the later stem development is inhibited by exogenous JA, as the exogenous JA can be potentially transported to the cells of the internode from the shoot apex. Therefore, systemic growth inhibition by JA may occur.

5.3 Stem cell maintenance in response to systemic wounding and exogenous JA

The reduced cell number of the SAM in wounded samples reveals that the SAM indeed senses and responds to the systemic wounding signals. In the inflorescence SAM, the top three layers contain stem cells and precursor cells that finally contribute to the components of floral primordia. In contrast to the inhibited stem growth, the lateral organ development is free from the effect of systemic wounding. It is intriguing to ask whether the top three layers are insulated from wounding or JA signals, or if these signals are immediately scavenged upon entry. The *in situ* hybridization results of the *JAZ* genes expression in the SAM with JA treatment favors the later hypothesis, as the mRNA expression domain of *JAZ2*, *JAZ3,* and *JAZ5* indeed expanded to the top three layers in the SAM with JA treatment (Figure 4.5).

The reduced *WUS* and *CLV3* cell number upon JA treatment indicates WUS-CLV3 regulatory system is repressed by exogenous JA. This negative effect is dose-dependent, as extending the duration of JA treatment leads to the enhanced reduction of *WUS* and *CLV3* expressing domain (Figure S4). Interestingly, unlike the result from JA treatment, systemic wounding did not significantly alter the number of *WUS* and *CLV3* cells, although there is a trend towards a reduction in the number of *WUS* cells in the wounded sample. This result suggests that SAM activity is either not affected by wounding or can somehow recover from the rhythmically induced wounding stress and the activated JA response following systemic wounding. However, if overloaded JA occurs in the SAM, the stem cell activity can be hampered. All these results highlight the robustness of the regulatory system of stem cell homeosis in response to wounding stress. The SAM potentially exhibits a self-renewal mechanism that counteracts the negative effects of systemic wounding and JA signaling in some level.

5.4 The systemic wounding response is mediated by the JA pathway

Given that wounding triggers various signaling responses apart from JA (León et al., 2001), the consistent phenotype of the stem growth observed upon wounding and JA treatment is not sufficient to validate that JA is the essential regulator of wounding-induced stem growth inhibition. However, the observation of the upregulated JA-responsive gene expression in the shoot apex and the less inhibited stem growth in the mutants of JA pathways upon wounding further prove the role of JA pathways in wounding-induced stem growth inhibition.

Four hours after wounding treatment in leaves, the expression of four JA early responsive markers (Figure 4.3), namely *JAZ10*, *JAZ7*, *LOX3,* and *VSP2*, shows upregulated in the shoot apex. The fold change of gene expression in wounded samples varied among genes, as these genes are expected to display different transcriptional upsurge time points in JA signaling (Zander et al., 2020). Moreover, mutants defective in JA signaling and biosynthesis display significantly reduced stem growth inhibition upon wounding treatment, highlighting that both JA biosynthesis and signaling pathways are essential for the shoot apex to perceive and respond to wounding signals. Interestingly, *jar1-11* displayed the same level of stem growth inhibition as WT upon systemic wounding (Figure 4.3). Although JAR1 is the key enzyme converting JA to bioactive JA-lle, it seems that JAR1 is not required for the JA response triggered by

systemic wounding in stem growth. Results from the systemic wounding indicate either other enzymes are involved in catalyzing JA-lle synthesis, or other bioactive forms are required for stem growth inhibition. It has been suggested that JAR1 does not regulate the inhibition of shoot growth by wounding but is required for the inhibition of root growth by exogenous JA treatment (Staswick et al., 1992; Zhang & Turner, 2008). Therefore, the function of JAR1 in response to JA and wounding could be uncoupled. The contrasting JAR1 functions in the shoot and the root reveal the complex and distinct regulation of wounding and JA responses across different tissues.

This tissue-specific regulation in response to JA is also evident from the varied composition of JA signaling cassettes in different tissues (Acosta et al., 2013). Consistent with this note, JA signaling machinery in the SAM is different from that in the root. According to the expression pattern of the receptors, repressors, and activators of JA signaling. Co-receptor COI1 evenly distributes in the SAM. While *JAZ* genes display varied gene expression patterns (Figure 4.4 and Figure 4.5). Interestingly, only the expression of *MYC3* out of the four *MYC* genes is detected in the SAM by *in situ* hybridization. In the root, MYC2 is considered as the crucial activator of JA response (Fernández-Calvo et al., 2011). However, this may not be the case in the SAM, if it is not expressed in the SAM.

In addition to JA biosynthesis and JA signaling, it is worth exploring whether JA transport is involved in the regulation of stem growth inhibition upon systemic wounding. It is disputable whether the JA molecule itself acts as the mobile signal in the long-distance wounding response transduction. In plants, the mobile electric signals driven by GLUTAMATE-RECEPTOR-LIKE(GLR3) proteins are considered as the pioneer massager of wounding signal transduction (Mousavi et al., 2013). However, increasing studies reveal that JA but not JA-lle can move from cell to cell through the phloem, and the mobile JA contributes to the wounding-induced systemic response (Schulze et al., 2019). JA transporters JAT3 and JAT4 in the phloem are also identified in *Arabidopsis* (Li et al., 2020; Li et al., 2017). It is worthwhile to test whether these transporters are involved in the regulation of JA-mediated stem growth inhibition by systemic wounding.

5.5 The role of WUS in the regulation of JA signaling

The role of WUS in the SAM response to JA-mediated systemic wounding signals is indispensable. From my study, WUS represses JA-responsive gene expression in the SAM, repelling the JA outburst in the stem cell region. In addition, WUS acts as a positive regulator in alleviating JA-induced stem growth inhibition.

WUS can respond to the JA activation in the SAM. Current results suggest that the short-term JA treatment triggers a weak WUS protein domain expansion, whereas long-term JA treatment represses *WUS* expression. No evidence so far suggests whether this transient WUS protein activation upon short-term JA treatment is a result of enhanced *WUS* gene expression. This enhanced protein accumulation is dynamic and reversible, indicating that the WUS response is quite fast and sensitive. Nevertheless, the current experimental system can be further improved in the future, as dissecting or sectioning the inflorescence may induce additional wounding signals, which might interfere with the direct effects of JA treatment. The PFA fixation before dissection and fast operation can significantly reduce the side effects. Moreover, the quantification method is required for precisely evaluating the changes in the WUS domain in the future.

Second, WUS represses JA-responsive gene expression when the JA level is low in the SAM, which may eliminate the negative effects of stress response on stem cell maintenance. In the shoot apex of *the clv3-10* mutant, overexpressed *WUS* represses the expression of early JA-responsive markers. Moreover, according to the RNA-seq and ChIP-seq profiles generated by my colleagues, genes involved in JA biosynthesis and signaling are consistently downregulated with inducible overexpression of *WUS* (Table S1). In addition, WUS directly targets genomic regions of most down-regulated genes in Table S1. All these results indicate WUS negatively regulates both JA biosynthesis and JA signaling in the SAM. Interestingly, MYC3 and WUS share many common targets in JA pathways (Zander et al., 2020). They probably compete in binding target sites, which allows typically gene expression on or off, depending on the JA level in the SAM.

On the other side, WUS selectively represses some gene expressions even when JA signaling is activated in the shoot apex. The expression of *LOX3,* required for JA biosynthesis, is still inhibited upon JA treatment under the *clv3-10* background (Figure 4.7). While the expression of JA signaling repressor *JAZ7* is even enhanced in *clv3-10*. Furthermore, WUS directly promotes *JAZ3* expression, which in turn represses JA-

responsive gene expression. These results suggest the transcriptional controls of the JA responsive gene by WUS may vary among genes, which may relate to the function of genes in JA signaling. It seems that WUS negatively regulates genes that promote JA response but not the genes that repress JA response.

Regarding the function of WUS in the regulation of JA-related plant developmental processes, WUS can reduce the level of inflorescence stem growth inhibition by JA and systemic wounding. The stem growth inhibition assay with JA treatment in *clv3-10* and *wus-7* elucidates that WUS is a positive regulator against the inhibition of stem growth by JA. The stimulated WUS activity upon JA treatment potentially enhances the repression of JA response by WUS and inhibits JA response from disturbing the cell identity maintenance in the SAM. As a result, stem development is less affected by reinforced stem cell homeostasis in the shoot apex.

5.6 The role of JAZ3 in response to JA signaling in the SAM

Different from other *JAZ* genes, *JAZ3* is specifically expressed in the organizing center and the rib zone as well as the pith region in the sub-SAM area (Figure 4.11). This specific expression pattern connects the SAM and the inflorescence stem, where systemic wounding signals are conveyed. Interestingly, J*AZ3* mRNA is expanded in the SAM with JA treatment, indicating the expression of *JAZ3* strongly responds to the exogenous JA in the SAM (Figure 4.5). Considering that *JAZ3* expression is promoted by both WUS and MYCs, this upregulated expression of *JAZ3* upon exogenous JA is likely achieved by both WUS and MYCs in the SAM. All these results suggest the regulation of J*AZ3* expression might be a pivotal node for stem cell maintenance in response to wounding and JA signals.

The current result suggests that JAZ3 is not a regulator in stem cell maintenance, as the *jaz3* mutants and *WUS:JAZ3* transgenic lines displayed WT-like SAM-related phenotypes. Although JAZ3 interacts with WUS, it seems not to be associated with the function of WUS in stem cell maintenance. Moreover, since JAZ3 interacts with WUS in the dimerization domain rather than the homeodomain of the WUS protein, it might not interfere with the function of WUS as a transcription factor in DNA binding, which is important for stem cell maintenance in the SAM.

On the other hand, JAZ3 is involved in the regulation of flowering control and inflorescence stem growth. While *jaz3-cr* and *jaz3/5/10* mutants bolt slightly later than

WT, *WUS:JAZ3* and *WUS:JAZ3Δ2* display earlier flowering phenotypes. It has been reported that JAZ proteins regulate flowering time by interacting with TARGET OF EAT1(TOE1) and TOE2 (Zhai et al., 2015). Overexpressing truncated JAZ1 protein without Jas domain under 35S promoter results in a significantly earlier flowering phenotype (Zhai et al., 2015). Interestingly, overexpressing *JAZ3* only in the *WUS* domain is sufficient to promote flowering. It is reasonable to speculate that the WUS-expressing domain contains the regulatory elements involved in the regulation of floral transition.

Together with WUS, JAZ3 alleviates the inflorescence stem growth inhibition by wounding and exogenous JA. This is potentially achieved by interacting with MYCs proteins and recruiting transcriptional repression complex, hence repressing JA-responsive gene expression. However, the interaction between WUS and JAZ3 suggests that JAZ3 may be also part of the WUS-directed transcriptional repression complex. *WUS:JAZ3* transgenic lines are resistant to wounding and exogenous JA treatment. These results further confirm that the *WUS* domain is crucial for the regulation of stem growth in response to wounding and JA treatment. The growth of the inflorescence stem in the *jaz3-cr* mutant is more sensitive to wounding treatment compared to WT. However, the significance of this phenotype varies among different biological replicates, indicating the presence of other similar regulators to JAZ3. The *jaz3/5/10* triple mutant did not show increased sensitivity to systemic wounding compared to the *jaz3-cr* single mutant. Its phenotype is even milder than that of the *jaz3-cr* single mutant. JAZ5 and JAZ10 may not be functionally redundant with JAZ3 in the stem growth regulation. However, the developmental phenotypes related to JA response have not been characterized in the *jaz3/5/10* triple mutant. It has been reported that the primary root growth of double mutant *jaz5/10* and *jaz3/10* is more sensitive to exogenous JA compared with WT, while *jaz3/5* displays WT-like primary root growth in response to exogenous JA (de Torres Zabala et al., 2016). Therefore, more genetic evidence is required to determine the roles of other JAZs in the regulation of inflorescence stem growth in response to wounding and exogenous JA.

5.7 The biological significance of the interaction between JAZ3 and WUS

The interaction between JAZ3 and WUS provides new insights into understanding the regulatory network in the SAM in response to environmental signals. However, the clear biological significance of this interaction is still not deciphered. Here, I propose three possible hypotheses based on my current results.

JAZ3 acts as the co-sensor of the wounding signal and JA together with WUS. *JAZ3* is expressed in the rib zone, which connects the inflorescence stem and the SAM. Therefore, JAZ3 might first perceive the systemic wounding signal which is induced in the rosette leaves. When the wounding signal is transmitted from the leaves to the stem, JAZ3 is degraded once JA signaling is activated, which somehow releases WUS from interacting with JAZ3 in the rib zone. Consequently, WUS is activated and represses the JA-responsive events in the SAM.

In the second hypothesis, WUS stabilizes JAZ3 by competing with COI1 for interacting with JAZ3 upon JA treatment. Therefore, JAZ3 can inhibit MYCs activity from promoting JA-responsive gene expression. Evidence that supports this hypothesis is that WUS and COI1 interact with JAZ3 both via the Jas and ZIM domains. However, no evidence suggests that JAZ3 protein is more stabilized in the presence of WUS so far.

Third, JAZ3 interacts with WUS and leads WUS to MYCs binding sites of the genomic regions of their targets, thereby shutting down the JA-responsive gene expression. MYCs also interact with JAZ3 and share common genomic binding sites with WUS. The most common DNA binding motif of MYC2 or MYC3 is the G-box (CA[C/T]GT[G/T]) motif (Zander et al., 2020), while WUS can bind to the G-box like (TCACGTGA) motif (Sloan et al., 2020). Moreover, JAZ3 needs the adaptor protein NINJA to recruit the TPL repression complex (Howe et al., 2018). However, NINJA is insufficient to repress the JA-responsive gene expression in the aerial part of the plants, unlike in the roots (Acosta et al., 2013). Therefore, other types of transcriptional repression machinery are required for JA signaling regulation in the SAM. The repression complex directed by WUS may act in the same regulatory pathway as NINJA.

5.8 TIFY8 is a regulator of stem cell maintenance

TIFY8 is an atypical TIFY protein. Its function in plant development is not well characterized yet. In this study, the function of TIFY8 as an important regulator of stem cell maintenance is uncovered.

TIFY8 is specifically expressed in the *WUS*-expressing domain, while its promoter activity indicates a broader expression pattern compared to the pattern of mRNA accumulation and protein accumulation in the SAM. This difference suggests the expression of *TIFY8* is likely under post-transcriptional regulations with yet unknown mechanisms. Despite the shared expression pattern between *WUS* and *TIFY8*, WUS does not regulate TIFY8 at either the transcriptional level or the translational level.

The interaction between TIFY8 and WUS sheds light on TIFY8 function at a molecular level. TIFY8 is characterized as a transcriptional repressor, which can interact with various transcription factors (Cuéllar Pérez et al., 2014). Therefore, it can be inferred that TIFY8 may be involved in the WUS-directed transcriptional repression complex. In addition, TIFY8 interacts with the dimerization domain of WUS, which contains an intrinsically disordered region. From this point of view, TIFY8 might act as an adaptor or chaperone, forming the protein complex with WUS to facilitate proper protein folding of WUS protein. Apart from this hypothesis, TIFY8 is possibly involved in the regulation of WUS homodimerization. WUS homodimerization is related to WUS regulation behavior towards its targets and its protein mobility. TIFY8 may fine-tune WUS activity through this process.

Genetic evidence, including the SAM-related phenotypes of the *tify8* single mutant and the *tif8 clv3* double mutant, confirms that TIFY8 functions in stem cell maintenance associated with WUS. Mutating *TIFY8* reduced the over-proliferation phenotype of the SAM in the *clv3-10* mutant. However, only the enlarged SAM phenotype, but not the phenotypes of misshaped flowers and siliques in the *clv3-10* mutant, was rescued by the mutation of *TIFY8*. This result indicates that TIFY8 is probably only involved in stem cell maintenance in the SAM but not in the floral meristems. Moreover, the phenotype of fasciated inflorescence in *CLV3:TIFY8* transgenic lines reveals that TIFY8 promotes cell proliferation and activates stem cell identity in the SAM. However, the molecular mechanism of TIFY8 function has not been deeply studied yet. Identifying the downstream WUS targets specifically regulated by TIFY8 might be a way to characterize the role of TIFY8 in stem cell maintenance at a molecular level.

TIFY8 is a stem cell regulator probably not only in the SAM. The interaction between TIFY8 and WOX5 is also observed by AP-FRET. Also, the expression pattern of *TIFY8* in the root tip is overlapped with that of WOX5. *WOX5* is the molecular identity marker of the quiescent center (QC) in the root apical meristem (Sarkar et al., 2007). The cells in the QC monitor the maintenance of stem cells in the root. The root stem cells give rise to other different cell types, including the columella cells in the distal position of the root and initial cells for each cell layer in the meristematic zone. Therefore, the function of TIFY8 is possibly also required for stem cell maintenance in the root. In *tify8-cr1*, an additional cell layer was observed in the columella stem cell region, indicating that TIFY8 may be involved in the columella stem cell maintenance. Furthermore, it is promising to investigate whether TIFY8 is a common interactor of WUSCHEL-related homeobox proteins and whether TIFY8 is involved in the stem cell maintenance of different tissues and different plant species.

5.9 Potential connection between TIFY8 and JAZ3 upon interacting with WUS

It is still unclear whether TIFY8 and JAZ3 act synergically or antagonistically associated with each other in the SAM. JAZ3 and TIFY8 are from the same protein family, and both contain the conserved ZIM domain. The expression pattern of *JAZ3* and *TIFY8* overlap with the *WUS*-expressing domain, though *JAZ3* is more restricted in the rib zone. JAZ3 and TIFY8 both interact with WUS, and the conserved ZIM domain is required for the interaction. On one hand, it is reasonable to deduce that JAZ3 and TIFY8 act synergistically to modulate WUS activity in response to JA signaling in the SAM. However, TIFY8 may not directly regulate JA response as JAZ3 does. First, TIFY8 lacks the conserved Jas domain and may not interact with JA co-receptor COI1 (Figure 4.23); Second, JA treatment did not significantly alter *TIFY8* mRNA accumulation (Figure 4.17), and the protein accumulation (Cuéllar Pérez et al., 2014). Third, *tify8* mutants, *TIFY8*-knockdown transgenic lines, and *TIFY8* over-expressing lines show WT-like response to JA treatment in terms of primary root growth inhibition assay (Cuéllar Pérez et al., 2014).

On the other hand, TIFY8 may compete with JAZ3 in interacting with WUS in some regulatory processes in the SAMs. It has been suggested that the expression pattern of *TIFY8* seems to be opposite to most of the expression pattern of *JAZ*s, in terms of the

data from Genevestigator and eFP browser as well as transgenic reporter lines (Cuéllar Pérez et al., 2014).

The biological function of TIFY8 and JAZ3 in the SAM is different. *JAZ3* is regulated by WUS at the transcriptional level, but *TIFY8* is not. Transgenic lines overexpressing *TIFY8* and t*ify8* CRISPR/Cas9 mutant display SAM-related phenotypes. On the contrary, genetic lines with impaired JAZ3 function or *JAZ3* overexpression exhibit WT-like SAM phenotypes. Overall, the role of JAZ3 in the SAM mainly relied on the response to JA, while the role of TIFY8 mainly relied on the regulation of stem cell maintenance. Notably, the *jaz3-cr tify8-cr1* double mutant displays a significantly later flowering phenotype than the WT (Figure 4.15 and Figure S9), suggesting TIFY8 synergizes JAZ in flowering regulation.

5.10 Conclusion

In this study, I first explored how the SAM responds to systemic wounding signals and how wounding signals modulate the inflorescence stem development and SAM morphology. The systemic wounding from the rosette leaves represses the inflorescence stem development possibly by reducing the cell number in the SAM. However, the number of stem cells is not significantly affected by the wounding signals. Moreover, wounding signal perception and response in the SAM is mainly mediated by JA pathways. At a molecular level, WUS represses the JA response in the SAM, which maintains stem cell homeosis and alleviates stem growth inhibition in response to JA outbursts. This process is achieved potentially by promoting *JAZ3* expression and interacting with JAZ3. Moreover, this study also uncovered the function of TIFY8 as a regulator of stem cell maintenance in both the SAM and the RAM. TIFY8 interacts with WUS and promotes cell proliferation in the SAM. In addition, TIFY8 also can interact with WOX5 and is potentially involved in the regulation the columella stem cell maintenance.

Overall, all these results elucidate a novel mechanism of wounding signal perception and transduction in the SAM and plant stem ontogenesis upon systemic wounding. Also, the characterized interplay between the stem cell regulatory loop and the JA signaling adds a new viewpoint of stem cell maintenance in response to stress signals. Moreover. all these results reveal the distinct roles of two TIFY proteins in the regulation of stem cell maintenance in different plant developmental processes.

6. References

Acosta, I. F., Gasperini, D., Chetelat, A., Stolz, S., Santuari, L., & Farmer, E. E. (2013). Role of NINJA in root jasmonate signaling. *Proc Natl Acad Sci U S A*, *110*(38), 15473-15478. https://doi.org/10.1073/pnas.1307910110

Agusti, J., & Greb, T. (2013). Going with the wind–adaptive dynamics of plant secondary meristems. *Mechanisms of development*, *130*(1), 34-44.

Andrade Galan, A. G., Doll, J., Saile, S. C., Wünsch, M., Roepenack-Lahaye, E. v., Pauwels, L., Goossens, A., Bresson, J., & Zentgraf, U. (2023). The Non-JAZ TIFY protein TIFY8 of Arabidopsis thaliana interacts with the HD-ZIP III transcription factor REVOLUTA and regulates leaf senescence. *International Journal of Molecular Sciences*, *24*(4), 3079.

Argueso, C. T., Raines, T., & Kieber, J. J. (2010). Cytokinin signaling and transcriptional networks. *Current opinion in plant biology*, *13*(5), 533-539.

Baekelandt, A., Pauwels, L., Wang, Z., Li, N., De Milde, L., Natran, A., Vermeersch, M., Li, Y., Goossens, A., & Inzé, D. (2018). Arabidopsis leaf flatness is regulated by PPD2 and NINJA through repression of CYCLIN D3 genes. *Plant physiology*, *178*(1), 217-232.

Bencivenga, S., Serrano-Mislata, A., Bush, M., Fox, S., & Sablowski, R. (2016). Control of Oriented Tissue Growth through Repression of Organ Boundary Genes Promotes Stem Morphogenesis. *Dev Cell*, *39*(2), 198-208. https://doi.org/10.1016/j.devcel.2016.08.013

Betsuyaku, S., Takahashi, F., Kinoshita, A., Miwa, H., Shinozaki, K., Fukuda, H., & Sawa, S. (2011). Mitogen-activated protein kinase regulated by the CLAVATA receptors contributes to shoot apical meristem homeostasis. *Plant and Cell Physiology*, *52*(1), 14-29.

Boter, M., Ruíz-Rivero, O., Abdeen, A., & Prat, S. (2004). Conserved MYC transcription factors play a key role in jasmonate signaling both in tomato and Arabidopsis. *Genes & development*, *18*(13), 1577-1591.

Brand, U., Fletcher, J. C., Hobe, M., Meyerowitz, E. M., & Simon, R. (2000). Dependence of stem cell fate in Arabidopsis on a feedback loop regulated by CLV3 activity. *Science*, *289*(5479), 617-619.

Buechel, S., Leibfried, A., To, J. P., Zhao, Z., Andersen, S. U., Kieber, J. J., & Lohmann, J. U. (2010). Role of A-type ARABIDOPSIS RESPONSE REGULATORS in meristem maintenance and regeneration. *European journal of cell biology*, *89*(2-3), 279-284.

Busch, W., Miotk, A., Ariel, F. D., Zhao, Z., Forner, J., Daum, G., Suzaki, T., Schuster, C., Schultheiss, S. J., & Leibfried, A. (2010). Transcriptional control of a plant stem cell niche. *Developmental cell*, *18*(5), 841-853.

Cai, X.-T., Xu, P., Zhao, P.-X., Liu, R., Yu, L.-H., & Xiang, C.-B. (2014). Arabidopsis ERF109 mediates cross-talk between jasmonic acid and auxin biosynthesis during lateral root formation. *Nature Communications*, *5*(1), 5833.

Campos, M. L., Kang, J.-H., & Howe, G. A. (2014). Jasmonate-triggered plant immunity. *Journal of chemical ecology*, *40*, 657-675.

Carles, C. C., & Fletcher, J. C. (2003). Shoot apical meristem maintenance: the art of a dynamic balance. *Trends in plant science*, *8*(8), 394-401.

Cevik, V., Kidd, B. N., Zhang, P., Hill, C., Kiddle, S., Denby, K. J., Holub, E. B., Cahill, D. M., Manners, J. M., Schenk, P. M., Beynon, J., & Kazan, K. (2012). MEDIATOR25 acts as an integrative hub for the regulation of jasmonate-responsive gene expression in Arabidopsis. *Plant Physiol*, *160*(1), 541-555. https://doi.org/10.1104/pp.112.202697

Chauvin, A., Caldelari, D., Wolfender, J. L., & Farmer, E. E. (2013). Four 13-lipoxygenases contribute to rapid jasmonate synthesis in wounded Arabidopsis thaliana leaves: a role for lipoxygenase 6 in responses to long-distance wound signals. *New Phytol*, *197*(2), 566-575. https://doi.org/10.1111/nph.12029

Chen, M.-K., Wilson, R. L., Palme, K., Ditengou, F. A., & Shpak, E. D. (2013). ERECTA family genes regulate auxin transport in the shoot apical meristem and forming leaf primordia. *Plant physiology*, *162*(4), 1978-1991.

Chen, Q., Sun, J., Zhai, Q., Zhou, W., Qi, L., Xu, L., Wang, B., Chen, R., Jiang, H., & Qi, J. (2011). The basic helix-loop-helix transcription factor MYC2 directly represses PLETHORA expression during jasmonate-mediated modulation of the root stem cell niche in Arabidopsis. *The Plant Cell*, *23*(9), 3335-3352.

Chen, R., Jiang, H., Li, L., Zhai, Q., Qi, L., Zhou, W., Liu, X., Li, H., Zheng, W., Sun, J., & Li, C. (2012). The Arabidopsis mediator subunit MED25 differentially regulates jasmonate and abscisic acid signaling through interacting with the MYC2 and ABI5 transcription factors. *Plant Cell*, *24*(7), 2898-2916. https://doi.org/10.1105/tpc.112.098277

Chickarmane, V. S., Gordon, S. P., Tarr, P. T., Heisler, M. G., & Meyerowitz, E. M. (2012). Cytokinin signaling as a positional cue for patterning the apical–basal axis of the growing Arabidopsis shoot meristem. *Proceedings of the National Academy of Sciences*, *109*(10), 4002-4007.

Chini, A., Fonseca, S., Fernandez, G., Adie, B., Chico, J. M., Lorenzo, O., García-Casado, G., López-Vidriero, I., Lozano, F., & Ponce, M. (2007). The JAZ family of repressors is the missing link in jasmonate signalling. *Nature*, *448*(7154), 666-671.

Chini, A., Gimenez-Ibanez, S., Goossens, A., & Solano, R. (2016). Redundancy and specificity in jasmonate signalling. *Current opinion in plant biology*, *33*, 147-156.

Clark, S. E., Running, M. P., & Meyerowitz, E. M. (1995). CLAVATA3 is a specific regulator of shoot and floral meristem development affecting the same processes as CLAVATA1. *Development*, *121*(7), 2057-2067.

Consortium, A. I. M., Dreze, M., Carvunis, A.-R., Charloteaux, B., Galli, M., Pevzner, S. J., Tasan, M., Ahn, Y.-Y., Balumuri, P., & Barabási, A.-L. (2011). Evidence for network evolution in an Arabidopsis interactome map. *Science*, *333*(6042), 601-607.

Cuéllar Pérez, A., Nagels Durand, A., Vanden Bossche, R., De Clercq, R., Persiau, G., Van Wees, S. C., Pieterse, C. M., Gevaert, K., De Jaeger, G., & Goossens, A. (2014). The non-JAZ TIFY protein TIFY8 from Arabidopsis thaliana is a transcriptional repressor. *PLoS One*, *9*(1), e84891.

Daum, G., Medzihradszky, A., Suzaki, T., & Lohmann, J. U. (2014). A mechanistic framework for noncell autonomous stem cell induction in Arabidopsis. *Proceedings of the National Academy of Sciences*, *111*(40), 14619-14624.

de Folter, S., & Immink, R. G. (2011). Yeast protein–protein interaction assays and screens. *Plant Transcription Factors: methods and protocols*, 145-165.

de Torres Zabala, M., Zhai, B., Jayaraman, S., Eleftheriadou, G., Winsbury, R., Yang, R., Truman, W., Tang, S., Smirnoff, N., & Grant, M. (2016). Novel JAZ co-operativity and unexpected JA dynamics underpin A rabidopsis defence responses to P seudomonas syringae infection. *New Phytologist*, *209*(3), 1120-1134.

Demole, E., Lederer, E., & Mercier, D. (1962). Isolement et détermination de la structure du jasmonate de méthyle, constituant odorant caractéristique de l'essence de jasmin. *Helvetica Chimica Acta*, *45*(2), 675-685.

DeYoung, B. J., Bickle, K. L., Schrage, K. J., Muskett, P., Patel, K., & Clark, S. E. (2006). The CLAVATA1-related BAM1, BAM2 and BAM3 receptor kinase-like proteins are required for meristem function in Arabidopsis. *The Plant Journal*, *45*(1), 1-16.

Dolzblasz, A., Nardmann, J., Clerici, E., Causier, B., van der Graaff, E., Chen, J., Davies, B., Werr, W., & Laux, T. (2016). Stem cell regulation by Arabidopsis WOX genes. *Molecular plant*, *9*(7), 1028-1039.

Farhangi-Abriz, S., & Ghassemi-Golezani, K. (2019). Jasmonates: Mechanisms and functions in abiotic stress tolerance of plants. *Biocatalysis and agricultural biotechnology*, *20*, 101210.

Fernández-Calvo, P., Chini, A., Fernández-Barbero, G., Chico, J.-M., Gimenez-Ibanez, S., Geerinck, J., Eeckhout, D., Schweizer, F., Godoy, M., & Franco-Zorrilla, J. M. (2011). The Arabidopsis bHLH transcription factors MYC3 and MYC4 are targets of JAZ repressors and act additively with MYC2 in the activation of jasmonate responses. *The Plant Cell*, *23*(2), 701-715.

Fornara, F., de Montaigu, A., & Coupland, G. (2010). SnapShot: control of flowering in Arabidopsis. *Cell*, *141*(3), 550-550. e552.

Forner, J., Pfeiffer, A., Langenecker, T., Manavella, P., & Lohmann, J. U. (2015). Germline-transmitted genome editing in Arabidopsis thaliana using TAL-effector-nucleases. *PLoS One*, *10*(3), e0121056.

Fuchs, M., & Lohmann, J. U. (2020). Aiming for the top: non-cell autonomous control of shoot stem cells in Arabidopsis. *Journal of plant research*, *133*(3), 297-309.

Galvan-Ampudia, C. S., Cerutti, G., Legrand, J., Brunoud, G., Martin-Arevalillo, R., Azais, R., Bayle, V., Moussu, S., Wenzl, C., & Jaillais, Y. (2020). Temporal integration of auxin information for the regulation of patterning. *Elife*, *9*, e55832.

Glauser, G., Dubugnon, L., Mousavi, S. A., Rudaz, S., Wolfender, J.-L., & Farmer, E. E. (2009). Velocity estimates for signal propagation leading to systemic jasmonic acid accumulation in wounded Arabidopsis. *Journal of Biological Chemistry*, *284*(50), 34506-34513.

Gordon, S. P., Chickarmane, V. S., Ohno, C., & Meyerowitz, E. M. (2009). Multiple feedback loops through cytokinin signaling control stem cell number within the Arabidopsis shoot meristem. *Proceedings of the National Academy of Sciences*, *106*(38), 16529-16534.

Graf, P., Dolzblasz, A., Würschum, T., Lenhard, M., Pfreundt, U., & Laux, T. (2010). MGOUN1 encodes an Arabidopsis type IB DNA topoisomerase required in stem cell regulation and to maintain developmentally regulated gene silencing. *The Plant Cell*, *22*(3), 716-728.

Greb, T., & Lohmann, J. U. (2016). Plant stem cells. *Current biology*, *26*(17), R816-R821.

Guo, Q., Yoshida, Y., Major, I. T., Wang, K., Sugimoto, K., Kapali, G., Havko, N. E., Benning, C., & Howe, G. A. (2018). JAZ repressors of metabolic defense promote growth and reproductive fitness in Arabidopsis. *Proc Natl Acad Sci U S A*, *115*(45), E10768-E10777. https://doi.org/10.1073/pnas.1811828115

Haecker, A., Groß-Hardt, R., Geiges, B., Sarkar, A., Breuninger, H., Herrmann, M., & Laux, T. (2004). Expression dynamics of WOX genes mark cell fate decisions during early embryonic patterning in Arabidopsis thaliana. *Development*, *131*(3), 657-668. https://doi.org/10.1242/dev.00963

Han, G. Z. (2017). Evolution of jasmonate biosynthesis and signaling mechanisms. *J Exp Bot*, *68*(6), 1323-1331. https://doi.org/10.1093/jxb/erw470

He, Y., Chung, E. H., Hubert, D. A., Tornero, P., & Dangl, J. L. (2012). Specific missense alleles of the arabidopsis jasmonic acid co-receptor COI1 regulate innate immune receptor accumulation and function. *PLoS Genet*, *8*(10), e1003018. https://doi.org/10.1371/journal.pgen.1003018

Hou, X., Lee, L. Y., Xia, K., Yan, Y., & Yu, H. (2010). DELLAs modulate jasmonate signaling via competitive binding to JAZs. *Dev Cell*, *19*(6), 884-894. https://doi.org/10.1016/j.devcel.2010.10.024

Howe, G. A., & Jander, G. (2008). Plant immunity to insect herbivores. *Annu Rev Plant Biol*, *59*, 41-66. https://doi.org/10.1146/annurev.arplant.59.032607.092825

Howe, G. A., Major, I. T., & Koo, A. J. (2018). Modularity in jasmonate signaling for multistress resilience. *Annual review of plant biology*, *69*, 387-415.

Huang, H., Liu, B., Liu, L., & Song, S. (2017). Jasmonate action in plant growth and development. *Journal of experimental botany*, *68*(6), 1349-1359.

Ilyas, N., Gull, R., Mazhar, R., Saeed, M., Kanwal, S., Shabir, S., & Bibi, F. (2017). Influence of salicylic acid and jasmonic acid on wheat under drought stress. *Communications in soil science and plant analysis*, *48*(22), 2715-2723.

Ishida, T., Tabata, R., Yamada, M., Aida, M., Mitsumasu, K., Fujiwara, M., Yamaguchi, K., Shigenobu, S., Higuchi, M., & Tsuji, H. (2014). Heterotrimeric G proteins control stem cell proliferation through CLAVATA signaling in Arabidopsis. *EMBO reports*, *15*(11), 1202-1209.

Ishiguro, S., Kawai-Oda, A., Ueda, J., Nishida, I., & Okada, K. (2001). The DEFECTIVE IN ANTHER DEHISCENCE1 gene encodes a novel phospholipase A1 catalyzing the initial step of jasmonic acid biosynthesis, which synchronizes pollen maturation, anther dehiscence, and flower opening in Arabidopsis. *The Plant Cell*, *13*(10), 2191-2209.

John, A., Smith, E. S., Jones, D. S., Soyars, C. L., & Nimchuk, Z. L. (2023). A network of CLAVATA receptors buffers auxin-dependent meristem maintenance. *Nat Plants*, *9*(8), 1306-1317. https://doi.org/10.1038/s41477-023-01485-y

Kazan, K., & Manners, J. M. (2013). MYC2: the master in action. *Mol Plant*, *6*(3), 686-703. https://doi.org/10.1093/mp/sss128

Kinoshita, A., Betsuyaku, S., Osakabe, Y., Mizuno, S., Nagawa, S., Stahl, Y., Simon, R., Yamaguchi-Shinozaki, K., Fukuda, H., & Sawa, S. (2010). RPK2 is an essential receptor-like kinase that transmits the CLV3 signal in Arabidopsis. *Development*, *137*(22), 3911-3920.

Lampropoulos, A., Sutikovic, Z., Wenzl, C., Maegele, I., Lohmann, J. U., & Forner, J. (2013). GreenGate-a novel, versatile, and efficient cloning system for plant transgenesis. *PLoS One*, *8*(12), e83043.

Landrein, B., Formosa-Jordan, P., Malivert, A., Schuster, C., Melnyk, C. W., Yang, W., Turnbull, C., Meyerowitz, E. M., Locke, J. C., & Jönsson, H. (2018). Nitrate modulates stem cell dynamics in Arabidopsis shoot meristems through cytokinins. *Proceedings of the National Academy of Sciences*, *115*(6), 1382-1387.

Larrieu, A., Champion, A., Legrand, J., Lavenus, J., Mast, D., Brunoud, G., Oh, J., Guyomarc'h, S., Pizot, M., & Farmer, E. E. (2015). A fluorescent hormone biosensor reveals the dynamics of jasmonate signalling in plants. *Nature Communications*, *6*(1), 6043.

Laux, T., Mayer, K. F., Berger, J., & Jürgens, G. (1996). The WUSCHEL gene is required for shoot and floral meristem integrity in Arabidopsis. *Development*, *122*(1), 87-96.

Leibfried, A., To, J. P., Busch, W., Stehling, S., Kehle, A., Demar, M., Kieber, J. J., & Lohmann, J. U. (2005). WUSCHEL controls meristem function by direct regulation of cytokinin-inducible response regulators. *Nature*, *438*(7071), 1172-1175.

León, J., Rojo, E., & Sánchez-Serrano, J. J. (2001). Wound signalling in plants. *Journal of experimental botany*, *52*(354), 1-9.

Leyser, H. O., & Furner, I. J. (1992). Characterisation of three shoot apical meristem mutants of Arabidopsis thaliana. *Development*, *116*(2), 397-403.

Li, M., Wang, F., Li, S., Yu, G., Wang, L., Li, Q., Zhu, X., Li, Z., Yuan, L., & Liu, P. (2020). Importers Drive Leaf-to-Leaf Jasmonic Acid Transmission in Wound-Induced Systemic Immunity. *Mol Plant*, *13*(10), 1485-1498. https://doi.org/10.1016/j.molp.2020.08.017

Li, Q., Zheng, J., Li, S., Huang, G., Skilling, S. J., Wang, L., Li, L., Li, M., Yuan, L., & Liu, P. (2017). Transporter-Mediated Nuclear Entry of Jasmonoyl-Isoleucine Is Essential for Jasmonate Signaling. *Mol Plant*, *10*(5), 695-708. https://doi.org/10.1016/j.molp.2017.01.010

Lorenzo, O., Chico, J. M., Saénchez-Serrano, J. J., & Solano, R. (2004). JASMONATE-INSENSITIVE1 encodes a MYC transcription factor essential to discriminate between different jasmonate-regulated defense responses in Arabidopsis. *The Plant Cell*, *16*(7), 1938-1950.

Luo, L., Zeng, J., Wu, H., Tian, Z., & Zhao, Z. (2018). A molecular framework for auxin-controlled homeostasis of shoot stem cells in Arabidopsis. *Molecular plant*, *11*(7), 899-913.

Ma, Y., Miotk, A., Šutiković, Z., Ermakova, O., Wenzl, C., Medzihradszky, A., Gaillochet, C., Forner, J., Utan, G., & Brackmann, K. (2019). WUSCHEL acts as an auxin response rheostat to maintain apical stem cells in Arabidopsis. *Nature Communications*, *10*(1), 5093.

Mahmud, S., Ullah, C., Kortz, A., Bhattacharyya, S., Yu, P., Gershenzon, J., & Vothknecht, U. C. (2022). Constitutive expression of JASMONATE RESISTANT 1 induces molecular changes that prime the plants to better withstand drought. *Plant Cell Environ*, *45*(10), 2906-2922. https://doi.org/10.1111/pce.14402

Mandel, T., Moreau, F., Kutsher, Y., Fletcher, J. C., Carles, C. C., & Williams, L. E. (2014). The ERECTA receptor kinase regulates Arabidopsis shoot apical meristem size, phyllotaxy and floral meristem identity. *Development*, *141*(4), 830-841.

Mayer, K. F., Schoof, H., Haecker, A., Lenhard, M., Jürgens, G., & Laux, T. (1998). Role of WUSCHEL in regulating stem cell fate in the Arabidopsis shoot meristem. *Cell*, *95*(6), 805-815.

Medzihradszky, A., Schneitz, K., & Lohmann, J. U. (2014). Detection of mRNA expression patterns by nonradioactive in situ hybridization on histological sections of floral tissue. *Flower Development: Methods and Protocols*, 275-293.

Melotto, M., Mecey, C., Niu, Y., Chung, H. S., Katsir, L., Yao, J., Zeng, W., Thines, B., Staswick, P., & Browse, J. (2008). A critical role of two positively charged amino acids in the Jas motif of Arabidopsis JAZ proteins in mediating coronatine-and jasmonoyl isoleucine-dependent interactions with the COI1 F-box protein. *The Plant Journal*, *55*(6), 979-988.

Meng, W. J., Cheng, Z. J., Sang, Y. L., Zhang, M. M., Rong, X. F., Wang, Z. W., Tang, Y. Y., & Zhang, X. S. (2017). Type-B ARABIDOPSIS RESPONSE REGULATORs specify the shoot stem cell niche by dual regulation of WUSCHEL. *The Plant Cell*, *29*(6), 1357-1372.

Meng, X., Wang, H., He, Y., Liu, Y., Walker, J. C., Torii, K. U., & Zhang, S. (2012). A MAPK cascade downstream of ERECTA receptor-like protein kinase regulates Arabidopsis inflorescence architecture by promoting localized cell proliferation. *The Plant Cell*, *24*(12), 4948-4960.

Mousavi, S. A., Chauvin, A., Pascaud, F., Kellenberger, S., & Farmer, E. E. (2013). GLUTAMATE RECEPTOR-LIKE genes mediate leaf-to-leaf wound signalling. *Nature*, *500*(7463), 422-426.

Muller, R., Bleckmann, A., & Simon, R. (2008). The receptor kinase CORYNE of Arabidopsis transmits the stem cell–limiting signal CLAVATA3 independently of CLAVATA1. *The Plant Cell*, *20*(4), 934-946.

Myers, R. J., Fichman, Y., Zandalinas, S. I., & Mittler, R. (2023). Jasmonic acid and salicylic acid modulate systemic reactive oxygen species signaling during stress responses. *Plant Physiol*, *191*(2), 862-873. https://doi.org/10.1093/plphys/kiac449

Nguyen, C. T., Martinoia, E., & Farmer, E. E. (2017). Emerging Jasmonate Transporters. *Mol Plant*, *10*(5), 659-661. https://doi.org/10.1016/j.molp.2017.03.007

Nimchuk, Z. L., Zhou, Y., Tarr, P. T., Peterson, B. A., & Meyerowitz, E. M. (2015). Plant stem cell maintenance by transcriptional cross-regulation of related receptor kinases. *Development*, *142*(6), 1043-1049.

Ohta, M., Matsui, K., Hiratsu, K., Shinshi, H., & Ohme-Takagi, M. (2001). Repression domains of class II ERF transcriptional repressors share an essential motif for active repression. *The Plant Cell*, *13*(8), 1959-1968.

Park, J. H., Halitschke, R., Kim, H. B., Baldwin, I. T., Feldmann, K. A., & Feyereisen, R. (2002). A knock-out mutation in allene oxide synthase results in male sterility and defective wound signal transduction in Arabidopsis due to a block in jasmonic acid biosynthesis. *Plant J*, *31*(1), 1-12. https://doi.org/10.1046/j.1365-313x.2002.01328.x

Pauwels, L., Barbero, G. F., Geerinck, J., Tilleman, S., Grunewald, W., Pérez, A. C., Chico, J. M., Bossche, R. V., Sewell, J., & Gil, E. (2010). NINJA connects the co-repressor TOPLESS to jasmonate signalling. *Nature*, *464*(7289), 788-791.

Pauwels, L., & Goossens, A. (2011). The JAZ proteins: a crucial interface in the jasmonate signaling cascade. *Plant Cell*, *23*(9), 3089-3100. https://doi.org/10.1105/tpc.111.089300

Perales, M., Rodriguez, K., Snipes, S., Yadav, R. K., Diaz-Mendoza, M., & Reddy, G. V. (2016). Threshold-dependent transcriptional discrimination underlies stem cell homeostasis. *Proceedings of the National Academy of Sciences*, *113*(41), E6298-E6306.

Pfeiffer, A., Janocha, D., Dong, Y., Medzihradszky, A., Schöne, S., Daum, G., Suzaki, T., Forner, J., Langenecker, T., & Rempel, E. (2016). Integration of light and metabolic signals for stem cell activation at the shoot apical meristem. *Elife*, *5*, e17023.

Pin, P., & Nilsson, O. (2012). The multifaceted roles of FLOWERING LOCUS T in plant development. *Plant, cell & environment*, *35*(10), 1742-1755.

Qi, T., Huang, H., Song, S., & Xie, D. (2015). Regulation of jasmonate-mediated stamen development and seed production by a bHLH-MYB complex in Arabidopsis. *The Plant Cell*, *27*(6), 1620-1633.

Qi, T., Song, S., Ren, Q., Wu, D., Huang, H., Chen, Y., Fan, M., Peng, W., Ren, C., & Xie, D. (2011). The Jasmonate-ZIM-domain proteins interact with the WD-Repeat/bHLH/MYB complexes to regulate Jasmonate-mediated anthocyanin accumulation and trichome initiation in Arabidopsis thaliana. *The Plant Cell*, *23*(5), 1795-1814.

Qi, T., Song, S., Ren, Q., Wu, D., Huang, H., Chen, Y., Fan, M., Peng, W., Ren, C., & Xie, D. (2011). The Jasmonate-ZIM-domain proteins interact with the WD-Repeat/bHLH/MYB complexes to regulate Jasmonate-mediated anthocyanin accumulation and trichome initiation in Arabidopsis thaliana. *Plant Cell*, *23*(5), 1795-1814. https://doi.org/10.1105/tpc.111.083261

Raza, A., Charagh, S., Zahid, Z., Mubarik, M. S., Javed, R., Siddiqui, M. H., & Hasanuzzaman, M. (2021). Jasmonic acid: a key frontier in conferring abiotic stress tolerance in plants. *Plant Cell Rep*, *40*(8), 1513-1541. https://doi.org/10.1007/s00299-020-02614-z

Reinhardt, D., Mandel, T., & Kuhlemeier, C. (2000). Auxin regulates the initiation and radial position of plant lateral organs. *The Plant Cell*, *12*(4), 507-518.

Rodriguez, K., Perales, M., Snipes, S., Yadav, R. K., Diaz-Mendoza, M., & Reddy, G. V. (2016). DNA-dependent homodimerization, sub-cellular partitioning, and protein destabilization control WUSCHEL levels and spatial patterning. *Proceedings of the National Academy of Sciences*, *113*(41), E6307-E6315.

Sarkar, A. K., Luijten, M., Miyashima, S., Lenhard, M., Hashimoto, T., Nakajima, K., Scheres, B., Heidstra, R., & Laux, T. (2007). Conserved factors regulate signalling in Arabidopsis thaliana shoot and root stem cell organizers. *Nature*, *446*(7137), 811-814.

Savatin, D. V., Gramegna, G., Modesti, V., & Cervone, F. (2014). Wounding in the plant tissue: the defense of a dangerous passage. *Frontiers in plant science*, *5*, 111139.

Schoof, H., Lenhard, M., Haecker, A., Mayer, K. F., Jürgens, G., & Laux, T. (2000). The stem cell population of Arabidopsis shoot meristems is maintained by a regulatory loop between the CLAVATA and WUSCHEL genes. *Cell*, *100*(6), 635-644.

Schulze, A., Zimmer, M., Mielke, S., Stellmach, H., Melnyk, C. W., Hause, B., & Gasperini, D. (2019). Wound-Induced Shoot-to-Root Relocation of JA-Ile Precursors Coordinates Arabidopsis Growth. *Mol Plant*, *12*(10), 1383-1394. https://doi.org/10.1016/j.molp.2019.05.013

Schweingruber, F. H., & Börner, A. (2018). *The plant stem: a microscopic aspect*. Springer.

Schweizer, F., Fernández-Calvo, P., Zander, M., Diez-Diaz, M., Fonseca, S., Glauser, G., Lewsey, M. G., Ecker, J. R., Solano, R., & Reymond, P. (2013). Arabidopsis basic helix-loop-helix transcription factors MYC2, MYC3, and MYC4 regulate glucosinolate biosynthesis, insect performance, and feeding behavior. *The Plant Cell*, *25*(8), 3117-3132.

Serrano-Mislata, A., Bencivenga, S., Bush, M., Schiessl, K., Boden, S., & Sablowski, R. (2017). DELLA genes restrict inflorescence meristem function independently of plant height. *Nature Plants*, *3*(9), 749-754.

Serrano-Mislata, A., & Sablowski, R. (2018). The pillars of land plants: new insights into stem development. *Curr Opin Plant Biol*, *45*(Pt A), 11-17. https://doi.org/10.1016/j.pbi.2018.04.016

Shaikhali, J., de Dios Barajas-Lopéz, J., Ötvös, K., Kremnev, D., Garcia, A. S., Srivastava, V., Wingsle, G., Bako, L., & Strand, Å. (2012). The CRYPTOCHROME1-dependent response to excess light is mediated through the transcriptional activators ZINC FINGER PROTEIN EXPRESSED IN INFLORESCENCE MERISTEM LIKE1 and ZML2 in Arabidopsis. *The Plant Cell*, *24*(7), 3009-3025.

Shikata, M., Matsuda, Y., Ando, K., Nishii, A., Takemura, M., Yokota, A., & Kohchi, T. (2004). Characterization of Arabidopsis ZIM, a member of a novel plant-specific GATA factor gene family. *J Exp Bot*, *55*(397), 631-639. https://doi.org/10.1093/jxb/erh078

Shikha, D., Jakhar, P., & Satbhai, S. B. (2023). Role of jasmonate signaling in the regulation of plant responses to nutrient deficiency. *Journal of experimental botany*, *74*(4), 1221-1243.

Sloan, J., Hakenjos, J. P., Gebert, M., Ermakova, O., Gumiero, A., Stier, G., Wild, K., Sinning, I., & Lohmann, J. U. (2020). Structural basis for the complex DNA binding behavior of the plant stem cell regulator WUSCHEL. *Nature Communications*, *11*(1), 2223.

Smyth, D. R., Bowman, J. L., & Meyerowitz, E. M. (1990). Early flower development in Arabidopsis. *The Plant Cell*, *2*(8), 755-767.

Somssich, M., Je, B. I., Simon, R., & Jackson, D. (2016). CLAVATA-WUSCHEL signaling in the shoot meristem. *Development*, *143*(18), 3238-3248.

Song, S., Qi, T., Fan, M., Zhang, X., Gao, H., Huang, H., Wu, D., Guo, H., & Xie, D. (2013). The bHLH subgroup IIId factors negatively regulate jasmonate-mediated plant defense and development. *PLoS Genet*, *9*(7), e1003653. https://doi.org/10.1371/journal.pgen.1003653

Song, S., Qi, T., Huang, H., Ren, Q., Wu, D., Chang, C., Peng, W., Liu, Y., Peng, J., & Xie, D. (2011). The jasmonate-ZIM domain proteins interact with the R2R3-MYB transcription factors MYB21 and MYB24 to affect jasmonate-regulated stamen development in Arabidopsis. *The Plant Cell*, *23*(3), 1000-1013.

Song, S.-K., Lee, M. M., & Clark, S. E. (2006). POL and PLL1 phosphatases are CLAVATA1 signaling intermediates required for Arabidopsis shoot and floral stem cells.

Staswick, P. E., Su, W., & Howell, S. H. (1992). Methyl jasmonate inhibition of root growth and induction of a leaf protein are decreased in an Arabidopsis thaliana mutant. *Proceedings of the National Academy of Sciences*, *89*(15), 6837-6840.

Staswick, P. E., & Tiryaki, I. (2004). The oxylipin signal jasmonic acid is activated by an enzyme that conjugates it to isoleucine in Arabidopsis. *The Plant Cell*, *16*(8), 2117-2127.

Stintzi, A., & Browse, J. (2000). The Arabidopsis male-sterile mutant, opr3, lacks the 12-oxophytodienoic acid reductase required for jasmonate synthesis. *Proceedings of the National Academy of Sciences*, *97*(19), 10625-10630.

Stone, J. M., Trotochaud, A. E., Walker, J. C., & Clark, S. E. (1998). Control of meristem development by CLAVATA1 receptor kinase and kinase-associated protein phosphatase interactions. *Plant physiology*, *117*(4), 1217-1225.

Suza, W. P., & Staswick, P. E. (2008). The role of JAR1 in jasmonoyl-L-isoleucine production during Arabidopsis wound response. *Planta*, *227*, 1221-1232.

Thines, B., Katsir, L., Melotto, M., Niu, Y., Mandaokar, A., Liu, G., Nomura, K., He, S. Y., Howe, G. A., & Browse, J. (2007). JAZ repressor proteins are targets of the SCF(COI1) complex during jasmonate signalling. *Nature*, *448*(7154), 661-665. https://doi.org/10.1038/nature05960

Thireault, C., Shyu, C., Yoshida, Y., St. Aubin, B., Campos, M. L., & Howe, G. A. (2015). Repression of jasmonate signaling by a non-TIFY JAZ protein in Arabidopsis. *The Plant Journal*, *82*(4), 669-679.

Vanholme, B., Grunewald, W., Bateman, A., Kohchi, T., & Gheysen, G. (2007). The tify family previously known as ZIM. *Trends Plant Sci*, *12*(6), 239-244. https://doi.org/10.1016/j.tplants.2007.04.004

Wager, A., & Browse, J. (2012). Social network: JAZ protein interactions expand our knowledge of jasmonate signaling. *Frontiers in plant science*, *3*, 41.

Wang, G., & Fiers, M. (2010). CLE peptide signaling during plant development. *Protoplasma*, *240*, 33-43.

Wang, H., Li, Y., Pan, J., Lou, D., Hu, Y., & Yu, D. (2017). The bHLH transcription factors MYC2, MYC3, and MYC4 are required for jasmonate-mediated inhibition of flowering in Arabidopsis. *Molecular plant*, *10*(11), 1461-1464.

Wang, J., Wu, D., Wang, Y., & Xie, D. (2019). Jasmonate action in plant defense against insects. *J Exp Bot*, *70*(13), 3391-3400. https://doi.org/10.1093/jxb/erz174

Wang, Z.-P., Xing, H.-L., Dong, L., Zhang, H.-Y., Han, C.-Y., Wang, X.-C., & Chen, Q.-J. (2015). Egg cell-specific promoter-controlled CRISPR/Cas9 efficiently generates homozygous mutants for multiple target genes in Arabidopsis in a single generation. *Genome biology*, *16*, 1-12.

Wasternack, C. (2015). How jasmonates earned their laurels: past and present. *Journal of plant growth regulation*, *34*, 761-794.

Wasternack, C., & Hause, B. (2013). Jasmonates: biosynthesis, perception, signal transduction and action in plant stress response, growth and development. An update to the 2007 review in Annals of Botany. *Ann Bot*, *111*(6), 1021-1058. https://doi.org/10.1093/aob/mct067

Wasternack, C., & Song, S. (2017). Jasmonates: biosynthesis, metabolism, and signaling by proteins activating and repressing transcription. *Journal of experimental botany*, *68*(6), 1303-1321.

Weigel, D., & Jürgens, G. (2002). Stem cells that make stems. *Nature*, *415*(6873), 751-754. https://doi.org/10.1038/415751a

Weits, D. A., Kunkowska, A. B., Kamps, N. C., Portz, K. M., Packbier, N. K., Nemec Venza, Z., Gaillochet, C., Lohmann, J. U., Pedersen, O., & van Dongen, J. T. (2019). An apical hypoxic niche sets the pace of shoot meristem activity. *Nature*, *569*(7758), 714-717.

Wenzl, C., & Lohmann, J. U. (2023). 3D imaging reveals apical stem cell responses to ambient temperature. *Cells & Development*, *175*, 203850.

White, D. W. (2006). PEAPOD regulates lamina size and curvature in Arabidopsis. *Proc Natl Acad Sci U S A*, *103*(35), 13238-13243. https://doi.org/10.1073/pnas.0604349103

Wu, H., Qu, X., Dong, Z., Luo, L., Shao, C., Forner, J., Lohmann, J. U., Su, M., Xu, M., & Liu, X. (2020). WUSCHEL triggers innate antiviral immunity in plant stem cells. *Science*, *370*(6513), 227-231.

Wu, J., & Baldwin, I. T. (2010). New insights into plant responses to the attack from insect herbivores. *Annual review of genetics*, *44*, 1-24.

Xie, D.-X., Feys, B. F., James, S., Nieto-Rostro, M., & Turner, J. G. (1998). COI1: an Arabidopsis gene required for jasmonate-regulated defense and fertility. *Science*, *280*(5366), 1091-1094.

Xin, W., Wang, Z., Liang, Y., Wang, Y., & Hu, Y. (2017). Dynamic expression reveals a two-step patterning of WUS and CLV3 during axillary shoot meristem formation in Arabidopsis. *Journal of plant physiology*, *214*, 1-6.

Yadav, R. K., Perales, M., Gruel, J., Girke, T., Jönsson, H., & Reddy, G. V. (2011). WUSCHEL protein movement mediates stem cell homeostasis in the Arabidopsis shoot apex. *Genes & development*, *25*(19), 2025-2030.

Yan, J., Zhang, C., Gu, M., Bai, Z., Zhang, W., Qi, T., Cheng, Z., Peng, W., Luo, H., Nan, F., Wang, Z., & Xie, D. (2009). The Arabidopsis CORONATINE INSENSITIVE1 protein is a jasmonate receptor. *Plant Cell*, *21*(8), 2220-2236. https://doi.org/10.1105/tpc.109.065730

Yoshida, S., Mandel, T., & Kuhlemeier, C. (2011). Stem cell activation by light guides plant organogenesis. *Genes & development*, *25*(13), 1439-1450.

Zander, M., Lewsey, M. G., Clark, N. M., Yin, L., Bartlett, A., Saldierna Guzmán, J. P., Hann, E., Langford, A. E., Jow, B., & Wise, A. (2020). Integrated multi-omics framework of the plant response to jasmonic acid. *Nature Plants*, *6*(3), 290-302.

Zarei, A., Korbes, A. P., Younessi, P., Montiel, G., Champion, A., & Memelink, J. (2011). Two GCC boxes and AP2/ERF-domain transcription factor ORA59 in jasmonate/ethylene-mediated activation of the PDF1.2 promoter in Arabidopsis. *Plant Mol Biol*, *75*(4-5), 321-331. https://doi.org/10.1007/s11103-010-9728-y

Zeng, J., Dong, Z., Wu, H., Tian, Z., & Zhao, Z. (2017). Redox regulation of plant stem cell fate. *The EMBO journal*, *36*(19), 2844-2855.

Zeng, J., Li, X., Ge, Q., Dong, Z., Luo, L., Tian, Z., & Zhao, Z. (2021). Endogenous stress-related signal directs shoot stem cell fate in Arabidopsis thaliana. *Nature Plants*, *7*(9), 1276-1287.

Zhai, Q., Zhang, X., Wu, F., Feng, H., Deng, L., Xu, L., Zhang, M., Wang, Q., & Li, C. (2015). Transcriptional Mechanism of Jasmonate Receptor COI1-Mediated Delay of Flowering Time in Arabidopsis. *Plant Cell*, *27*(10), 2814-2828. https://doi.org/10.1105/tpc.15.00619

Zhang, G., Liu, W., Gu, Z., Wu, S., E, Y., Zhou, W., Lin, J., & Xu, L. (2023). Roles of the wound hormone jasmonate in plant regeneration. *Journal of experimental botany*, *74*(4), 1198-1206.

Zhang, G., Zhao, F., Chen, L., Pan, Y., Sun, L., Bao, N., Zhang, T., Cui, C.-X., Qiu, Z., & Zhang, Y. (2019). Jasmonate-mediated wound signalling promotes plant regeneration. *Nature Plants*, *5*(5), 491-497.

Zhang, Y., & Turner, J. G. (2008). Wound-induced endogenous jasmonates stunt plant growth by inhibiting mitosis. *PLoS One*, *3*(11), e3699. https://doi.org/10.1371/journal.pone.0003699

Zhao, L., Xie, L., Zhang, Q., Ouyang, W., Deng, L., Guan, P., Ma, M., Li, Y., Zhang, Y., & Xiao, Q. (2020). Integrative analysis of reference epigenomes in 20 rice varieties. *Nature Communications*, *11*(1), 2658.

Zhao, Z., Andersen, S. U., Ljung, K., Dolezal, K., Miotk, A., Schultheiss, S. J., & Lohmann, J. U. (2010). Hormonal control of the shoot stem-cell niche. *Nature*, *465*(7301), 1089-1092.

Zhou, W., Lozano-Torres, J. L., Blilou, I., Zhang, X., Zhai, Q., Smant, G., Li, C., & Scheres, B. (2019). A jasmonate signaling network activates root stem cells and promotes regeneration. *Cell*, *177*(4), 942-956. e914.

Zhou, Y., Liu, X., Engstrom, E. M., Nimchuk, Z. L., Pruneda-Paz, J. L., Tarr, P. T., Yan, A., Kay, S. A., & Meyerowitz, E. M. (2015). Control of plant stem cell function by conserved interacting transcriptional regulators. *Nature*, *517*(7534), 377-380.

Zhou, Y., Yan, A., Han, H., Li, T., Geng, Y., Liu, X., & Meyerowitz, E. M. (2018). HAIRY MERISTEM with WUSCHEL confines CLAVATA3 expression to the outer apical meristem layers. *Science*, *361*(6401), 502-506.

Zhu, Z., An, F., Feng, Y., Li, P., Xue, L., A, M., Jiang, Z., Kim, J. M., To, T. K., Li, W., Zhang, X., Yu, Q., Dong, Z., Chen, W. Q., Seki, M., Zhou, J. M., & Guo, H. (2011). Derepression of ethylene-stabilized transcription factors (EIN3/EIL1) mediates jasmonate and ethylene signaling synergy in Arabidopsis. *Proc Natl Acad Sci U S A*, *108*(30), 12539-12544. https://doi.org/10.1073/pnas.1103959108

Züst, T., & Agrawal, A. A. (2017). Trade-offs between plant growth and defense against insect herbivory: an emerging mechanistic synthesis. *Annual review of plant biology*, *68*, 513-534.

Publications

Zeng J, Zhao X, Liang Z, Hidalgo I, Gebert M, **Fan P**, Wenzl C, Gornik S, Lohmann, J. U. (2023). Nitric oxide controls shoot meristem activity via regulation of DNA methylation. Nature Communications, 14(1), 8001.

Wang L, **Fan P**, Jimenez-Gongora T, Zhang D, Ding X, Medina-Puche L, Lozano-Durán R. (2022). The V2 Protein from the Geminivirus Tomato Yellow Leaf Curl Virus Largely Associates to the Endoplasmic Reticulum and Promotes the accumulation of the Viral C4 Protein in a Silencing Suppression-Independent Manner. Viruses, 14(12), 2804.

Wang L, Tan H, Medina-Puche L, Wu M, Garnelo Gomez B, Gao M, Shi C, Jimenez-Gongora T, **Fan P,** Ding X, Zhang D, Ding Y, Rosas-Diaz T, Liu Y, Aguilar E, Fu X, Lozano-Durán R (2022). Combinatorial interactions between viral proteins expand the potential functional landscape of the tomato yellow leaf curl proteome. PLoS Pathog. 18;18:e1010909.

Fan P[*], Aguilar E[*], Bradai M, Xue H, Wang H, Rosas-Diaz T, Tang W, Wolf S, Zhang H, Xu L, Lozano-Durán R (2021). The receptor-like kinases BAM1 and BAM2 are required for root xylem patterning. PNAS. 2021 Mar 23;118(12):e2022547118. doi: 10.1073/pnas.2022547118.

[*] Equal contribution

Garnelo Gomez B, Rosas-Diaz T, Shi C, **Fan P**, Zhang D, Rufian JS, Lozano-Duran R (2020). The viral silencing suppressor P19 interacts with the receptor-like kinases BAM1 and BAM2 and suppresses the cell-to-cell movement of RNA silencing independently of its ability to bind sRNA. New Phytol, doi: 10.1111/nhp.16981.

Rosas-Diaz T, Zhang D, **Fan P**, Wang L, Ding X, Jiang Y, Jimenez-Gongora T, Medina-Puche L, Zhao Z, Feng Z, Zhang G, Liu X, Bejarano ER, Tan L, Zhang H, Zhu JK, Xing W, Faulkner C, Nagawa S, Lozano-Duran R (2018). A virus-targeted plant receptor-like kinase promotes cell-to-cell spread of RNAi. PNAS. 2018 Feb 6;115(6):1388-1393. doi: 10.1073/pnas.1715556115.

Fan P, Chen D, He Y, Zhou Q, Tian Y & Gao L. (2016). Alleviating salt stress in tomato seedlings using Arthrobacter and Bacillus megaterium isolated from the rhizosphere of wild plants grown on saline–alkaline lands. International Journal of Phytoremediation, 18(11), 1113-1121.

Acknowledgments

Firstly, I would like to thank my supervisor Prof. Jan Lohmann for his support and guidance to my Ph.D study. The academic atmosphere of freedom and equality he created for the lab motivated me to be fully immersed in the journey of scientific exploration and discovery. Also, he always provided me with necessary suggestions and advice when I was at the critical intersection of my Ph.D project, which greatly benefits my future studies.

Secondly, I would like to thank all my colleagues in Jan Lohmann's lab. Their help and support allowed me to conduct scientific research efficiently in the lab. It is a great honor and pleasure to work with them. For my Ph.D project, I would like to especially thank Dr. Yanfei Ma for his supervision and support regarding the experimental work as well as the guidance in developing my Ph.D project when I first came to the lab. Also, I would like to thank Dr. Christian Wenzl for the support of microscopy and imaging analysis. I also thank Dr. Jian Zeng, Dr. XinAi Zhao, and Dr. Sharmila Singh for the experimental guidance. Thanks to Katja Piiper and Lotte Bald for the efficient assistance to the lab work. Many thanks to Dr. Jiao Zhao from Thomas Greb lab for providing the resources for the Y2H experiment and Dr. Sheng-kai Sun from Rüdiger Hell lab for providing *jar1-11* and *aos1-1* mutants.

Next, I would like to thank all the members of my TAC committee including Prof. Thomas Greb, Prof. Michael Raissig, and Prof. Rosa Lozano-Durán. Their feedback and suggestions from every TAC meeting always brought new insights to my projects, which led me to think about my project from different perspectives. Also, I would like to thank Heidelberg University and Centre for Organismal Studies (COS) for providing such an advanced scientific platform and pleasant working environment.

Finally, I would like to thank my parents and my husband Wencong Zhu. They always unconditionally understand and support every decision I make in my life. Special thanks to the GeminiTeam, they always support me just like my family. Without their support, I could not have come so far in this journey. I would like to thank *Arabidopsis thaliana* in the end, the silent friend I have been working with for the past eight years. This small and great plant opened the wonderful scientific world to me and what I learned from them is not only biological knowledge but also the philosophy of life.

Appendix

Supplementary figures:

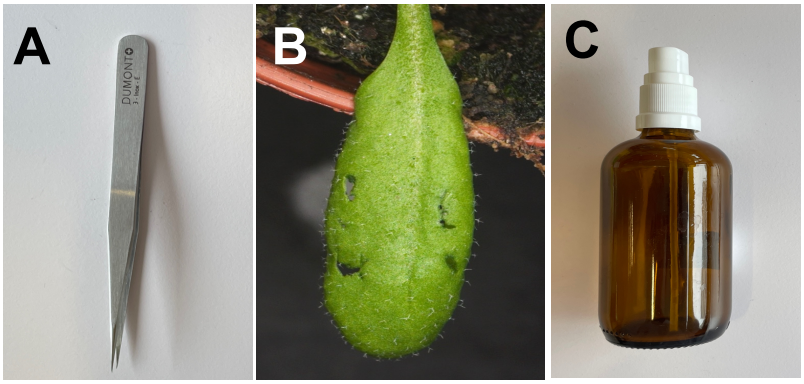


Figure S1: Additional information for the long-term wounding and JA treatment. **A**, forceps used for wounding leaves. **B**, a leaf that is wounded on the first day. **C**, the spray bottle used for JA treatment.

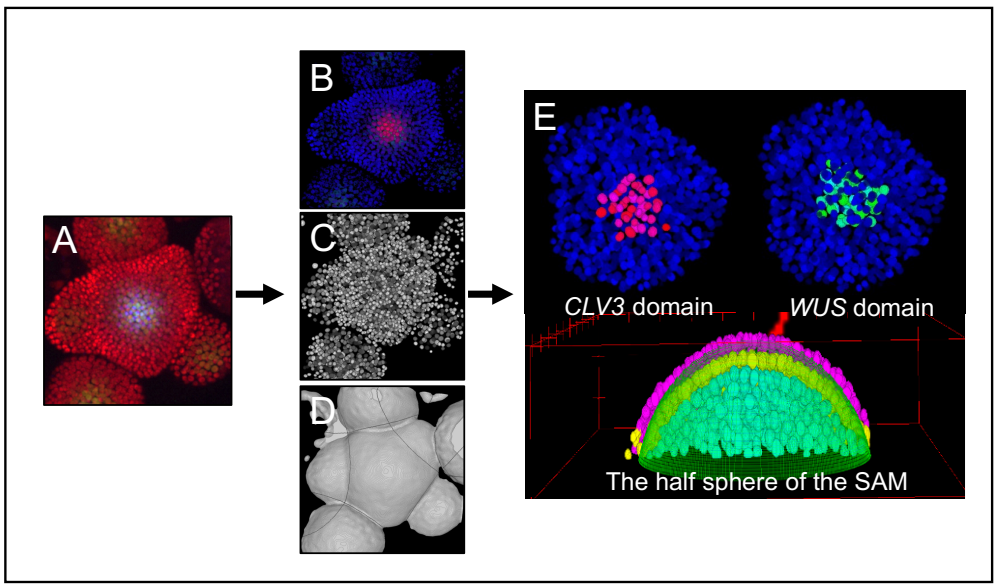


Figure S2: A brief illustration of the triple reporter (*TR7*) computational analysis pipeline. The image files captured by the confocal microscope (**A**) were first converted into multichannel image stacks in the tagged image file format (TIFF) (**B**). The converted images were then used to generate the files for 3D nuclear segmentation (**C**) and the files for the 3D mask (**D**). After the three types of files (**B-D**) were ready, the analysis pipeline was executed as described by Wenzl and Lohmann (2023). In the analysis pipeline, the following parameters were assessed: the size of the SAM, the cell number of the SAM, the cell number of the *WUS*-expressing domain, and the cell number of the *CLV3*-expressing domain (**E**).

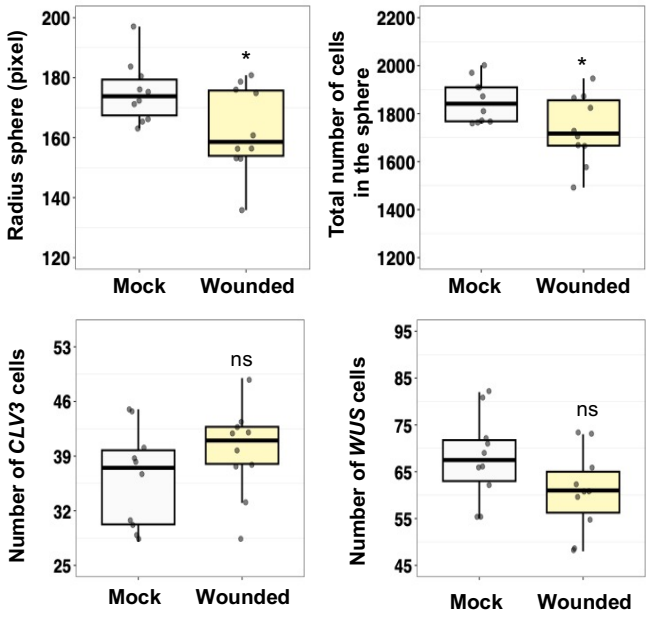


Figure S3: The third biological replicate of SAM morphological analysis following the seven-day wounding treatment. SAM morphological analysis of mock and wounded samples were performed using the computational image analysis pipeline. N=10. Statistical analysis: two-tailed Student's t-tests, *P < 0.05, ns =not significant.

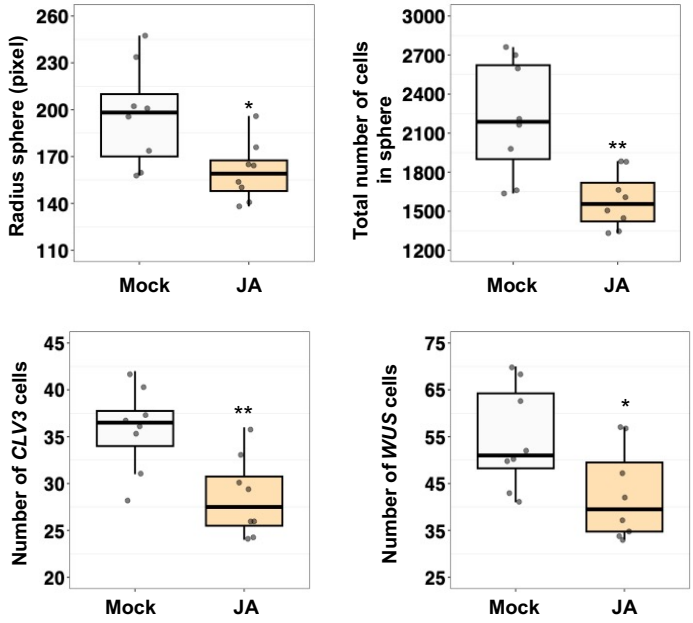


Figure S4: SAM morphological analysis following a nine-day JA treatment. SAM morphology analysis of mock and JA-treated SAMs was performed using computational image analysis pipeline. N=8. Statistical analysis: two-tailed Student's t-tests, *P < 0.05, **P < 0.01.

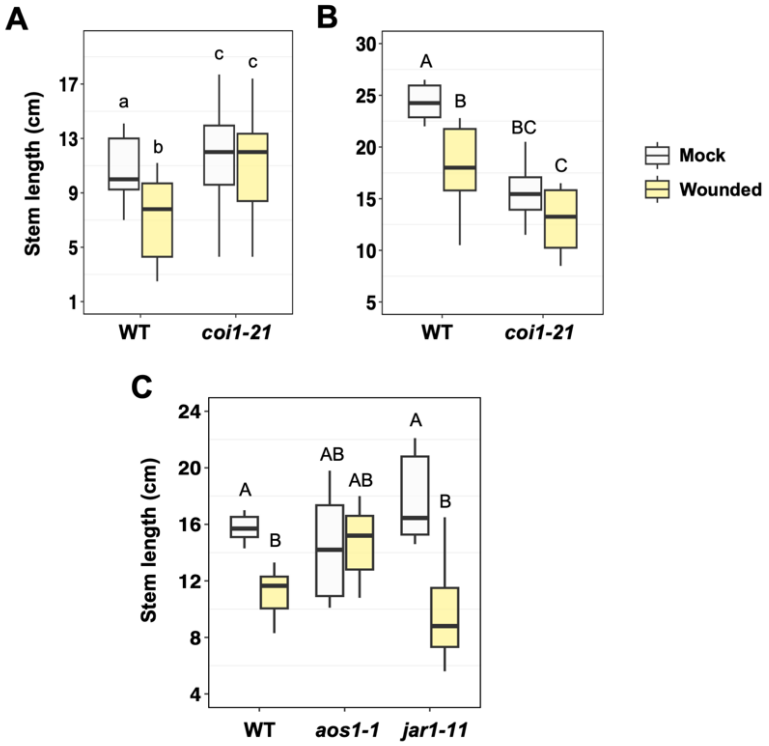


Figure S5: The long-term wounding treatment with mutants in the JA pathways. A-B, the two additional biological replicates for measuring the stem length of WT and *coi1-21* upon wounding treatment. **C**, one additional biological replicate for measuring the stem length of WT, *aos1-1*, and *jar1-11* upon wounding treatment. Statistical analysis: One-way ANOVA (Tukey's test). $P < 0.01$ with capital letters, $P < 0.05$ with lowercase. N=10.

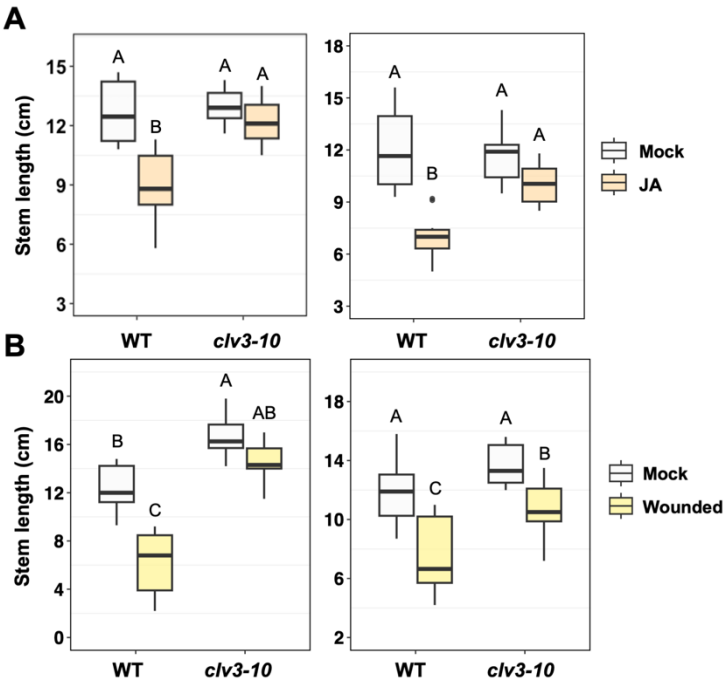


Figure S6: Long-term wounding or JA treatment with *clv3-10*. A, the two additional biological replicates for measuring the stem length of WT and *clv3-10* with the seven-day JA treatment. **B**, the two additional biological replicates for measuring the stem length of WT and *clv3-10* with the seven-day wounding treatment. Statistical analysis: One-way ANOVA (Tukey's test). $P < 0.01$. N=10.

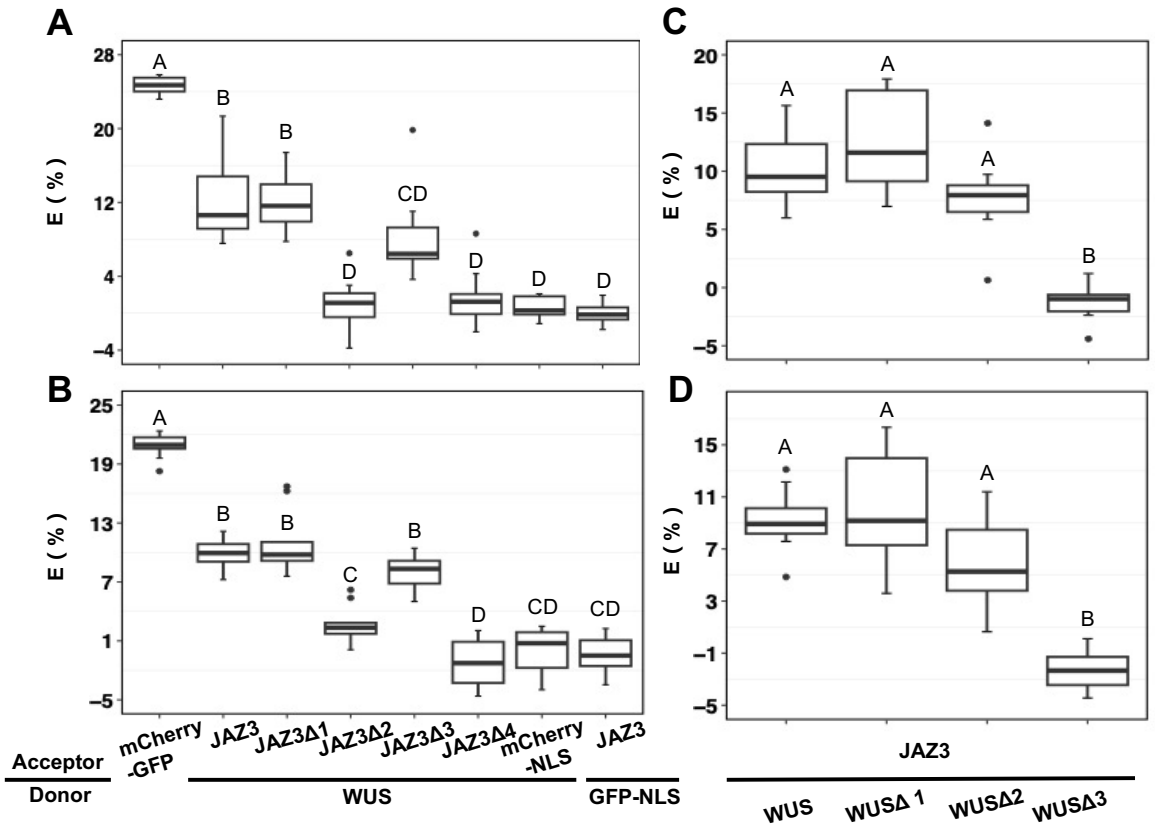


Figure S7: WUS interacts with JAZ3 by the AP- FRET assay. A-B: the two additional biological replicates of AP-FRET experiments for interaction between WUS and truncated versions of JAZ3. **C-D**, the two additional biological replicates of AP-FRET experiments of interaction between truncated versions of WUS and JAZ3. The efficiencies of eight to ten nuclei were calculated in one biological replicate. Statistics were analyzed using one-way ANOVA with the Tukey test ($P<0.01$).

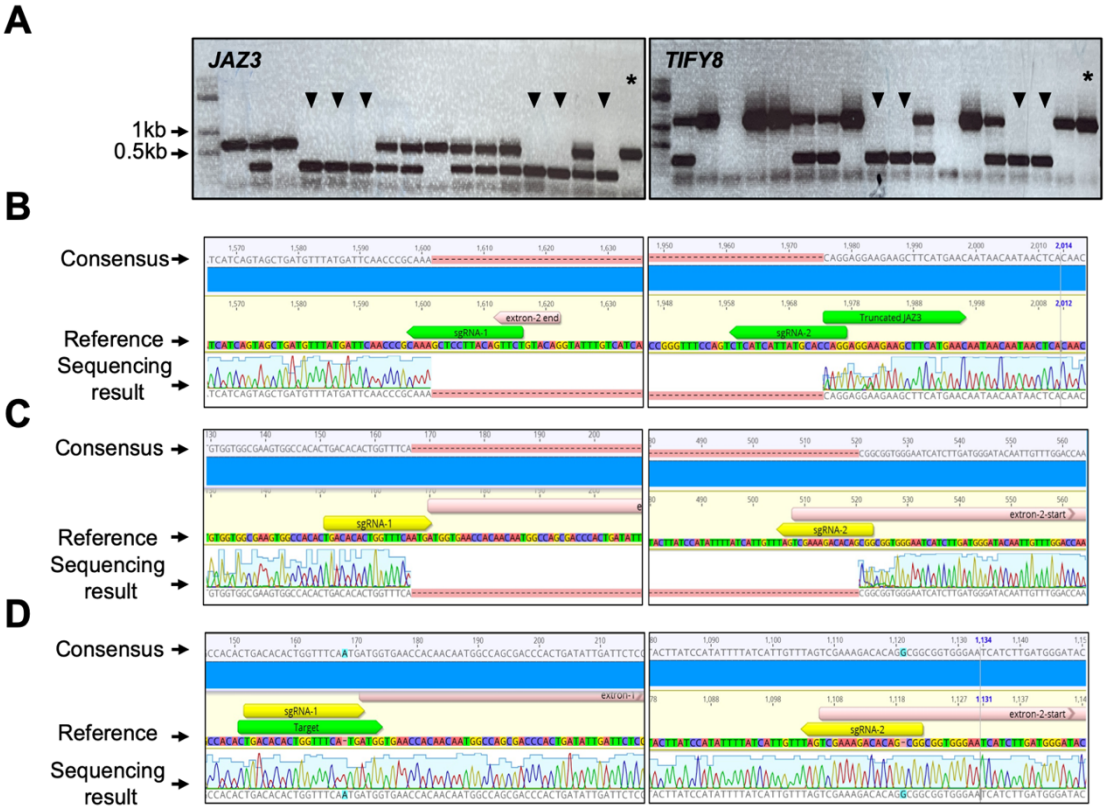


Figure S8: Identification of the mutants generated by CRISPR/Cas9 genome editing system. **A**, representative images of the PCR results for genotyping *jaz3-cr* and *tify8-cr1*. Arrowheads indicate the PCR fragments amplified from the homozygous mutants. The size of fragments: ~240bp for *jaz3-cr* and ~ 232 bp for *tify8-cr1*. Asterisks indicate the PCR fragments amplified from WT or heterozygous plants. The size of fragments: ~ 616bp for *jaz3-cr* and ~1185bp for *tify8-cr1*. **B-D**, Representative results of the sequencing alignment for the edited sequences in the homozygous mutants. The genomic sequences of respective genes were aligned with the Sanger sequencing results of *jaz3-cr* **(B)**, *tify8-cr1* **(C)**, or *tify8-cr2* **(D).** Images were downloaded from Genious (9.1.8).

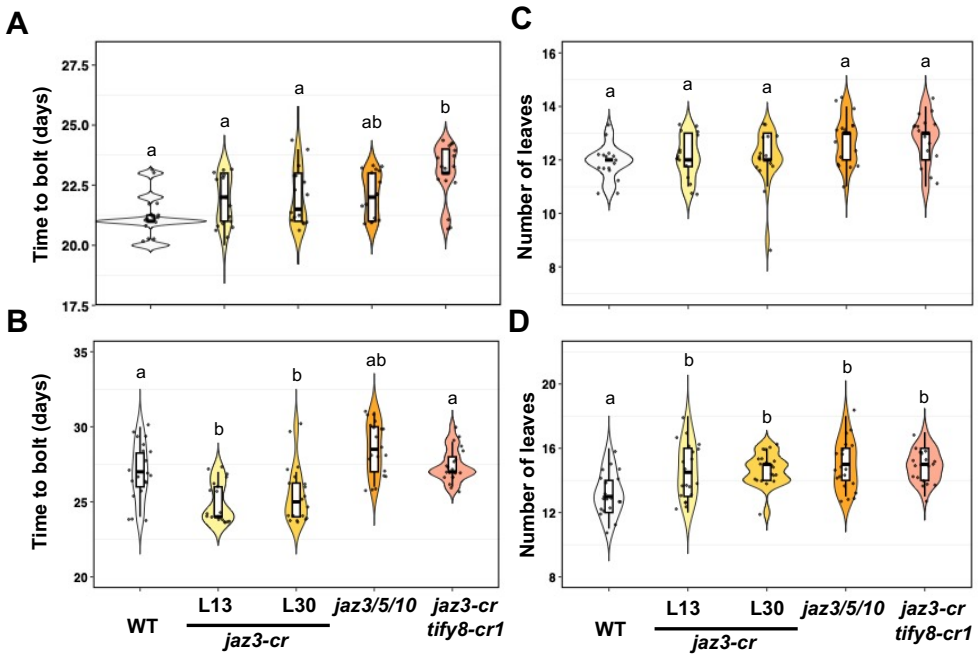


Figure S9: Flowering phenotypes of JAZ3-related mutants. A-B, the two additional biological replicates for measuring the time to bolt. **C-D**, the two additional biological replicates for measuring the number of leaves after bolting. Statistics were analyzed using the Kruskal-Wallis test followed by Dunn's multiple comparison test (P<0.05). **A, C**: n=16. **B, D**: n =20.

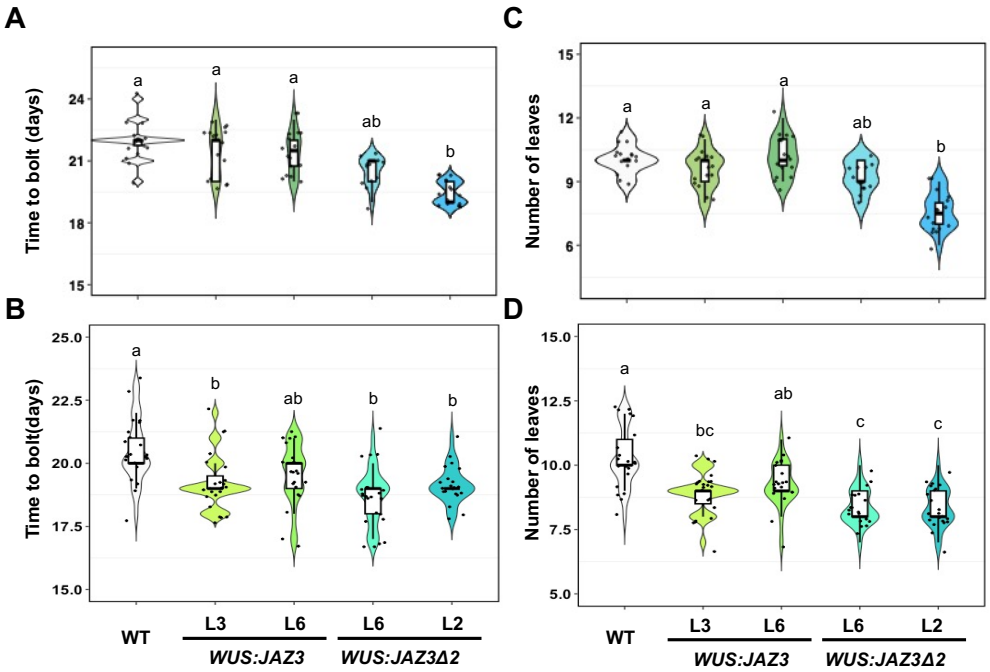


Figure S10: Flowering phenotypes of JAZ3-related transgenic lines. A-B, the two additional biological replicates for measuring the time to bolt. **C-D**, the two additional biological replicates for measuring the number of leaves after bolting. Statistics were analyzed using the Kruskal-Wallis test followed by Dunn's multiple comparison test (P<0.05). **A, C:** n=12-16. B, D: n=24.

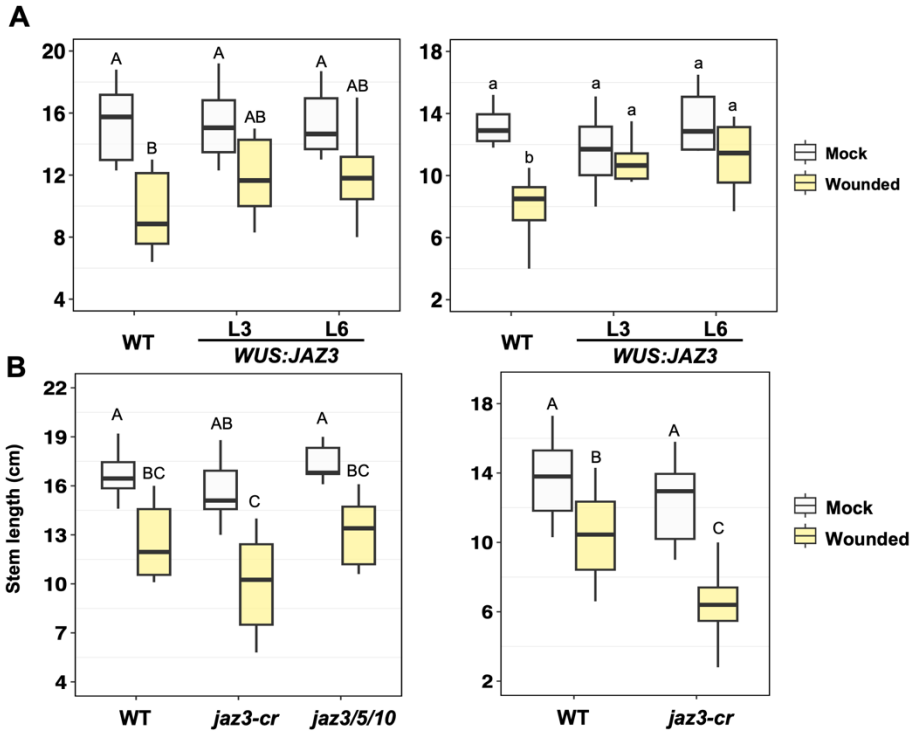


Figure S11: The long-term wounding treatment with *WUS:JAZ3* and *jaz3-cr*. A, the two additional biological replicates for measuring the stem length of WT and *WUS:JAZ3* upon wounding treatment. N=8-10. **B**, the two additional biological replicates for measuring the stem length of WT, *jaz3-cr,* and *jaz3/5/10* upon wounding treatment. N=10-12. Statistical analysis: One-way ANOVA (Tukey's test). P < 0.01 with capital letters, P < 0.05 with lowercase.

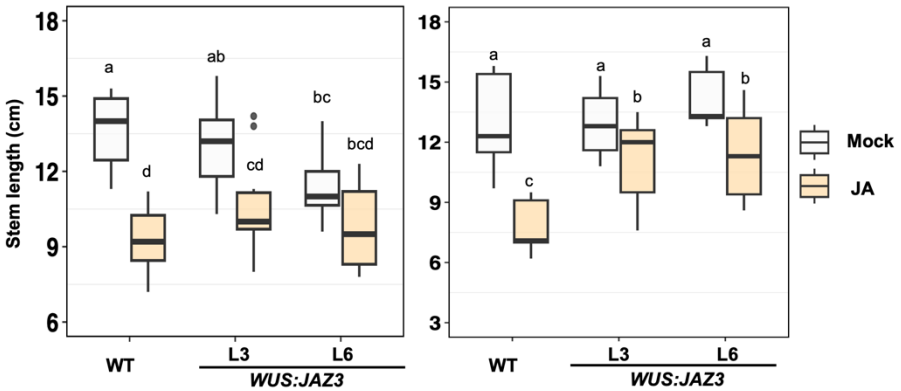


Figure S12: The long-term JA treatment with *WUS:JAZ3*. the two additional biological replicates for measuring the stem length of WT and *WUS:JAZ3* upon JA treatment. N=9-10. Statistical analysis: One-way ANOVA (Tukey's test). P < 0.01 with capital letters, P < 0.05 with lowercase.

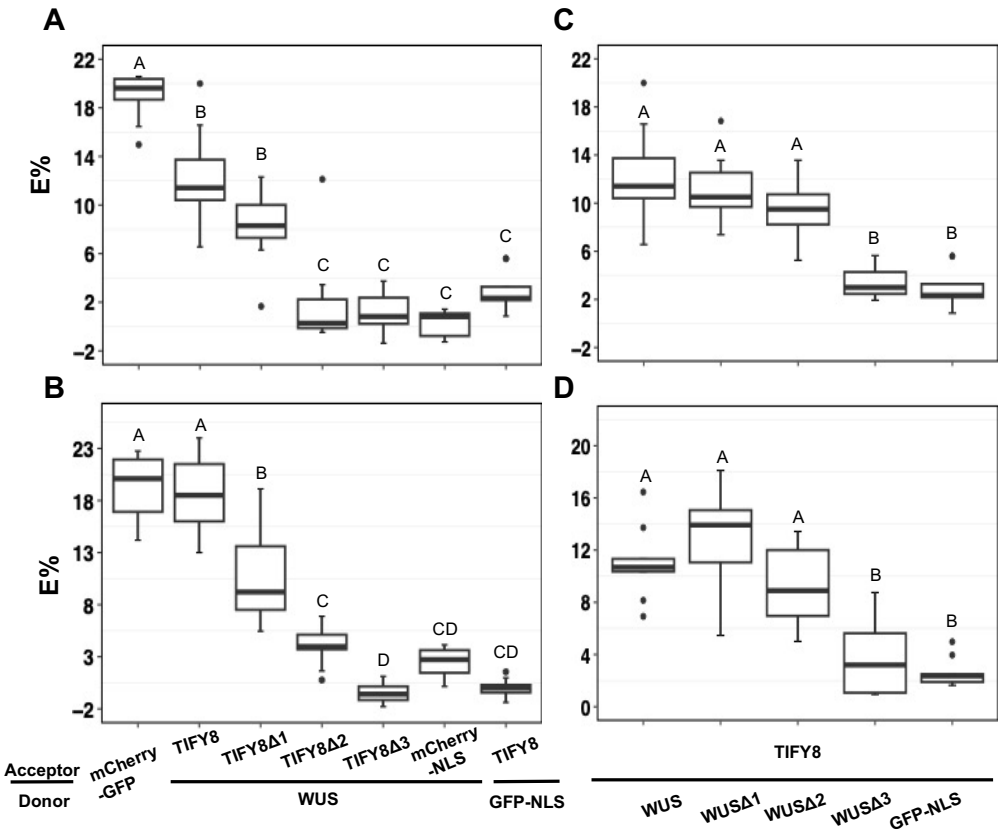


Figure S13: WUS interacts with TIFY8 by AP- FRET assay. A-B: the two additional biological replicates of AP-FRET experiments for protein interaction between WUS and truncated versions of TIFY8. **C-D**, the two additional biological replicates of AP-FRET experiments of protein interaction between truncated versions of WUS and TIFY8. The efficiencies of eight to ten nuclei were calculated in one biological replicate. Statistics were analyzed using one-way ANOVA with the Tukey test ($P<0.01$). **A** and **C** share the same result of the combination of TIFY8-mCherry + WUS-GFP and TIFY8-mCherry + GFP-NLS, as the experiments are conducted in the same batch.

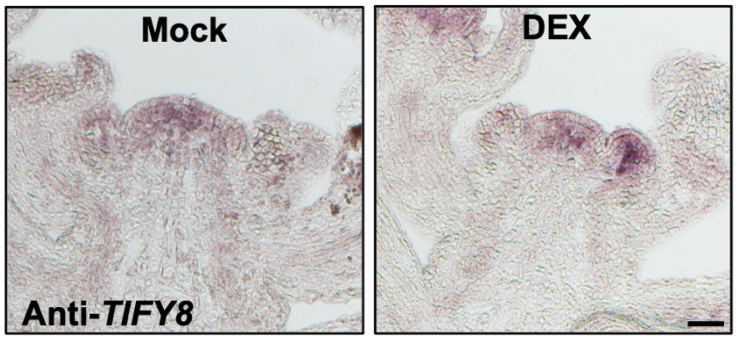


Figure S14: Expression pattern of *TIFY8* upon inducible WUS overexpression. Expression pattern of *TIFY8* in the SAM of *UBQ10: mCherry-GR-linker-WUS* line with or without DEX treatment. mCherry-WUS-GR in the SAM was induced by spaying 10 μM DEX solution on the shoot apex. Samples were collected 2 hours after the treatment.

Supplementary tables:

Table S1: The list of candidate genes related to JA pathways

Genes are selected based on the data from yeast-two hybrid screening and the data from the ChIP-seq and RNA-seq (Ma et al., 2019). [1]: Targets are selected based on the peaks with significant WUS protein enrichment detected in the ChIP-seq. [2]: Genes are selected from the list of those showing significantly differential expression upon inducible overexpression of WUS (p-value< 0.05) in the RNA-seq. NT: not found.[3] Data is kindly provided by Dr. Athanasios Lampropoulos.

Part 1: JA signaling

AGI	Gene Name	If targeted by WUS?[1]	log2FC in RNA-seq [2]	WUS protein interactor? [3]
AT1G19180	JAZ1	NO	-0.49706217595453	No
AT1G74950	JAZ2	YES	-0.64817997668341	No
AT1G17380	JAZ5	YES	NT	No
AT1G72450	JAZ6	YES	-0.818190264480813	No
AT5G20900	JAZ12	NO	0.331534155092977	No
AT1G70700	TIFY7	YES	NT	No
AT3G17860	JAZ3	YES	NT	Yes
AT1G32640	MYC2	YES	-0.827624961025022	No
AT4G17880	MYC4	NO	-0.384052803509705	No
AT5G64810	WRKY51	YES	-0.974239138666889	No
AT2G46370	JAR1	YES	-0.366581188717293	No
AT4G32570	TIFY8	NO	0.352660705534755	Yes

Part 2: JA biosynthesis

AGI	Gene Name	If targeted by WUS? [1]	log2FC in RNA-seq [2]	WUS protein interactor? [3]
AT5G42650	AOS	YES	-1.89011312079554	No
AT3G25770	AOC2	YES	-2.06745703816161	No
AT1G72520	LOX4	YES	-1.07418063850471	No
AT3G25760	AOC1	YES	-1.45929046761127	No
AT1G76680	OPR1	YES	-1.38977946953355	No
AT1G19640	JMT	YES	-3.19401605915253	No
AT1G17420	LOX3	YES	-1.19495063685111	No
AT1G76690	OPR2	NO	-0.531776551948296	No
AT1G20510	OPCL1	NO	-0.693028694083209	No
AT1G05800	DGL	NO	-1.28768596480486	No
AT2G06050	OPR3	NO	-0.343819163916897	No
AT3G25780	AOC3	NO	-1.27058355540215	No

Table S2: Plant materials used in this study

Mutants		
Name	**Ecotype**	**Reference**
clv3-10	Col-0	Forner et al., 2015
coi1-21	Col-0	He et al., 2012
wus-7	L*er*	Graf et al., 2010
jar1-11	Col-0	Suza & Staswick, 2008
aos1-1	Col-0	Myers et al., 2023
jaz3/5/10	Col-0	de Torres Zabala et al., 2016
tify8-cr1	Col-0	this study
jaz3-cr L13	Col-0	this study
jaz3-cr L30	Col-0	this study
tify8-cr1 clv3-10	Col-0	this study
tify8-cr2 clv3-10	Col-0	this study
jaz3-cr tify8-cr1	Col-0	this study
Transgenic lines		
Name	**Ecotype**	**Reference**
TR7	Col-0	Wenzl & Lohmann, 2023
GD44	*wus-am*	Daum et al., 2014
UBQ10: mCherry-GR-WUS	Col-0	Ma et al., 2019
UBQ10: mCherry-GR	Col-0	Ma et al., 2019
COI1:COI1-GFP	Col-0	Larrieu et al., 2015
WUS:JAZ3 L3	Col-0	this study
WUS:JAZ3 L6	Col-0	this study
WUS:JAZ3Δ2 L2	Col-0	this study
WUS:JAZ3Δ2 L6	Col-0	this study
WUS:JAZ3/TR7 L4	*TR7*	this study
WUS:JAZ3/TR7 L11	*TR7*	this study
WUS:JAZ3 /clv3-10 L4	*clv3-10*	this study
WUS:JAZ3/clv3-10 L10	*clv3-10*	this study
WUS:JAZ3/clv3-10 L12	*clv3-10*	this study
WUS:TIFY8/TR7 L1	*TR7*	this study
WUS:TIFY8/TR7 L4	*TR7*	this study
CLV3:TIFY8/TR7 L7	*TR7*	this study
CLV3:TIFY8/TR7 L8	*TR7*	this study
JAZ3: GFP-NLS	Col-0	this study
TIFY8:GFP-NLS	Col-0	this study
TIFY8:TIFY8$_{CDS}$-GFP	Col-0	this study

TIFY8:GFP-NLS/UBQ10: mCherry-GR-WUS	*UBQ10: mCherry-GR-WUS*	this study
TIFY8:TIFY8$_{CDS}$-GFP/UBQ10: mCherry-GR-WUS	*UBQ10: mCherry-GR-WUS*	this study

Table S3: GreenGate Modules generated in this study

ID	content	backbone
PFF001	coding sequence of JAZ5	pGGC000
PFF002	coding sequence of MYC2	pGGC000
PFF003	coding sequence of JAZ3	pGGC000
PFF004	coding sequence of TIFY8	pGGC000
PFF006	coding sequence of JAZ6	pGGC000
PFF007	coding sequence of JAZ1	pGGC000
PFF008	coding sequence of JAZ2	pGGC000
PFF009	coding sequence of MYC4	pGGC000
PFF017	coding sequence of JAZ3Δ4 version	pGGC000
PFF018	coding sequence of JAZ3Δ1 version	pGGC000
PFF014	coding sequence of JAZ3Δ2 version	pGGC000
PFF019	coding sequence of JAZ3Δ3 version	pGGC000
PFF020	coding sequence of TIFY8Δ2 version	pGGC000
PFF021	coding sequence of TIFY8Δ3 version	pGGC000
PFF022	coding sequence of TIFY8Δ1 version	pGGC000
PFF023	coding sequence of WUSΔ1 version	pGGC000
PFF024	coding sequence of WUSΔ2 version	pGGC000
PFF025	coding sequence of WUSΔ3 version	pGGC000
PFF027	TIFY8 promoter	pGGA000
PFF030	JAZ3 terminator	pGGE000
PFF031	TIFY8 terminator	pGGE000
PFF039	JA3 promoter	pGGA000
PFF041	coding sequence of MYC3	pGGC000
PFF042	coding sequence of MYC5	pGGC000

Table S4: GreenGate vectors generated in this study

ID	content	Modules
PFF052	WUS:JAZ3	A003-B003-PFF003-D017-E002-F005-Z003
PFF053	WUS:TIFY8	A003-B003-PFF004-D017-E002-F005-Z003
PFF062	WUS:JAZ3Δ2	A003-B003-PFF014-D017-E002-F005-Z003
PFF068	CLV3:TIFY8	A033-B003-PFF004-D017-E008-F005-Z003
PFF084	35S:mCherry-JAZ3	A004-B008-PFF003-D017-E001-F005-Z003
PFF089	35S:TIFY8-mCherry	A004-B003-PFF004-D010-E001-F005-Z003
PFF090	TIFY8-CC	gRNAs for *TIFY8* integrated in PHEE401E
PFF092	JAZ3-CC	gRNAs for *JAZ3* integrated in PHEE401E
PFF094	35S:mCherry-JAZ3Δ2	A004-B008-PFF014-D017-E001-F005-Z003
PFF095	35S:mCherry-JAZ3	A004-B008-PFF003-D017-E001-F005-Z003
PFF096	35S:mCherry-TIFY8	A004-B008-PFF004-D017-E001-F005-Z003
PFF097	35S:mCherry-JAZ3Δ1	A004-B008-PFF018-D017-E001-F005-Z003
PFF098	35S:mCherry-JAZ3Δ3	A004-B008-PFF019-D017-E001-F005-Z003
PFF099	35S:mCherry-JAZ3Δ4	A004-B008-PFF017-D017-E001-F005-Z003
PFF100	35S:TIFY8Δ1-mCherry	A004-B003-PFF022-D010-E001-F005-Z003
PFF101	35S:TIFY8Δ2-mCherry	A004-B003-PFF020-D010-E001-F005-Z003
PFF102	35S:TIFY8Δ3-mCherry	A004-B003-PFF021-D010-E001-F005-Z003
PFF106	35S:WUSΔ1-GFP	A004-B003-PFF023-D011-E001-F005-Z003
PFF107	35S:WUSΔ2-GFP	A004-B003-PFF024-D011-E001-F005-Z003
PFF108	35S:WUSΔ3-GFP	A004-B003-PFF025-D011-E001-F005-Z003
PFF111	TIFY8:GFP-NLS	PFF027-B003-C012-D017-PFF030-F005-Z003
PFF114	JAZ3:GFP-JAZ3CDS	PFF039-B025-PFF003-D017-PFF031-F005-Z003
PFF115	TIFY8:TIFY8CDS-GFP	PFF027-B003-PFF004-D001-PFF030-F005-Z003
PFF153	JAZ3: GFP-NLS	PFF039-B003-C012-D017-PFF031-F005-Z003
PFF164	35S:WOX5-GFP	A004-B003-C333-D011-E001-F005-Z003

Table S5: Primers used in this study

Primers for cloning:

Name	Sequence	Comments
JAZ3-F	aacaGGTCTCaggctcaacaATGGAGAGA GATTTTCTCGG	C module of JAZ3
JAZ3-R	aacaGGTCTCtctgaGGTTGCAGAGCTGAGAG AAGAA	C module of JAZ3
JAZ3Δ2-R	aacaGGTCTCtctgaCACTGTTGGAGCCATTAC	C module of truncated JAZ3
JAZ3Δ3-F	aacaGGTCTCaggctcaacaATGAACTGGTCTTTC TCAAA	C module of truncated JAZ3
JAZ3Δ1-R	aacaGGTCTCtctgaCTTGTCTAAGCAATATGG	C module of truncated JAZ3
JAZ3Δ4-F	aacaGGTCTCaggctcaacaATGGGTTCCTCTATG CCTC	C module of truncated JAZ3
TIFY8-F	aacaGGTCTCaggctcaacaATGATGGTGAACCA CAACAA	C module of TIFY8
TIFY8-R	aacaGGTCTCtctgaTGTGGCTTCTTTTTCAGG ATCT	C module of TIFY8
TIFY8Δ1-F	aacaGGTCTCaggctcaacaATGACTCCTTCCAC GGCTTC	C module of truncated TIFY8
TIFY8Δ2-F	aacaGGTCTCaggctcaacaATGAATGTGAATCC TTTGGC	C module of truncated TIFY8
TIFY8Δ3-R	aacaGGTCTCtctgaCCGATTTCCGGTATTTGA AGG	C module of truncated TIFY8
TIFY8-pro-F	aacaGGTCTCaacctTCCTGAAGAGCCTCGATT TT	TIFY8 promoter
TIFY8-pro-R	aacaGGTCTCttgttGAAACCAGTGTGTCAGTG TGG	TIFY8 promoter
JAZ3-pro-F	aacaGGTCTCaacctGCCATCAAAGGATCCACT AA	JAZ3 promoter
JAZ3-pro-R	aacaGGTCTCttgttCTATAATAAAGACACAGC CC	JAZ3 promoter
WUS-F	aacaGGTCTCaggctcaacaATGGAGCCGCCACA G	C module of truncated WUS
WUSΔ1-R	aacaGGTCTCtctgaACCAAACAGAGGCTTTGC T	C module of truncated WUS
WUSΔ2-R	aacaGGTCTCtctgaTCCACCTACGTTGTTGTA AT	C module of truncated WUS
JAZ3-T-F	aacaGGTCTCactgcTTTCATCTACAGTAAGAA GG	JAZ3 terminator
JAZ3-T-R	aacaGGTCTCttagtCGAATTCCGCCTTTTTCTT C	JAZ3 terminator

TIFY8-T-F	aacaGGTCTCactgcTTAAAGTCTGAATATGAGAG	TIFY8 terminator
TIFY8-T-R	aacaGGTCTCttagtTGCAGATATGAAAGAAGATT	TIFY8 terminator
TIFY8-Y2H-F	ACTAGAATTCATGATGGTGAACCACAACAA	TIFY8 for Yeast two-hybrid
TIFY8-Y2H-R	TAGTGGATCCTCATGTGGCTTCTTTTTCAG	TIFY8 for Yeast two-hybrid
JAZ3-Y2H-F	ACTAGAATTCATGGAGAGAGATTTTCTCGG	TIFY8 for Yeast two-hybrid
JAZ3-Y2H-R2	TAGTCTCGAGTTAGGTTGCAGAGCTGAGAG	TIFY8 for Yeast two-hybrid
JAZ6-F	aacaGGTCTCaggctcaacaATGTCAACGGGACAAGCGCCG	C module of JAZ6
JAZ6-R	aacaGGTCTCtctgaAAGCTTGAGTTCAAGGTTTTTGGAA	C module of JAZ6
JAZ2-F	aacaGGTCTCaggctcaacaATGTCGAGTTTTTCTGCCGAGTGT	C module of JAZ2
JAZ2-R	aacaGGTCTCtctgaCCGTGAACTGAGCCAAGCTGG	C module of JAZ2
JAZ5-F	aacaGGTCTCaggctcaacaATGTCGTCGAGCAATGAAAATGCT	C module of JAZ5
JAZ5-R	aacaGGTCTCtctgaTAGCCTTAGATCGAGATCTTTCGA	C module of JAZ5
MYC2-F	aacaGGTCTCaggctcaacaATGACTGATTACCGGCTACAACCA	C module of MYC2
MYC2-R	aacaGGTCTCtctgaACCGATTTTTGAAATCAAACTTGCT	C module of MYC2
MYC3-F	aacaGGTCTCaggctcaacaATGAACGGCACAACATCATC	C module of MYC3
MYC3-R	aacaGGTCTCtctgaATAGTTTTCTCCGACTTTCG	C module of MYC3
MYC4-F	aacaGGTCTCaggctcaacaATGTCTCCGACGAATGTTCAAG	C module of MYC4
MYC4-R	aacaGGTCTCtctgaTGGACATTCTCCAACTTTCTC	C module of MYC4
MYC5-F	aacaGGTCTCaggctcaacaATGATTAATACCGACGAT	C module of MYC5
MYC5-R	aacaGGTCTCtctgaGCTAATTTTCGACATCAAC	C module of MYC5

Primers for CRISPR/Cas9 constructs:

Name	Sequence	Comments
TIFY8-CC-F	ATATATGGTCTCG**ATTGTGACACAC TGGTTTCATGA**GTTTTAGAGCTAGA AATAGC	cloning construct for CRISPR-Cas9 *tify8* mutant
TIFY8-CC-R	ATTATTGGTCTCG**AAAC**CCGCTGTG TCTTTCGACTACAATCTCTTAGTCGA CTCTAC	cloning construct for CRISPR-Cas9 *tify8* mutant
JAZ3-CC-F	ATATATGGTCTCG**ATTG**AGAACTGT AAGGAGCTTTGGTTTTAGAGCTAGA AATAGC	cloning construct for CRISPR-Cas9 *jaz3*mutant
JAZ3-CC-R	ATTATTGGTCTCG**AAAC**CCTGGTGC ATAATGATGAGCAATCTCTTAGTCG ACTCTAC	cloning construct for CRISPR-Cas9 *jaz3*mutant

Primers for genotyping:

Name	Sequence	Comments
JAZ3-CC-F1	TCTCAGTTTCTATCCTTCAG	genetyping CRISPR-Cas9 *jaz3* mutant
JAZ3-CC-R2	ATCCTCACTCCCTGAGAGTA	genetyping CRISPR-Cas9 *jaz3* mutant
JAZ3-CC-R1	TCAGTAGTCCCTACAATGG	genetyping CRISPR-Cas9 *jaz3* mutant
TIFY8-CC-F1	ACGCTGATGAGGTTTTGAGCT	genetyping CRISPR-Cas9 *tify8* mutant
TIFY8-CC-R2	TGGGTGCTCCTGAGTCGTGA	genetyping CRISPR-Cas9 *tify8* mutant
TIFY8-CC-F2	TGTCCATGAAATAATACTCT	genetyping CRISPR-Cas9 *tify8* mutant
WUS-F	TTGAAGCTGGGATATGGCTT	genetyping *wus-7* mutant
WUS-R	ggagcaaatcaaaatcctcaa	genetyping *wus-7*mutant
CLV3-F	CAAAGACGAAGGGTTTAGGAC	genetyping *clv3-10* mutant
CLV3-R	CGTAATGCTATAGACATCTTCGT TT	genetyping *clv3-10* mutant
jar1-11-LP	CTGTGCAATGTGGATCAAATG	genetyping *jar1-11* mutant
jar1-11-RP	GCTCTGGAACTAGTCAAGGCC	genetyping *jar1-11* mutant
aos-LP	CGAGAAATTAACGGAGCTTCC	genetyping *aos1-1* mutant
aos-RP	CTAACCGGAGGCTACCGTATC	genetyping *aos1-1* mutant
LBb1.3	ATTTTGCCGATTTCGGAAC	genetyping T-DNA insertion mutant
pWUS-g-F	CTCCACCAGATATCCTCTGA	genetyping *WUS:JAZ3* and *WUS:TIFY8*

JAZ3-g-R	ACCAGTTCATTCCTCTGTTG	genetyping *WUS:JAZ3* and *WUS:JAZ3Δ2*
TIFY8-g-R	CGGAGACGAGAATCAATATC	genetyping *WUS:TIFY8* and *CLV3:TIFY8*
pCLV3-g-F	CCCTTGTAGGCTTACGCTAT	genetyping *CLV3:TIFY8*

Primers for qPCR :

Name	Sequence	Comments
LOX3-q-F	TGGTGGCCGGAGTTATCAAC	qPCR for gene expression
LOX3-q-R	GGATTAACCGCCGCATCAAC	qPCR for gene expression
VSP2-q-F	AAAACCGTGTGCAAAGAGGC	qPCR for gene expression
VSP2-q-R	TAACCACAACCAGTACGCCC	qPCR for gene expression
JAZ7-q-F	ACCCATCTTGAGGCTAACGC	qPCR for gene expression
JAZ7-q-R	ACGGTGGTAAGGGGAAGTTG	qPCR for gene expression
JAZ10-q-F	GGAGAAAGTCACTGCAACGT	qPCR for gene expression
JAZ10-q-R	TAGCAACGACGAAGAAGGCT	qPCR for gene expression
JAZ3-q-F	TCGCCACACTGAGTTTCTCC	qPCR for gene expression
JAZ3-q-R	AGGGAAACAGAAGCGATGCA	qPCR for gene expression
JAZ3-IP-F1	CGATTCACATGTCGCATGC	qPCR for gene expression
JAZ3-IP-R1	CTAAATAGAGCTTCGCCGG	qPCR for ChIP
JAZ3-IP-F2	GGGTTAGACTCACGCGCTA	qPCR for ChIP
JAZ3-IP-R2	CATCGTCGTGCAGTGTGTG	qPCR for ChIP
JAZ3-IP-F3	TGACATAATCACATGAGGAT	qPCR for ChIP
JAZ3-IP-R3	GATTAATCGGATGGTACTAT	qPCR for ChIP
JAZ3-IP-F4	CGGACCACATGCATCTTATA	qPCR for ChIP
JAZ3-IP-R4	CCTCATGTGATTATGTCATC	qPCR for ChIP
JAZ3-IP-F5	CGCTTTGTAGGTCCACTTTTGA	qPCR for ChIP
JAZ3-IP-R5	ACACGTCATTTTCTCCAGCC	qPCR for ChIP

Supplemental information (uploaded on the attached CD):

The additional images of *in situ* hybridization and images captured by confocal microscopies in this study.